Fall 2011

# Population pharmacokinetic/pharmacodynamic modeling of insulin kinetics

Lanyi Xie
*University of Iowa*

# POPULATION PHARMACOKINETIC/PHARMACODYNAMIC MODELING OF INSULIN KINETICS

by

Lanyi Xie

An Abstract

Of a thesis submitted in partial fulfillment
of the requirements for the Doctor of
Philosophy degree in Pharmacy
in the Graduate College of
The University of Iowa

December 2011

Thesis Supervisor: Professor Peter Veng-Pedersen

# ABSTRACT

The development of type 2 diabetes over time involves defects in insulin action and insulin secretion. Defects in insulin action alone can be compensated with appropriate hyperinsulinemia. However, the progressive loss of pancreatic beta-cell function leads eventually to the development of persistent hyperglycemia that characterizes type 2 diabetes. Insulin secretion patterns reflect two phases when beta-cells are exposed to acute and sustained glucose stimulation. Through the study and understanding of the roles of these two phases in the regulation of glucose homeostasis, it is clear that insulin must not only be secreted in sufficient amounts, but also at the right time. In type 2 diabetes, the timing and magnitude of insulin secretion are altered, and an abnormal first-phase release initiates before the onset of the disease. Only a few pharmacokinetic/pharmacodynamic (PK/PD) models have considered the biphasic nature of insulin secretion. This study is aimed at describing the biphasic dynamics of insulin secretion through developing a PK/PD model based on current knowledge of the cellular mechanism of biphasic insulin secretion.

The objectives of this work are to 1) evaluate the insulin-glucose kinetics using nonparametric analysis, 2) develop a physiologically based mechanistic PK/PD model to dynamically describe the biphasic insulin secretion, 3) evaluate the impact of ethnicity on insulin secretion kinetics following an intravenous glucose administration using population analysis and 4) extend the proposed model to oral glucose administration and utilize the co-secretion kinetics of insulin and C-peptide in a population PK/PD analysis of the prehepatic insulin secretion.

Population analysis was done using a nonlinear mixed-effects model combined with the proposed PK/PD model to estimate population parameters and their variations between- and within-subjects and the covariates' effects on model parameters. The proposed model describes biphasic insulin behavior, accounts for first-phase insulin

secretion, and also applies to oral glucose administration for estimating prehepatic insulin secretion *in vivo* and in liver extraction. This is done by an analysis that simultaneously uses plasma insulin and C-peptide concentrations. A significantly higher first-phase insulin secretion was identified in healthy youths of African-American compared to Caucasians. The analysis showed no significant differences in the clearance of insulin from the plasma and the liver extraction of insulin between subjects with various levels of glucose tolerance. Obesity leads to a higher insulin production rate and lower elimination rate from the plasma than normal weight subjects. Also, type 2 diabetes and impaired glucose tolerance were found to reduce insulin production rate and resulted in a delayed insulin secretion from the beta-cells.

Abstract Approved: _____
Thesis Supervisor

_____
Title and Department

_____
Date

# POPULATION PHARMACOKINETIC/PHARMACODYNAMIC MODELING OF INSULIN KINETICS

by

Lanyi Xie

A thesis submitted in partial fulfillment
of the requirements for the Doctor of
Philosophy degree in Pharmacy in the Graduate College of
The University of Iowa

December 2011

Thesis Supervisor: Professor Peter Veng-Pedersen

Graduate College
The University of Iowa
Iowa City, Iowa

CERTIFICATE OF APPROVAL

_____

PH.D. THESIS

_____

This is to certify that the Ph.D. thesis of

Lanyi Xie

has been approved by the Examining Committee
for the thesis requirement for the Doctor of Philosophy
degree in Pharmacy at the December 2011 graduation.

Thesis Committee: _____
Peter Veng-Pedersen, Thesis Supervisor

_____
David G. Rethwisch

_____
Daryl J. Murry

_____
Jennifer Fiegel

_____
Lawrene L. Fleckenstein

To My Parents and Friends

## ACKNOWLEDGMENTS

It is my pleasure to thank all those who have made this thesis possible. First and foremost, I would like to thank my advisor, Professor Peter Veng-Pedersen, for his guidance, encouragement and support throughout my graduate career. He is an excellent mentor and has always provided precious direction when I was lost. Without his mentorship and devotion to my Ph.D. education, it would not have been possible for me to fully develop my potential in research or to mature as a professional.

I would also like to thank Dr. Robert P. Hoffman for providing clinical data collected from African-American and Caucasian youths, and for his comments on my journal manuscripts, and sincerely thank Dr. Alexandra Kautzky-Willer at Medical University of Vienna in Austria and Dr. Ele Ferrannini at University of Pisa School of Medicine in Italy for providing data from clinical trials involving oral glucose tolerance tests.

I also wish to thank all the members of the College of Pharmacy faculty and staff for their help during my research study. Specifically, I would like to thank the members of my comprehensive exam and dissertation defense committee, Dr. Fleckenstein, Dr. Murry, Dr. Fiegel, Dr. Rethwisch, and Dr. Flanagan for their direction, dedication and advice about this research. I also want to thank my former and current lab mates, Neeraj Gupta, Kevin Freise, Chih-Wei Lin, Matthew Rosebraugh, Mohammad Saleh, and Mohammed El-Komy.

Finally, a sincere thank to my parents for their encouragement, unconditional love and understanding.

## ABSTRACT

The development of type 2 diabetes over time involves defects in insulin action and insulin secretion. Defects in insulin action alone can be compensated with appropriate hyperinsulinemia. However, the progressive loss of pancreatic beta-cell function leads eventually to the development of persistent hyperglycemia that characterizes type 2 diabetes. Insulin secretion patterns reflect two phases when beta-cells are exposed to acute and sustained glucose stimulation. Through the study and understanding of the roles of these two phases in the regulation of glucose homeostasis, it is clear that insulin must not only be secreted in sufficient amounts, but also at the right time. In type 2 diabetes, the timing and magnitude of insulin secretion are altered, and an abnormal first-phase release initiates before the onset of the disease. Only a few pharmacokinetic/pharmacodynamic (PK/PD) models have considered the biphasic nature of insulin secretion. This study is aimed at describing the biphasic dynamics of insulin secretion through developing a PK/PD model based on current knowledge of the cellular mechanism of biphasic insulin secretion.

The objectives of this work are to 1) evaluate the insulin-glucose kinetics using nonparametric analysis, 2) develop a physiologically based mechanistic PK/PD model to dynamically describe the biphasic insulin secretion, 3) evaluate the impact of ethnicity on insulin secretion kinetics following an intravenous glucose administration using population analysis and 4) extend the proposed model to oral glucose administration and utilize the co-secretion kinetics of insulin and C-peptide in a population PK/PD analysis of the prehepatic insulin secretion.

Population analysis was done using a nonlinear mixed-effects model combined with the proposed PK/PD model to estimate population parameters and their variations between- and within-subjects and the covariates' effects on model parameters. The proposed model describes biphasic insulin behavior, accounts for first-phase insulin

secretion, and also applies to oral glucose administration for estimating prehepatic insulin secretion *in vivo* and in liver extraction. This is done by an analysis that simultaneously uses plasma insulin and C-peptide concentrations. A significantly higher first-phase insulin secretion was identified in healthy youths of African-American compared to Caucasians. The analysis showed no significant differences in the clearance of insulin from the plasma and the liver extraction of insulin between subjects with various levels of glucose tolerance. Obesity leads to a higher insulin production rate and lower elimination rate from the plasma than normal weight subjects. Also, type 2 diabetes and impaired glucose tolerance were found to reduce insulin production rate and resulted in a delayed insulin secretion from the beta-cells.

**TABLE OF CONTENTS**

## LIST OF TABLES

## LIST OF FIGURES

## LIST OF SYMBOLS AND ABBREVIATIONS

| | |
|---|---|
| AIC | Akaike information criteria |
| $AIR_g$ | Acute insulin response to glucose stimulation |
| BMI | Body mass index |
| AUC | Area under the curve |
| $C_G(t)$ | Plasma glucose concentration |
| $C_I(t)$ | Plasma insulin concentration |
| CP | C-peptide |
| $C_{P_1}(t)$ | C-peptide concentration in central compartment |
| $C_{P_2}(t)$ | C-peptide concentration in peripheral tissues |
| CrCl | creatinine clearance rate |
| CV | Coefficient of variation |
| CPSR(t) | C-peptide secretion rate from beta-cells |
| EGP(t) | Endogenous glucose production |
| EM | Expectation-maximization |
| FPG | Fasting plasma glucose |
| FSI | Fasting serum insulin |
| FSIVGTT | Frequently sampled intravenous glucose tolerance test |
| G(t) | Glucose mass |
| $HbA_{1c}$ | hemoglobin $A_{1c}$ |
| HOMA | Homeostatic model assessment |
| HOMA-IR | Insulin resistance measured by Homeostatic model assessment |
| HOMA-B | Beta-cell function measured by Homeostatic model assessment |
| I(t) | Insulin mass |

| | |
|---|---|
| IDR(t) | Insulin delivery rate |
| IGT | Impaired glucose tolerance |
| IM-IVGTT | Insulin modified intravenous glucose tolerance test |
| $I_R(t)$ | Reserved insulin pool |
| $I_{RR}(t)$ | Readily releasable insulin pool |
| ISR | Insulin secretion rate |
| IT2S | Iterative two-stage approach |
| IV | Intravenous |
| IVGTT | Intravenous glucose tolerance test |
| NLME | Nonlinear mixed-effects model |
| NPD | Naïve pooled data approach |
| NGT | Normal glucose tolerance |
| OGTT | Oral glucose tolerance test |
| PD | Pharmacodynamic |
| PK | Pharmacokinetic |
| RSE% | Relative standard error |
| SAEM | Stochastic approximation of expectation-maximization |
| SD | Standard deviation |
| SE | Standard error of the mean |
| STS | Standard two-stage approach |
| T1D | Type 1 diabetes |
| T2D | Type 2 diabetes |
| U | International unit |

# CHAPTER 1. INTRODUCTION

## 1.1 Background

Diabetes is a group of metabolic disorders characterized by chronic hyperglycemia which can lead to a dysfunction and damage of various organs, such as eyes, kidney, heart and nerves. It is one of the major public health threats in the United States. According to the Center for Disease Control (CDC) 2007 report (1), the prevalence of diabetes is 7.8% which equates to 23.6 million people who have diabetes. Furthermore, 25.9% of adults aged 20 years and older have prediabetes. The national cost of diabetes in 2007 is $174 billion. Type 1 diabetes (T1D) is characterized by the inability of the pancreas to produce insulin, thus insulin injections are required to survive. Type 2 diabetes (T2D) usually begins with insulin resistance, and subsequent inadequate insulin secretion. In adults, T2D accounts for about 90% to 95% of all diagnosed cases of diabetes.

For these reasons, early diagnosis and adequate treatment are important to decrease the long-term adverse effects of diabetes. Insulin resistance has been considered the major factor that contributes to the development of T2D. However, insulin resistance alone does not appear to be enough to cause diabetes. The development of overt diabetes is associated with a decline in beta-cell secretion. In patients with T2D or at the early stage of type 2 diabetes, the first-phase secretion is lost. In addition, recent evidence (2) found that defects in beta-cells' insulin secretion occurred earlier than previously understood. Therefore, reliable estimation of insulin secretion is required in understanding the pathogenesis of T2D.

The study of beta-cell secretory function can significantly benefit from PK/PD modeling because measuring insulin secretion from the pancreas is invasive and clinically impossible in human. The mechanism underlying the biphasic nature of insulin secretion is still not fully understood, but there have been new findings in recent years.

Population analysis is useful in detecting the impact of various covariates such as ethnicity, obesity, and glucose tolerance on insulin secretion. Thus, population analysis is valuable for a better understanding of the pathogenesis of diabetes.

### 1.2 Insulin

The discovery of insulin by Banting, Best, Macleod, and Collip in 1921 (3) changed the treatment of diabetes forever. Insulin is a small protein hormone with a molecular weight of 5800 Daltons and structured with 51 amino acids in two chains, the A and B chain, closely linked by two disulfide bonds (4). Insulin is produced by the beta-cells of the islets of Langerhans which are groups of tightly aggregated endocrine cells (such as the α-cell, β-cell, δ-cell and PP-cell) scattered throughout the pancreatic tissue (5). The biosynthetic cascade of insulin is outlined in Figure 1.1. Insulin is initially produced as a single-chain preproinsulin (6) and secreted to the endoplasmic reticulum. Within the endoplasmic reticulum, the signal sequence of preproinsulin is removed and the polypeptide is folded into proinsulin (7). Proinsulin is then converted to insulin by clipping a C-peptide (CP) segment that links the A and B chains during transportation from the endoplasmic reticulum to the Golgi apparatus (8-10). There are two normal cleavage sites indicated by the arrows in the Figure 1.1. Finally, the resulting insulin molecules along with the CP segments are packaged together into secretory granules for secretion or degradation.

### 1.3 Regulation of blood glucose between meals

Plasma glucose levels are maintained in a narrow range between 70 to 120 mg/dl in healthy individuals between meals. Tight control depends on the interplay between many hormones that regulate glucose production and disposal. Insulin is the primary hormone that lowers glucose concentrations, while glucagon produced by the alpha-cells of pancreas is the major hormone that counters insulin's effects. During the fasting state (Figure 1.2B), insulin concentrations are at the basal level and the low blood glucose

triggers the secretion of glucagon. Glucagon stimulates breakdown of glycogen into glucose via gluconeogenesis in the liver (11, 12). During the fed state (Figure 1.2A), consumption of carbohydrates increases glucose concentration in the blood. The rise in glucose stimulates the release of insulin from beta-cells and minimizes glucagon secretion. This promotes glucose uptake into liver- storing glucose as energy for later use and suppressing hepatic production of glucose. Insulin also stimulates glucose uptake into muscle and adipose tissues. In mammals, up to 75% of insulin-dependent glucose disposal occurs in skeletal muscle (13-15). Adipose tissue accounts for only a small fraction (5%-15%).

**1.4 Insulin clearance**

Insulin clearance includes hepatic extraction, peripheral utilization and degradation. Insulin is stored in beta-cells as secretory granules. Only a small amount of insulin granules undergo exocytosis, the majority is retained in the so-called intracellular storage pool (16, 17). The storage pool is not static and is replenished constantly. Young granules are preferentially released, while the granules that do not undergo exocytosis are ultimately degraded in the cell. The intracellular degradation is a slow process with an a estimated half-life of 3-5 days (18).

The elimination half-life of insulin from plasma is a brief 4-6 minutes, as would be expected in order to react rapidly to changes in glucose levels (19, 20). The liver and kidneys are the primary sites of insulin clearance. The liver removes approximately 50% of insulin released from the pancreas (21, 22), but the number varies widely under different physiological conditions (23, 24). The kidneys are the major sites that remove insulin from the systemic circulation, removing 50% of peripheral insulin (25-27) via glomerular filtration and degradation (26-28). It is reported that 99% of filtered insulin is reabsorbed by the proximal tubule cells (29) and then degraded. Relatively small amounts of insulin are excreted into the urine. The insulin not removed by the liver and kidneys is

cleared by other tissues. All insulin-sensitive cells are involved in clearance and degradation, but muscle accounts for the majority of insulin removal.

### 1.5 Biphasic insulin secretion

Insulin secretion shows a biphasic pattern (Figure 1.3) in healthy people when the pancreas is exposed to an abrupt and sustained rise in glucose, as observed in a glucose clamp test or intravenous gluocose tolerance test (IVGTT). The first-phase is defined by an early burst in insulin secretion within a few minutes, while the following second-phase develops gradually. The magnitude of both the first and second-phase is dose dependent. In addition, repeating the stimulus leads to a subsequent increase in insulin response (30) as shown in Figure 1.4. In the study of perfused rat pancreas in response to repeated stimulation by glucose in short intervals, the first-phase insulin response is not found. If longer time intervals are used, an augmentation of the first-phase insulin secretion is observed at the second stimulation. Thus, the magnitude of first-phase secretion is dependent on the pancreas' past history of glucose stimulation.

The first-phase is necessary for the maintenance of glucose homeostasis. The primary role of first-phase insulin secretion is to suppress hepatic glucose production quickly (31). The abolition of first-phase insulin secretion in normal subjects causes excessive postprandial glycemia (31, 32). The loss of first-phase secretion is quite common in both T1D (33-35) and T2D (36). A number of studies have shown that a reduction or a complete loss of the first-phase secretion is characteristic during the transformation from normal glucose to impaired glucose tolerance and eventually overt T2D. There are no distinct first-phase insulin secretions under normal physiological conditions, even after meals.

It has been found that 99% of insulin granules are secreted from beta-cells via regulated secretion (18), but the mechanism underlying biphasic exocytosis is not well understood. One main explanation suggests that biphasic secretion is related to the

existence of distinct insulin pools in the beta-cells in terms of the distance to the beta-cell membrane (16, 37, 38). The 'readily releasable' pool refers to insulin granules docked on the cell membrane that can be released directly in response to the stimulus, thus leading to first-phase secretion. Second-phase insulin secretion is derived from newly synthesized insulin granules within the cell. These granules need to translocate to the membrane before exocytosis. Recent investigations revealed that the first- and second-phase exocytosis are mechanistically different (39, 40). The evidence demonstrates docked insulin fuses with the membrane only at the site of a syntaxin 1A (Synt 1A) cluster during the first-phase, while the insulin released during the second-phase is independent of these Synt 1A clusters.

### 1.6 Assessment of insulin sensitivity, insulin resistance and beta-cell function

The liver plays a key role in glucose metabolism. Under the control of various hormones primarily insulin, the liver stores or releases glucose as needed by the whole body. The liver, skeletal muscles and adipose tissues are the three major insulin-sensitive organs involved in glucose homeostasis. Impairment of insulin sensitivity and beta-cell function are the two important components in the progression from glucose tolerance to T2D. Some common methods and indices used to evaluate insulin sensitivity through glucose metabolism include: glucose clamp tests, frequently sampled intravenous glucose tolerance test (FSIVGTT) with minimal model, fasting glucose, and insulin concentration.

**Insulin sensitivity** is the capacity of cells to process glucose in response to insulin, including peripheral glucose uptake and hepatic glucose output. Thus, insulin sensitivity has two aspects, but it is most frequently used to refer to glucose uptake by peripheral tissues.

**Insulin resistance** is the reciprocal concept of insulin sensitivity, which is defined by the condition that insulin works less effectively at lowering blood glucose.

**Beta-cell function** refers to the insulin secretory capacity of beta-cells. Beta-cell dysfunction is the major feature of impaired glucose tolerance and T2D.

### *1.6.1 Glucose clamp technique*

The glucose clamp technique is a method for assessing insulin sensitivity and insulin resistance. Two types of glucose clamps commonly used are the euglycemic hyperinsulinemic clamp (41) for insulin sensitivity and hyperglycemic clamp for the assessment of beta-cell function.

In the euglycemic hyperinsulinemic test, a hyperinsulinemic plateau is created by a constant exogenous insulin infusion, while blood glucose is 'clamped' to a desired level (e.g. 5 mmol/l) by infusing glucose at an adjustable rate. Under the condition of insulin infusion, hepatic glucose output is suppressed. Once steady state is reached, glucose metabolic rate is equal to glucose infusion rate. In particular, insulin sensitivity is directly related to the mean glucose infusion rate (*M*) and insulin resistance is inversely related to M. The index (*M/I*) of insulin sensitivity is calculated by dividing M with insulin concentration (*I*) at the steady state. The euglycemic clamp has shown good reproducibility (42, 43) and is commonly accepted as the gold standard for measuring insulin sensitivity *in vivo*. However, the test remains time-consuming, costly and labor-intensive.

The insulin secretory capacity of beta-cells can be evaluated by the hyperglycemic clamp test. Biphasic insulin secretion is induced by initiating a glucose bolus to quickly raise glucose concentration and then a continuous glucose infusion is started to maintain a desired elevated glucose concentration. The index ($AIR_g$) for first-phase secretion is usually calculated as the area under the curve of insulin concentration over the basal level in the first 10 minutes, while the mean insulin concentration of last the 20-30 minutes (44, 45) of the clamp test is often used as the index of second-phase secretion.

The hyperglycemic clamp test can also be used to estimate insulin sensitivity, but the resulting index is not as reliable as the euglycemic clamp test since glucose disposal becomes glucose dependent at higher glucose levels (46).

### *1.6.2 HOMA model assessment*

Homeostatic model assessment (HOMA) (47) is a method that can estimate insulin resistance and beta-cell function from fasting glucose and insulin concentrations. It is derived from a mathematical model (48) that describes the interaction between beta-cell function and insulin resistance to give predictions of basal insulin and glucose concentration. An approximation of the solution of the mathematical model is given as:

$$HOMA-IR = G_b \times I_b / 22.5 \qquad \text{Eq. 1.1}$$

$$HOMA-\%B = 20 \times I_b / (G_b - 3.5) \qquad \text{Eq. 1.2}$$

where $G_b$ and $I_b$ are fasting glucose and insulin concentrations in mmol/l and μU/ml, respectively; HOMA-IR is an index of insulin resistance and has a value of 1 or 100% for normal basal glucose and insulin concentration.

The HOMA approach only requires fasting insulin and glucose concentration, thus can be useful in epidemiological studies. It should be recognized that the results from HOMA may disagree with other methods, for example the index estimated from glucose clamp test (49-51).

### *1.6.3 Intravenous glucose tolerance test*

A widely acceptable alternative for estimation of insulin sensitivity is the minimal model analysis of frequently sampled intravenous glucose tolerance test (FSIVGTT) (52-56). An IV bolus of glucose infusion is administered over a short time period, for example 1 minute. Then, blood samples are collected at frequent intervals to measure plasma insulin and glucose levels. By modeling glucose disposal, the model allows for estimation of the insulin sensitivity index ($S_I$) through curve-fitting (see Chapter 2.1.1 for

details). The minimal model of insulin sensitivity has been validated in many studies compared to the clamp technique (57-59). However, a problem arises when a subject, such as a diabetes patient, has insufficient endogenous insulin secretion for glucose disposal. For example, the $S_I$ value could be negative for a subject with diabetes. For this reason, insulin-modified IVGTT (IM-IVGTT, an insulin infusion between 20-25 minutes for instance) has been developed to provide a more meaningful and general estimation of insulin sensitivity (60, 61). Compared to the glucose clamp test for the estimation of insulin sensitivity, the minimal model method is experimentally simple, but requires a more complex analysis.

The intravenous glucose tolerance test (IVGTT) triggers biphasic insulin secretion in which one or two peaks are observed in the insulin concentration profile. The common index for first-phase insulin secretion during IVGTT is called 'acute insulin response to glucose' (*AIRg*). *AIRg* is calculated as the area under the curve (*AUC*) above the basal level of insulin or C-peptide concentration time course during the first peak (54), such as from 0 to 10 minutes. Mathematical models of insulin secretion in IVGTT (often FSIVGTT protocol is used) have been developed and provide indices to describe beta-cell sensitivity to glucose in the first-phase and second-phase (see Chapter 2.2.1 for details).

### *1.6.4 Oral glucose tolerance test*

OGTT is a simple procedure in clinical practice to evaluate glucose tolerance. After overnight fast, a standard glucose load (75g) is taken orally by the subject, the status of glucose tolerance is then determined according to the glucose concentration at a specific time, for example 120 minute. OGTT reflects the efficiency of the body to dispose of glucose after an oral load. It mimics physiological conditions of glucose and insulin responses more closely than conditions of the glucose clamp and IVGTT. In addition, OGTT also represents a metabolic test which reflects insulin sensitivity and

beta-cell function. Several empirical indices from OGTT have been proposed, taking into account both fasting and dynamic post-glucose load plasma glucose and insulin levels, such as Matsuda index, Stumvoll index, and Gutt index.

**Matsuda index** is an insulin sensitivity index derived by DeFronzo and Matsuda in 1999 (62). It is an overall reflection of hepatic and muscle sensitivity to insulin and expressed as**:**

$$ISI_{Matsuda} = \frac{10{,}000}{\sqrt{G_b I_b G_m I_m}} \qquad \text{Eq. 1.3}$$

where $G_b$ (mg/dl) and $I_b$ (mU/l) are fasting basal plasma glucose and insulin concentrations, respectively; $G_m$ and $I_m$ are mean concentrations of glucose and insulin during the entair OGTT and 10,000 is a scaling factor. The fasting baseline reflects hepatic insulin sensitivity, whereas the mean of the dynamic data primarily represents skeletal muscle's insulin sensitivity. $ISI_{Matsuda}$ correlates reasonably well with estimates of the whole body insulin sensitivity determined by the glucose clamp (62, 63).

Abdul-Ghani and colleagues (64) demonstrated that the insulin secretion/insulin resistance index (disposition) was a reliable predictor of T2D onset under the following conditions: when the insulin sensitivity is calculated as $ISI_{Matsuda}$, and when the insulin secretion index is calculated by dividing the increment in plasma insulin at 30 min ( $\Delta I_{0-30}$ ) by the increment in plasma glucose at 30 min ( $\Delta G_{0-30}$ ) of OGTT ( $\Delta I_{0-30} / \Delta G_{0-30}$ ).

**Gutt index** of insulin sensitivity ($ISI_{0,120}$) is derived based on the plasma glucose and serum insulin concentrations at time 0 and 120 min during OGTT (65). The $ISI_{0,120}$ is defined as:

$$ISI_{0,120} = \frac{MCR}{\log(MSI)} \qquad \text{Eq. 1.4}$$

$$MCR = \frac{m}{MPG} \qquad \text{Eq. 1.5}$$

where *MCR* is the metabolic clearance rate calculated by Eq. 1.5; *MSI* is the mean serum insulin concentration (mU/l) obtained at time 0 and 120 min of OGTT; *MPG* is the mean plasma glucose calculated from the mean of plasma glucose concentrations at time 0 ($G_0$) and 120 min ($G_{120}$); and *m* is the glucose uptake rate in peripheral tissues in the unit of mg/min calculated by Eq. 1.6:

$$m = \frac{75000 + (G_0 - G_{120}) \times 0.19\ BW}{120} \qquad \text{Eq. 1.6}$$

where 0.19 is a glucose distribution space (1) normalized according to body weight and *BW* is the body weight in kg.

The $ISI_{0,120}$ correlates well with the estimates obtained from the euglycemic clamp and is thought to be superior to the HOMA method (65-67).

**Stumvoll index** of insulin sensitivity ($ISI_{est}$) (68) is derived from BMI, and plasma insulin and glucose concentrations obtained during an OGTT. It is calculated as:

$$ISI_{est} = 0.226 - 0.0032\ BMI - 0.0000645\ I_{120} - 0.0037\ G_{90} \qquad \text{Eq. 1.7}$$

where *BMI* (kg/m$^2$) is body mass index and $I_{120}$ is plasma insulin concentration (pmol/l) at 120 min and $G_{90}$ is plasma glucose concentration (mmol/l) at 90 min. The units of $ISI_{est}$ are $\mu mol \cdot kg^{-1} \cdot min^{-1} \cdot pM^{-1}$. According to the Stumvoll *et al.*, this empirical index highly correlates with measured insulin sensitivity form euglycemic hyperinsulinemic clamp values in 104 health subjects

**Insulinogenic index** of insulin secretion. Insulin secretion following oral glucose administration is a more complicated process to analyze than the response to IV glucose stimulation because responding gut hormones exaggerate insulin secretion from the beta-cells. Also, it is difficult to determine the exact amount of glucose taken by the body after oral glucose administration due to unknown bioavailability. The most common empirical index is insulinogenic index (*IGI*) (69) which is calculated as the change in insulin

response relative to the change in glucose stimulus over the first 30 min period according to the following equation:

$$IGI = \frac{I_{30} - I_0}{G_{30} - G_0} \quad \text{Eq. 1.8}$$

Serum insulin (pmol/l) and plasma glucose concentrations (mmol/l) at 30 minutes after glucose intake in Eq. 1.6 can be replaced with concentrations at 15 minutes or other period of time in literatures (69, 70). The index *IGI* reflects the integrated beta-cell response to glucose and glucose-dependent gut hormones. However, it does not reflect specific mechanisms of insulin secretion, such as first-phase insulin secretion.

**Stumvoll index** of insulin secretion. Beta-cell function as reflected by first-phase and second-phase during OGTT can be empirically assessed by the 0 and 30 min plasma insulin levels and 30 min plasma glucose level. The parameters, $PH_1$ and $PH_2$, represent insulin index (68) for first- and second-phase, respectively, and are described as:

$$PH_1 = 1283 + 1.829\ I_{30} - 138.7\ G_{30} + 3.772\ I_0 \quad \text{Eq. 1.9}$$

$$PH_2 = 287 + 0.4164\ I_{30} - 26.07\ G_{30} + 0.9226\ I_0 \quad \text{Eq. 1.10}$$

$PH_1$ and $PH_2$ show reasonable accuracy relative to the hyperglycaemic clamp method and appear better than other commonly used simple approaches (68).

These empirical indices of insulin sensitivity and beta-cell function from the OGTT can be easily implemented in epidemiological studies, large clinical trials, and clinical research investigations.

### *1.6.5 C-peptide based analysis*

Simple measurement of insulin plasma concentration is still used as an indication for the assessment of beta-cell secretory function in many studies. However, a drawback is that plasma insulin concentration inaccurately reflects pancreatic insulin secretion because insulin experiences first-pass metabolism before insulin's entrance into the systemic blood circulation. Pancreatic insulin secretion rates may be directly measured by

inserting catheters into the artery and vein, but this technique is invasive and not practical in a clinical research setting.

To avoid the problem of hepatic extraction, an alternative approach is to make use of C-peptide (CP) concentrations. CP is secreted with insulin in equimolar amounts (71-73) and, unlike insulin, is not extracted by the liver (74-76). Furthermore, the clearance of CP (exclusively through the kidneys) is nearly constant over a wide range of CP concentrations (77, 78). These characteristics make CP a suitable marker for insulin secretion. Plasma or serum CP levels are normally utilized for evaluation of insulin secretion under steady state conditions. However, the dynamic secretion profiles of insulin and CP are not equivalent because CP has a longer half-life, approximately 30 minutes (77), relative to the half-life of insulin (4 minutes). Since plasma CP concentrations do not change proportionally to the changes in the pancreatic insulin secretion rate, this approach has limitations under dynamic conditions. Rather, the deconvolution technique and mathematical modeling with CP disposition kinetics (see Chapter 2) can provide a more precise estimation and assessment of insulin secretion under dynamic conditions.

### *1.6.6 Deconvolution analysis*

Deconvolution as a mathematical operation was introduced to reconstruct insulin secretion profile from CP concentration by Eaton *et al.* (79). This approach is currently one of the most common methods for quantifying insulin secretion.

C-peptide disposition is thought to be linear within a wide range of concentrations, thus the plasma CP concentration, $C_P(t)$, can be calculated in terms of the dynamics of insulin secretion rate, $ISR(t)$, by the convolution integral:

$$C_P(t) = \int h(t-\tau) ISR(\tau) d\tau \qquad \text{Eq. 1.7}$$

where *ISR(t)* is the unknown endogenous insulin secretion rate, and *h(t)* is the plasma response to a unit impulse. The *ISR(t)* therefore can be estimated by deconvolution approach. To perform deconvolution, *h(t)* must be known. A two-compartment model is commonly used to represent *h(t)* in the deconvolution of insulin secretion rate. In the original approach proposed by Eaton et al, the CP kinetics is determined by a bolus injection of biosynthetic CP in each individual and fitting a two-compartment model to determine *h(t)*. In a later study (80), the deconvolution technique has been simplified by developing a method to approximated the individual *h(t)* using a population-based regression model instead of individual estimation. The deconvolution technique is valuable in reconstructing beta-cell insulin secretion and not limited to specific glucose administration routes.

In summary, several methods and protocols are available for the evaluation of insulin sensitivity and beta-cell function, each with its own advantages and limitations. The euglycemic clamp method is the gold standard for insulin sensitivity estimation although it is laborious, expensive, and not suitable for large scale studies. The HOMA method is simple and can be used for population studies, but only reflects steady-state glucose-insulin interactions. The evaluation of beta-cell function is complicated because beta-cells are able to adapt to insulin resistance and maintain normal glucose tolerance (81-83).

### 1.7 Type 2 diabetes and insulin resistance

The criteria for abnormal glucose tolerance are shown in Figure 1.5. Diagnostic criteria of diabetes include: fasting plasma glucose (FPG) be greater or equal to 126 mg/dl (7.0 mmol/l) or plasma glucose 2 hours after a 75g OGTT be greater or equal to 200 mg/dl (11.1 mmol/l). Fasting glucose is preferred as the diagnostic test for diabetes because of its simplicity and convenience. If fasting glucose concentration is in the diabetic range, an OGTT is not required for confirmation. On the other hand, if a subject

has an elevated fasting glucose level, but below the diagnostic range, an OGTT is needed on a subsequent day to confirm or exclude diabetes or impaired glucose tolerance (IGT).

The majority of diabetes cases fall into two distinct categories, type 1 diabetes (T1D) and type 2 diabetes (T2D). T1D is normally defined by the pancreas not producing enough insulin due to autoimmune-destruction of beta-cells (84), thus patients with T1D need exogenous insulin treatment for survival. T2D is the most common form of diabetes, however, specific etiology of this form has not been clearly defined. It is known that destruction of beta-cells does not occur and both insulin resistance and relative insulin deficiency arise in T2D. T2D patients do not need insulin treatment to survive, although ultimately many patients rely on it for optimal glycemic control.

Insulin resistance is seen in the early prediabetic stage in a majority of T2D patients and is a good clinical predictor of subsequent development of T2D (85). When insulin resistance exists, the muscle, fat, and liver cells do not respond properly to insulin. However, the development of diabetes appears to involve an additional defect in insulin secretion. In the absence of a defect in beta-cell function, individuals can compensate for insulin resistance with appropriate hyperinsulinemia (Figure 1.6). Hence, many individuals with marked insulin resistance may never progress to T2D. Insulin resistance is associated with abnormal conditions in a variety of tissue functions and metabolic processes of the body (86, 87), such as cardiovascular disease, high blood pressure, and abnormal levels of cholesterol and triglycerides. Having conditions such as these increases the risk of developing T2D.

Obesity has been strongly associated with insulin resistance in individuals with normal glucose tolerance as well as patients with T2D (85). This association is not only related to the degree of obesity, but is also dependent particularly on body fat distribution. Individuals with greater degrees of central adiposity (belly fat) are more resistant to the actions of insulin than those with peripheral body fat (88). There is evidence that increased production of proinflammatory cytokines, non-esterified fatty

acids (NEFAs), glycerol, and other factors from adipose tissues may cause insulin resistance and contribute to development of T2D (89, 90). Insulin resistance can also be caused by genetics (91) and environmental factors. Some people may inherit from their parents a disposition toward insulin resistance. A variety of environmental factors such as viruses, stress, traumas, illnesses, and pregnancy have shown some influence on insulin resistance.

### 1.8 Motivations of the thesis

T2D has 7.2% prevalence and 25.9% adults have prediabetes in USA. Long-term effects of T2D include heart disease, nerve damage, blindness and kidney disease. Early diagnosis is thus important in the prevention of long-term adverse effect of T2D. Defect in first-phase insulin secretion can be a clinical predictor of T2D, which starts long before the development of T2D. Therefore, reliable estimation of insulin release is crucial in understanding the development of T2D. PK/PD modeling provides a potential alternative for the assesment of beta-cell secretory function because direct measurement of insulin secretion is difficult; it needs to insert catherters into hepatic vein and artery. In this thesis, a novel mechanism-based PK/PD model will be proposed for quantifying insulin secretion, particularly the biphasic behavior of insulin secretion. We hope this model can help us to better understand biphasic insulin secretion and the prevention of T2D.

### 1.9 Objectives and specific aims

The main objective of this work is to develop a mechanistic PK/PD model that can characterize insulin secretion in response to glucose stimulation for better understanding the development of type 2 diabetes.

Specific aim 1: To determine the differences in insulin secretion response after an IV glucose stimulation between African-American and Caucasian youths using a noncompartmental approach.

Specific aim 2: To formulate a novel physiologically based mechanistic PK/PD model aimed at dynamically evaluating the biphasic insulin secretion.

Specific aim 3: To evaluate the impact of ethnicity on insulin secretion kinetics using a population modeling approach.

Specific aim 4: To extend the proposed model for oral glucose administration by making use of the co-secretion kinetics of insulin and glucose and to identify covariates' effects on prehepatic insulin secretion using a population approach.

**1.10 Hypotheses**

The central hypothesis of this work is that insulin secretion in response to elevated blood concentrations of glucose can be described and characterized by a PK/PD model.

Hypothesis 1: Quantifiable differences in insulin secretion response to glucose challenge exist between African-American and Caucasians youths.

Hypothesis 2: The plasma insulin concentrations after glucose challenge can be accurately described using a PK/PD model based on the cellular mechanism of biphasic insulin secretion.

Hypothesis 3: The proposed model is able to identify kinetic parameters that cause the differences in insulin secretion response to IV glucose stimulation between African-American and Caucasian youth using population analysis.

Hypothesis 4: The proposed model can simultaneously characterize the insulin and C-peptide secretion responses to an oral glucose load and thus evaluate prehepatic insulin secretion.

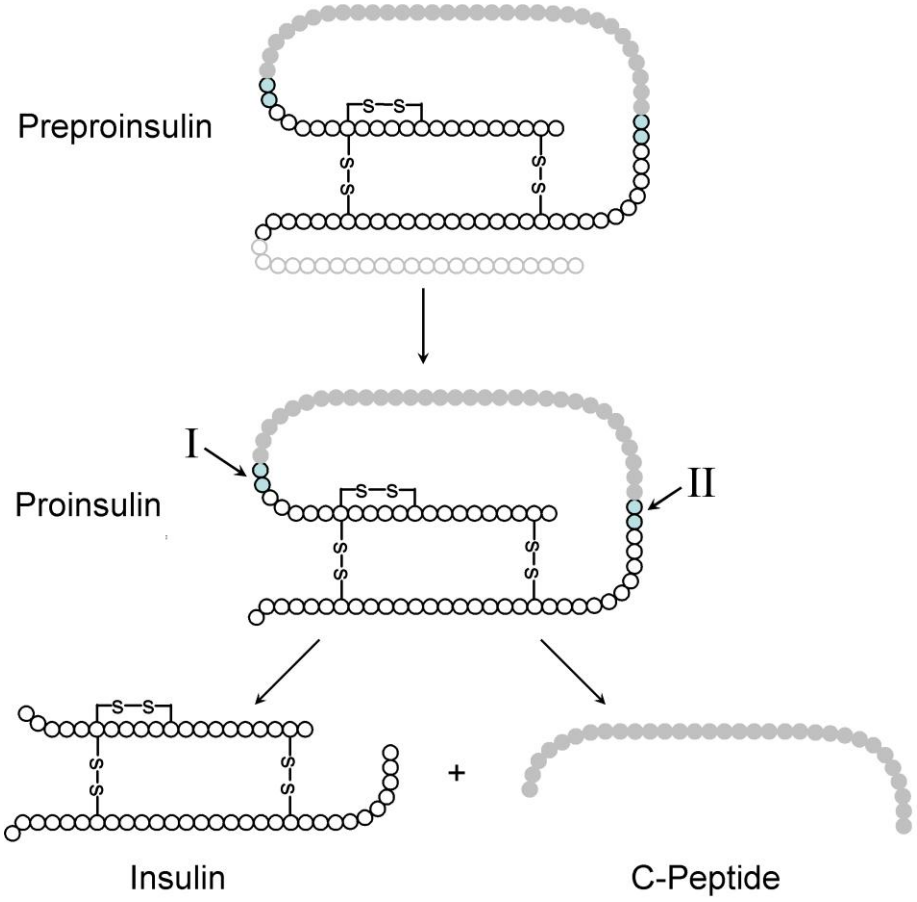


Figure 1.1. Conversion of preproinsulin to insulin.

Insulin production involves several intermediate steps. Initially, preproinsulin is secreted into the endoplasmaic reticulum. Then its N-terminal signal sequence is removed during a post-translational process to form proinsulin. Subsequently, the proinsulin is clipped at two positions (I and II) to release the C-peptide. C-peptide and active insulin are finally packaged into secretory granules for storage.

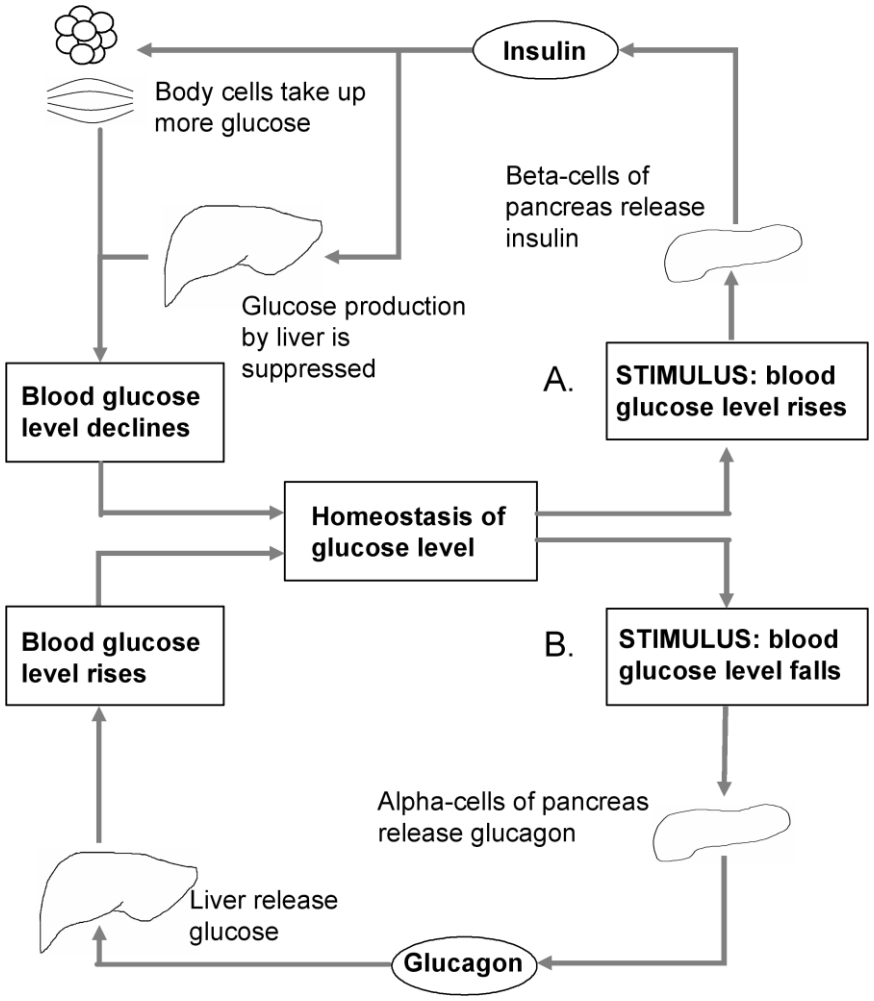


Figure 1.2. Glucose homeostasis between meals.

A: Feeding state. A rise in blood glucose stimulates the release of insulin from beta-cells, causing glucose uptake by body cells, such as fat and muscle, and suppression in glucose production by liver.
B: Fasting state. A fall in blood glucose stimulates alpha-cell of pancreas to secrete glucagons, promoting liver to release glucose.

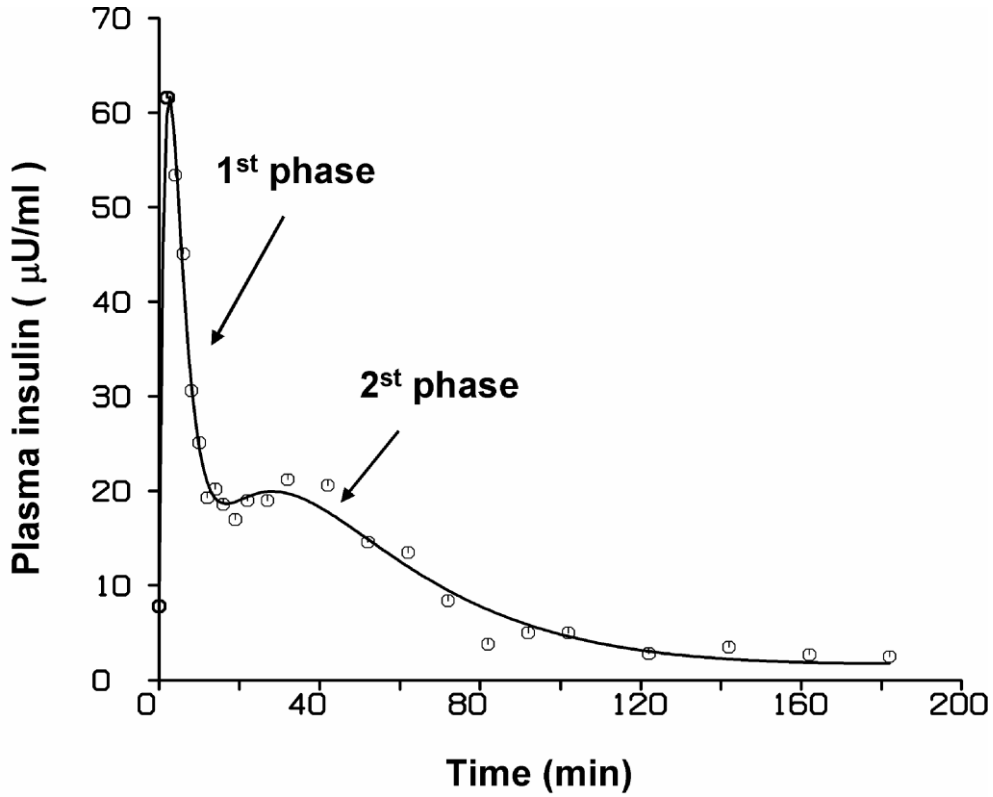


Figure 1.3. Biphasic insulin response to intravenous glucose administration in a healthy subject.

Circles indicate observed insulin plasma concentrations and the solid line is the predictions estimated by the proposed model in the Chapter 4. The first-phase is the period from 0 to 20 minutes and the second-phase is from 20 minute to the end of the test.

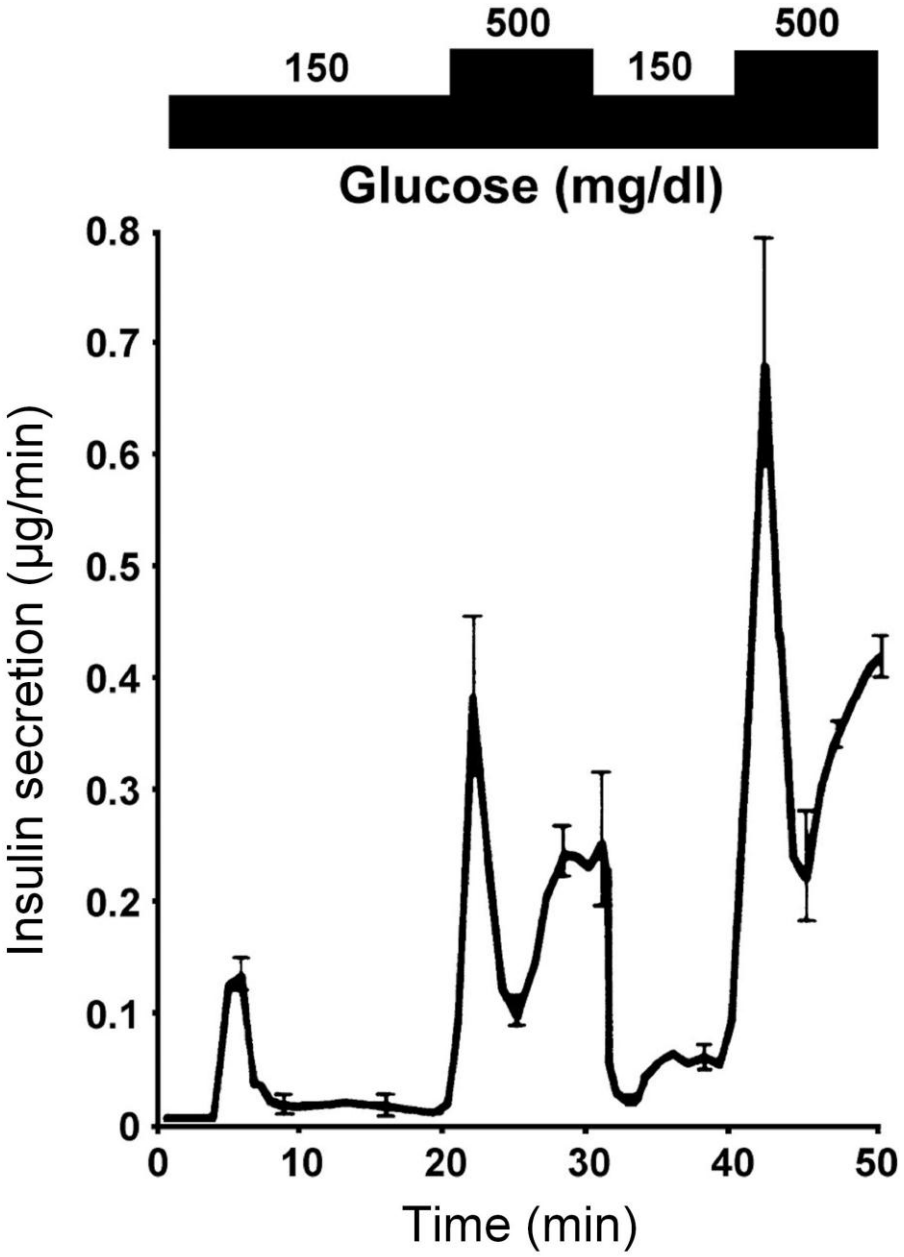


Figure 1.4. Insulin secretion in perfused rat pancreas in response to square wave of glucose stimulations.

Plotted from O'Connor *et al.* (30)

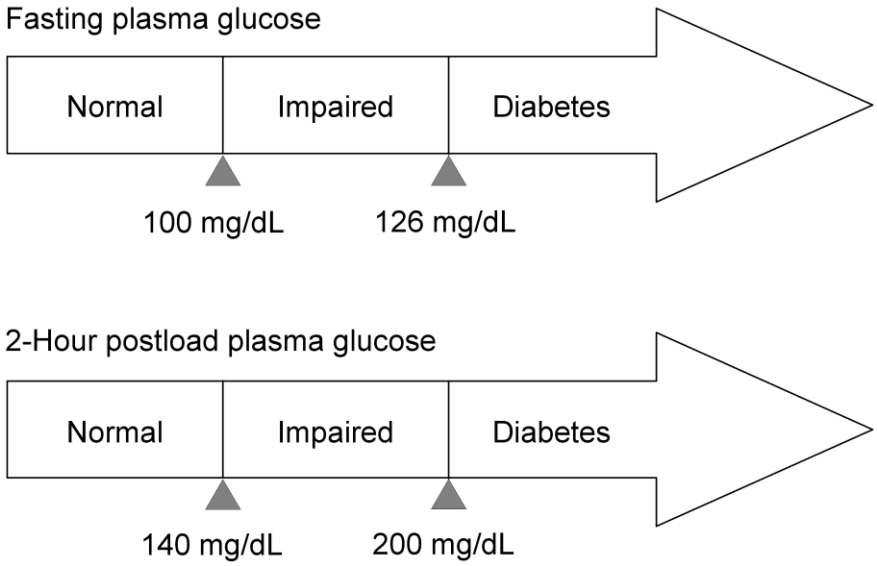


Figure 1.5. Diagnostic criteria for diabetes and related stages of glycemia

The criteria for abnormal glucoe tolerance can be classified based on fasting plasma glucose and 2-hour postload plasma glucose of a 75g oral glucose tolerance test (OGTT). Diabetes is diagnosed when fasting plasma glucose is greater or equal to 126 mg/dl or plasma glucose 2 hours after an OGTT is greater or equal to 200 mg/dl. Impaired glucose tolerance is defined as having fasting plasma glucose level of at least 100 mg/dl or 2-hour postload plasma glucose level of at least 140 mg/dl.

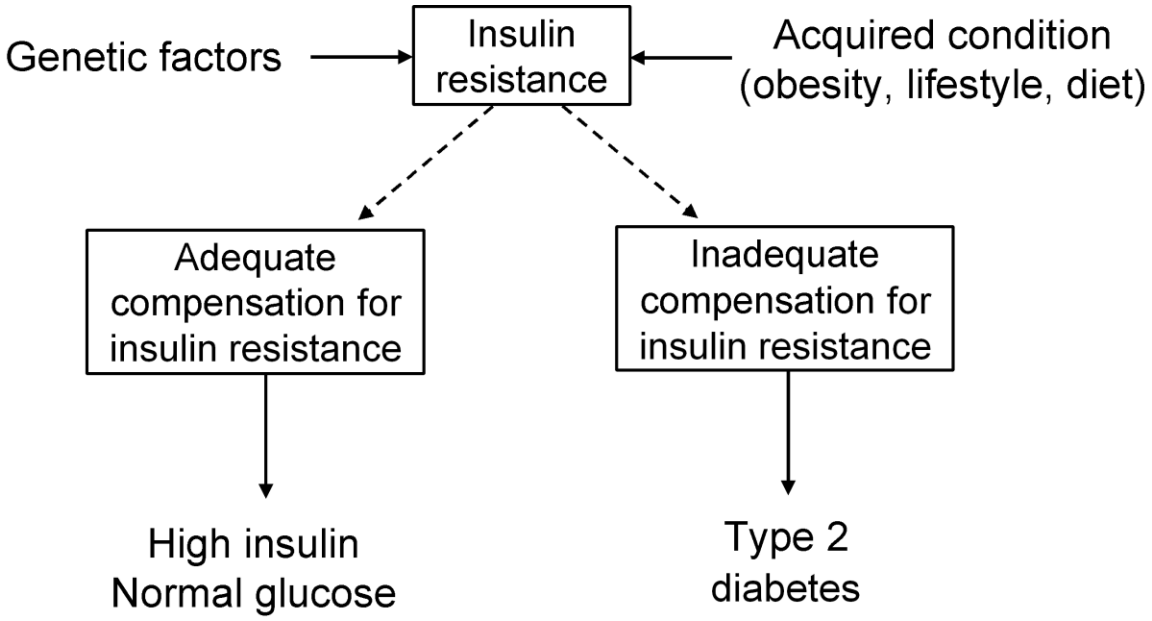


Figure 1.6. Pathophysiology for type 2 diabetes: insulin resistance and decreased insulin secretion.

Insulin resistance is seen in the early prediabetic stage in a majority of type 2 diabetes (T2D). It is defined by the condition that insulin works less effectively at lowein blood glucose. In the absence of a defect in beta-cell function, individuals can compensate for insulin resistance with appropriate hyperinsulinemia and normal glucose level. When beta-cells fail to compensate insulin resistance, blood glucose concentration rises and T2D is developed.

# CHAPTER 2. PK/PD MODELING GLUCOSE METABOLISM AND INSULIN SECRETION

Diabetes has been an increasing public health problem in many countries since the 20th century. Numerous mechanistic (pharmacokinetic/pharmacokinetic) PK/PD models have been developed for the study of the glucose-insulin system. This chapter reviews and discusses the recent advances in the PK/PD modeling of glucose-insulin system, and mainly focuses on modeling methods rather than model applications to specific problems. Particular emphasis is given to 1) assessment of insulin sensitivity, 2) insulin secretion and 3) insulin-glucose feedback and disease progression.

One of the key characteristics of the glucose-insulin system is the feedback loop between glucose and insulin. An increase in glucose concentration stimulates production of insulin, and insulin in turn stimulates disappearance of glucose and suppresses the hepatic glucose production. The hyperglycemia in type 2 diabetes (T2D) can be caused by decreased uptake of glucose into skeletal muscles (peripheral insulin resistance), increased hepatic glucose production (hepatic insulin resistance) and decreased insulin secretion (loss of beta-cell function).

Most of the earlier models were developed as alternatives to evaluate insulin sensitivity *in vivo* without the need of performing the complex glucose clamp test. Among them, the minimal model (56), applied to the intravenous glucose tolerance test (IVGTT), originally published in 1979 is the most commonly used research model. The minimal model is relatively simple and describes glucose disposal with a single compartment and an insulin compartment for insulin's regulation of the glucose clearancel. The minimal model yields indices for the evaluation of the effects of both glucose and insulin on glucose disposal. The major limitations of the model are that it can not distinguish between peripheral insulin sensitivity and hepatic insulin sensitivity. Numerous extensions and variants of the minimal model have been proposed to

overcome its limitation, including the use of a two-compartment model (92) for glucose kinetics, the application of hot glucose IVGTT (93, 94) to determine hepatic insulin sensitivity, and inclusion of more elaborate control mechanisms of glucose clearance.

As T2D is also characterized by a decrease in insulin secretion, it is essential to evaluate the beta-cell's secretory ability. Models have thus been developed to describe the relationship between glucose-stimulated beta-cell function and hepatic insulin secretion. A single compartment model (55) has been proposed to describe insulin kinetics and assess beta-cell function in response to the IVGTT, but it seems the single compartment does not represent insulin's biphasic time course accurately. The prehepatic insulin secretion rate can be estimated by analyzing plasma C-peptide (CP) concentrations because CP and insulin are secreted in equimolar amounts and CP is not extracted by the liver (76, 79, 95). In the combined model (96), the co-secretion kinetics of insulin and CP are used to simultaneously describe insulin and CP time courses and calculate hepatic extraction. The model developed by Gupta et al (97) has the advantage of being based on the physiological process of biphasic insulin release. It is aimed at early detection of the prediabetic condition. In order to more accurately represent insulin secretion, a model with incorporating a delay-compartment mechanism (98) has been proposed.

Other types of models (99-102) described in this chapter explore the glucose-insulin feedback relationship and disease progression. More mechanistic models have been developed with the goal of being able to improve early diagnosis of diabetes or prediabetes and provide further insights into the glucose-insulin system. Disease progression analysis of T2D is a new area of PK/PD analysis. The disease progression model is important in the evaluation of an antidiabetic drug's effect on disease progression.

## 2.1 Modeling of insulin sensitivity

Diabetes is a major health concern in many countries. For this reason, understanding the etiology of diabetes as well as early diagnosis has been of major research interest in the past decades. Most of the earlier studies have focused on the assessment of insulin sensitivity. Although, the glucose clamp tests can be used to experimentally determine insulin sensitivity, these methods require extensive experimental manipulation and carry risks to patients due to administration of glucose via intravenous infusion. Therefore, model-based methods for insulin sensitivity have been developed to provide suitable alternatives.

The most widely used model for the assessment of insulin sensitivity is the minimal model (55, 56) originally developed by Bergman *et al.* By analyzing the data from IVGTT, the minimal model provides estimates of insulin sensitivity ($S_I$) and glucose effectiveness ($S_G$) without the need to perform a complex glucose clamp procedure. The main problem of the original minimal model is it does not represent glucose systems very well, thus indices extracted from the model are inaccurate in certain situations, such as biased estimates of $S_I$ and $S_G$ in patients with T2D. It has been suggested that the inaccuracy is caused by oversimplification of glucose kinetics with a single compartment model and/or a poor description of the control of insulin and glucose on glucose disposal. Some models with two-compartments (92, 94) for glucose kinetics have been developed to improve the estimation of model-derived $S_I$ and $S_G$. Labeled glucose in the IVGTT (93, 103) can be used to differentiate insulin sensitivity between peripheral tissues and the liver. This approach is able to determine only the peripheral tissues' responses to increased glucose ($S_G$) and insulin ($S_I$) because the tracer's kinetics are not influenced by hepatic glucose production. Studies with a tracer-based IVGTT have demonstrated this method allows for precise estimation of $S_I$ and $S_G$ (103).

### *2.1.1 Minimal model of glucose disappearance*

The minimal model coupled with the intravenous glucose tolerance test (IVGTT) provides characteristic parameters for insulin sensitivity. Insulin's functions include two aspects: targeting peripheral tissues to increase uptake of glucose and acting on the liver to suppress glucose production. The original minimal model (Figure 2.1) proposed by Bergman *et al.* (56) describes insulin kinetics with a single compartment and consider physiological control processes by introducing a remote insulin compartment, $I_r$. By way of the $I_r$, insulin promotes glucose disappearance into peripheral tissues and the liver, and inhibits glucose production by liver. The utilization rate of glucose by peripheral tissues, $R_P(t)$, is split into insulin-independent and insulin-dependent components described as:

$$R_p(t) = k_1 C_G(t) + k_4 I_r(t) C_G(t) \qquad \text{Eq. 2.1}$$

where $k_1$ is a rate constant related to the insulin-independent disposal process and $k_4$ is a rate constant related to the insulin-dependent glucose disposal process through peripheral tissues.

The liver is the major site of releasing glucose to the blood. The minimal model also describes the production of glucose as insulin-dependent and independent. When insulin level is increased during the IVGTT, the release of glucose is suppressed and the net output of glucose from the liver, $R_L(t)$, is modeled as:

$$R_L(t) = B_0 - [k_5 C_G(t) + k_6 I_r(t) C_G(t)] \qquad \text{Eq. 2.2}$$

where $B_0$ is the net hepatic output when plasma glucose concentration is zero, $k_5$ is insulin-independent rate constant and $k_6$ is a rate constant associated with insulin-dependent hepatic glucose production.

A single compartment is used for the glucose kinetics. Therefore, the rate change in plasma glucose is described as:

Eq. 2.3

In this equation, $C_G(t)$ is the plasma glucose concentration and $C_{G_b}$ is the basal plasma glucose level. During the IVGTT, insulin enters the remote compartment and the rate change of insulin in the remote compartment is:

$$\frac{dI_r(t)}{dt} = k_2[C_I(t) - C_{I_b}] - k_3 I_r(t) \qquad I_r(0) = 0 \qquad \text{Eq. 2.4}$$

where $C_I(t)$ is plasma insulin concentration, $C_{I_b}$ is the basal plasma insulin concentration and $k_2$ and $k_3$ are rate constant. It is impossible to identify the parameters $k_1$, $k_5$ , $k_4$ and $k_6$ simultaneously, thus the above equations for the kinetics of glucose and insulin need to be reparameterized as below:

$$\frac{dC_G(t)}{dt} = (p_1 - X(t))C_G(t) + p_4 \qquad \text{Eq. 2.5}$$

$$\frac{dX}{dt} = p_2 X(t) + p_3 C_I(t) \qquad X(0) = 0 \qquad \text{Eq. 2.6}$$

In which,

$$X(t) = (k_4 + k_6) I_r(t) \qquad \text{Eq. 2.7}$$

$$p_1 = -(k_1 + k_5) \qquad \text{Eq. 2.8}$$

$$p_2 = -k_3 \qquad \text{Eq. 2.9}$$

$$p_3 = k_2(k_4 + k_6) \qquad \text{Eq. 2.10}$$

$$p_4 = B_0 \qquad \text{Eq. 2.11}$$

At the basal steady state Eq. 2.5 and Eq. 2.6 are equal to zero, and $p_4$ is equal to:

$$p_4 = p_1 C_{G_b} \qquad \text{Eq. 2.12}$$

The model uses insulin concentrations as a forcing function. Interpolations are required to obtain glucose concentrations for estimation of the parameters. The model defines glucose effectiveness ($E$) as the enhancement of glucose disappearance due to an increase in the plasma glucose concentration:

$$E \equiv \frac{\partial[dC_G(t)/dt]}{\partial C_G(t)} \qquad \text{Eq. 2.13}$$

Two indices for assessment of insulin sensitivity ($S_I$) and glucose effectives ($S_G$,) are then derived at the steady state:

$$S_I \equiv \left.\frac{\partial E}{\partial C_I(t)}\right|_{SS} = p_1 \qquad \text{Eq. 2.14}$$

$$S_G \equiv E_{SS} = \frac{p_3}{p_2} \qquad \text{Eq. 2.15}$$

The minimal model estimate of insulin sensitivity ($S_I$) has been validated in many studies versus the glucose clamp tests and is the currently used method in research on glucose tolerance. The minimal model method requires less experimental expertise compared to glucose clamp techniques. The $S_I$ reflects the entire body's (peripheral tissues and the liver) sensitivity to insulin. An injection of labeled glucose during the IVGTT is a way to estimate peripheral sensitivity to glucose. The effect of glucose ($S_G$) itself, aside from the circulating insulin level and the sensitivity of tissues to insulin, is also an important factor that can affect glucose levels (104). However, controversy exists in regards to the accuracy of $S_G$. The study from Finegood and colleagues (105) indicates an interaction exists between insulin and $S_G$ resulting in an inaccurate $S_G$. On the other hand, Vicini *et al.* (106) did not find such an interaction.

### *2.1.2 Tracer-based minimal model of glucose disappearance*

A hot IVGTT (i.e. an injection of isotopically-labeled glucose together with unlabeled glucose) can greatly enhance the power of the minimal model method. The minimal model with a regular IVGTT is intrinsically unable to distinguish the processes of hepatic glucose production and tissues-specific glucose disposal. While, the tracer-based minimal model is able to yield a set of metabolic indices that characterize glucose disposal by tissues only. Furthermore, it may be possible to estimate the profile of hepatic glucose production during the test from the unlabeled and labeled glucose concentrations.

The tracer-based minimal model of glucose tracer disappearance (93) is shown in Figure 2.2. When tracer is injected with cold glucose, the tracer reflects only the glucose disappearance process. All variables of the tracer-based model are the same as defined in the regular minimal mode (see Chapter 2.1.1) except as declared here. A new equation for the kinetics of hot glucose is expressed as:

$$\frac{dC_G^{\ *}(t)}{dt} = -R_d^*(t) = -(R_{dP}^* + R_{dL}^*) \qquad \text{Eq. 2.16}$$

The asterisk denotes 'tracer'. The total disappearance rate of the tracer, $R_d^*(t)$, is the rate of utilization of labeled glucose by liver ($R_{dL}^*(t)$) and peripheral tissues ($R_{dP}^*(t)$). The variable $R_{dP}^*(t)$ is modeled using the same function as Eq. 2.1 of the regular minimal model:

$$R_{dP}^*(t) = \frac{R_{dP}}{C_G(t)} C_G^*(t) = k_1^P C_G^*(t) + k_4^P C_G^*(t) I_r(t) \qquad \text{Eq. 2.17}$$

where the superscript *p* denotes peripheral tissues.

For the hepatic utilization of glucose, it is not appropriate to use Eq. 2.2 of the regular minimal model since it defines only the net output of hepatic glucose. Cobelli *et al.* (93) assumed a similar dependence of $R_{dL}$ on $C_G^*(t)$ and $I_r(t)$ as in Eq. 2.17. Thus, $R_{dL}$ is described by:

$$R_{dL}^*(t) = k_1^L C_G^*(t) + k_4^L C_G^*(t) I_r(t) \qquad \text{Eq.2.18}$$

where $k_1^L$ and $k_4^L$ are rate constant responsible for liver uptake. The $R_d^*(t)$ is expressed as following:

$$R_d^*(t) = (k_1^P + k_1^L) C_G^*(t) + (k_4^P + k_4^L) C_G^*(t) I_r(t) \qquad \text{Eq. 2.19}$$

Substitute Eq. 2.19 into Eq. 2.16, the rate change in glucose tracer is described as:

$$\begin{aligned} \frac{dC_G^*(t)}{dt} &= (k_1^P + k_1^L) C_G^*(t) + (k_4^P + k_4^L) C_G^*(t) I_r(t) \quad C_G^*(0) = C_{G0}^* \\ &= [k_1 + k_4 C_G^*(t)] I_r(t) \end{aligned} \qquad \text{Eq. 2.20}$$

where $C^*_{G0}$ is the initial tracer glucose concentration, $k_1^L$ and $k_1^P$ are lumped as $k_1$, and $k_4^L$ and $k_4^P$ as $k_4$ in order to achieve identifiability of the model. The new tracer-based minimal model is then expressed as:

$$\frac{dC^*_G(t)}{dt} = -[p_1^* + X^*(t)]C^*_G(t) \qquad C^*_G(0) = G^*_{G0} \qquad \text{Eq. 2.21}$$

$$\frac{dX^*(t)}{dt} = -p_2^* X^*(t) + p_3^*[I(t) - I_b] \quad X^*(0) = 0 \qquad \text{Eq. 2.22}$$

$$X^*(t) = (k_4^L + k_4^P) I_r(t) \qquad \text{Eq. 2.23}$$

$$p_1^* = k_1^L + k_1^P \qquad \text{Eq. 2.24}$$

$$p_2^* = k_3 \qquad \text{Eq. 2.25}$$

$$p_3^* = k_2(k_4^L + k_4^P) \qquad \text{Eq. 2.26}$$

The tracer-based minimal model describes tracer glucose uptake by the liver and peripheral tissues and is able to provide the metabolic parameters that reflect utilization processes only. Similar to the way the insulin sensitivity ($S_I$) and glucose effectiveness ($S_I$) are derived in the regular minimal model, the tracer-determined indices are defined as:

$$S_I^* = \frac{p_3^*}{p_2^*} = \frac{k_2(k_4^L + k_4^P)}{k_3} \qquad \text{Eq. 2.27}$$

$$S_G^* = p_1^* = k_1^L + k_1^P \qquad \text{Eq. 2.28}$$

The major advantage of the tracer-based minimal model is its ability to evaluate insulin's actions on tissues only. Its application to insulin resistance would be valuable to better understand the tissue-specific mechanisms in glucose metabolism. This method, according to the report by Avogaro (103), also allows a more precise estimation of insulin sensitivity in T2D patients with marked insulin resistance compared to the cold minimal model method. However, the estimation of glucose effectiveness and insulin

sensitivity from both, unlabeled and labeled minimal model, have been found to be inconsistent (103).

### *2.1.3 Two-compartment minimal model*

Insulin sensitivity ($S_I$) and glucose effectiveness ($S_G$) are two important indices that characterize the efficiency of the glucose-insulin system in regulating glucose homeostasis. The single compartment minimal model description of glucose kinetics is the most popular method used in clinical and epidemiological studies to estimate indices under the IVGTT or labeled IVGTT. However, studies have shown that the indices estimated using the single compartment minimal model are biased (105, 107, 108). $S_I$ is underestimated, although correlated well with the index measured from the glucose clamp technique, while $S_G$ is overestimated. In addition, the time course of hepatic glucose production based on the deconvolution method is unreliable using single compartment kinetics for glucose. It has been shown that inappropriate modeling, i.e. single compartment description of glucose disposition, is the major source of bias in the estimation of $S_I$ and $S_G$. To overcome this limitation of the original minimal model, a two-compartment model (Figure 2.3) of glucose kinetics has been developed by Cobelli *et al.* (92).

The two-compartment model evolved from the original single compartment model, in which a second, nonaccessible compartment is appended to it, and the only difference is the exchange between the accessible and non assessable pools. The model is described as:

$$\frac{G_1(t)}{dt} = -[p_1 + k_{21} + X(t)]G_1(t) + k_{12}G_2(t) + p_1G_b \qquad G_1(0) = G_{1b} + D \qquad \text{Eq. 2.29}$$

$$\frac{G_2(t)}{dt} = k_{21}G_1(t) - k_{12}G_2(t) \quad G_2(0) = G_{2b} \qquad \text{Eq. 2.30}$$

$$X(t) = -p_2X(t) + p_3[C_I(t) - C_{I_b}] \qquad X(0) = 0 \qquad \text{Eq. 2.31}$$

$$C_G(t) = G_1(t)/V_1 \quad \text{Eq. 2.32}$$

where $G_1$ and $G_2$ are the glucose masses in the accessible (plasma) and nonaccessible compartments, respectively; $G_{1b}$ and $G_{2b}$ are the basal steady state glucose mass in the accessible and nonaccessible compartment, respectively; $V_1$ is the volume of the accessible compartment; $k_{12}$ and $k_{21}$ are rate parameters that describe the exchange processes between the two-compartments; $D$, $C_G$, $C_I$, $X$, $p_1$, $p_2$ and $p_3$ are variables and parameters defined as for the single compartment minimal model. Like the original minimal model, the two-compartment model of glucose effectiveness ($S_G^2$) and insulin sensitivity ($S_I^2$) are derived as:

$$S_G^2 = \frac{\partial[dG_1(t)/dt]}{dC_G(t)} = p_1 V_1 = S_G V_1 \quad \text{Eq. 2.33}$$

$$S_I^2 = \frac{\partial^2[dG_1(t)/dt]}{\partial C_G(t)\partial I(t)} = \frac{p_3}{p_2} V_1 = S_I V_1 \quad \text{Eq. 2.34}$$

According to the authors, the indices from the two-compartment model for glucose effectiveness and insulin sensitivity are in agreement with measurements from the literature using the glucose clamp technique. The two-compartment model improves the accuracy of the estimation of insulin sensitivity and glucose effectiveness over the single compartment model. The estimates of indices from the two-compartment method are more similar to the glucose clamp results than the results from a single compartment model.

The two-compartment model differs from the classic minimal model (one-compartment model) only in allowing an exchange of glucose between the accessible and the nonaccessible compartment and introducing extra two parameters. However, extra complexity leads to an identifiability issue (92) which means some parameters may not be indentifiable. This problem can be avoided by making use of prior knowledge of parameters (Bayesian approach) or performing glucose tracer kinetic studies to add additional information to glucose exchange (92, 109, 110).

Overall, two-compartment glucose kinetics using the labeled IVGTT or unlabeled IVGTT coupled with the Bayesian approach improves the accuracy of glucose effectiveness and insulin sensitivity estimates compared to the classic one-compartment minimal model (92, 110). Specifically, the improvement in glucose effectiveness is more significant relative to the improvement in insulin sensitivity.

### *2.1.4 Two-compartment minimal model with endogenous glucose production*

In response to glucose stimulation, insulin secretion is increased and resulting hyperinsulinemia stimulates glucose uptake in peripheral tissues and suppresses hepatic glucose production. During the process of T2D progression, the liver becomes resistant to the suppressive effect of insulin on glucose production. It is thus necessary to quantify and assess the endogenous glucose production (EGP). The single compartment minimal model has been used to estimate EGP by deconvolution approach with labeled and unlabeled glucose data. However, the resulting time course of EGP is physiologically unreasonable. There are two possible sources for the error. One is the monocompartmental description of glucose kinetics (111, 112), the other one is the misrepresentation of insulin and glucose control on glucose kinetics.

Krudys (113) and his colleagues developed a two-compartment minimal model incorporating indirect pharmacodynamic (PD) effects of insulin and glucose on EGP. The structure of the model is shown in Figure 2.4A. Considering glucose metabolism, the model splits the utilization of glucose into two categories: insulin-independent glucose disposal occurring in the accessible pool and insulin-dependent glucose disposal occurring in the nonaccessible pool. Insulin-independent tissues, such as central nervous system and red blood cells, have a constant glucose uptake. Based on this physiological model, the insulin-independent uptake, $k_{01}$, has two components, a constant and a dynamic component inversely proportional to glucose amount:

$$k_{01}(t) = k_P + \frac{R_{d,0}}{V_1 C_G(t)} \quad \text{Eq. 2.35}$$

where $k_p$ is the constant term of glucose disposal from accessible compartment, $R_{d,0}$ is a constant that accounts for the glucose effect on its clearance, $V_1$ is the volume of the accessible pool, and $C_G(t)$ is the glucose concentration in the assessable pool.

Insulin-dependent glucose disposal from the nonasscessible pool is regulated by insulin in a remote compartment, $X(t)$, through parameter $k_{02}$, and is described by:

$$k_{02} + X(t) \quad \text{Eq. 2.36}$$

An additional relationship among model parameters was taken into account to improve the identifiability of the model parameter, in which the insulin-independent glucose disposal is three times as large as the insulin-dependent glucose disposal at the basal steady state. This relationship is given by:

$$k_P + \frac{R_{d,0}}{V_1 C_{G_b}} = \frac{3k_{21}k_{02}}{k_{02} + k_{12}} \quad \text{Eq. 2.37}$$

The model assumes a hypothetical PD compartment representing the glucose in the liver as commonly used in PD study. The amount of releasable glucose in the hypothetical compartment was described by:

$$\frac{dG_L(t)}{dt} = k_{in}[1 - H_1(t)] - k_{out}[1 - H_2(t)]\, G_L(t) \quad \text{Eq. 2.38}$$

where $G_L(t)$ is the amount of glucose in the liver, $k_{in}$ is zero-order rate constant of hepatic glucose production, and $k_{out}$ is the first-order rate constant of hepatic glucose output, and $H_1(t)$ and $H_2(t)$ are inhibitory functions describing the control of glucose and remote insulin to inhibit the EGP, respectively. The inhibition of EGP by the plasma glucose concentration is modeled as:

$$H_1(t) = \frac{C_G(t)}{C_{G_b}(t) + C_G(t)} \quad \text{Eq. 2.39}$$

where $C_G(t)$ is plasma glucose concentration and $C_{G_b}$ is basal plasma glucose concentration. It was assumed that the glucose inhibition of its own production is half the maximal effect under basal state. Thus, the insulin's inhibition effect on EGP is described by the following equation:

$$H_2(t) = \frac{X(t)}{IC_{50} + X(t)} \qquad \text{Eq. 2.40}$$

where $IC_{50}$ characterizes the insulin's action to produce 50% of maximum inhibition of glucose release. At steady state, $C_G(t) = C_{G_b}$ and $X(t) = 0$, giving the initial condition:

$$G_L(0) = \frac{k_{in}}{2 \times k_{out}} \qquad \text{Eq. 2.41}$$

PD modeling of EGP is then incorporated into the two-compartment model. The equations described the new model are:

$$\frac{dG_L(t)}{dt} = k_{in}[1 - H_1(t)] - k_{out}[1 - H_2(t)]G_L(t) \qquad G_L(0) = \frac{k_{in}}{2 \times k_{out}} \qquad \text{Eq. 2.42}$$

$$\frac{dEG_1(t)}{dt} = -[k_P + \frac{F_{01}}{V_1 C_G(t)} + k_{21}]EG_1(t) + k_{12}EG_2(t) + k_{out}[1 - H_2(t)]G_L(t) \qquad EG_1(0) = C_{G_b}V_1 \qquad \text{Eq. 2.43}$$

$$\frac{dEG_2}{dt} = k_{21}EG_1(t) - [k_{02} + X(t) + k_{12}]EG_2(t) \qquad EG_2(0) = k_{21}C_{G_b}V_1/(k_{12} + k_{02}) \qquad \text{Eq. 2.44}$$

$$\frac{dX(t)}{dt} = -k_b\{X(t) - s_k[I(t) - I_b]\} \qquad X(0) = 0 \qquad \text{Eq. 2.45}$$

$$Ge(t) = \frac{EG_1(t)}{V_1} \qquad \text{Eq. 2.46}$$

where $EG_1(t)$ and $EG_2(t)$ represent endogenous glucose masses in the accessible (plasma) and nonaccessible compartments, respectively, and $Ge(t)$ denotes the endogenous glucose concentration.

The time course of EGP is able to be estimated according to the following equation:

$$EGP(t) = k_{out}[1 - H_2(t)]G_L(t) \qquad \text{Eq. 2.47}$$

where the right term of the equation represents the hepatic output from the hypothetical liver compartment.

According the authors, the EGP estimates of healthy subjects obtained from this model are in agreement (113) with estimations from the deconvolution and the model-independent tracer-to-tracee clamp technique (performed on the same subjects). In addition, the model provides a new index, $IC_{50}$, for the assessment of insulin sensitivity in the inhibition of EGP. $IC_{50}$ is defined as the required amount of insulin in the remote compartment to attain 50% inhibition in EGP.

It is possible to provide model-derived parameters to characterize the glucose disposal process only from the tracer-based proposed model (Figure 2.4B). Briefly, the proposed two compartment tracer minimal model is described by:

$$\frac{dG_1^*(t)}{dt} = -\left\{k_P + \frac{F_{01}}{V_1 C_G^*(t)} + k_{21}\right\}G_1^*(t) + k_{12}G_2^*(t) \qquad G_1^*(0) = D^* \qquad \text{Eq. 2.48}$$

$$\frac{dG_2^*}{dt} = -[k_{02} + X^*(t) + k_{12}]G_2^* + k_{21}G_1^* \qquad G_2^*(0) = 0 \qquad \text{Eq. 2.49}$$

$$\frac{dX^*(t)}{dt} = -k_b X^*(t) + k_a[I(t) - I_b] \qquad X^*(0) = 0 \qquad \text{Eq. 2.50}$$

$$C_G^* = \frac{G_1^*(t)}{V_1} \qquad \text{Eq. 2.51}$$

where $G_1^*(t)$ and $G_2^*(t)$ are the tracer mass in the accessible and nonaccessible compartment, respectively; $X^*$ denotes insulin in remote pool; $k_p$, $k_{21}$, $k_{12}$, and $k_{02}$ are constant parameters; and $k_a$ and $k_b$ are parameters associated with insulin action.

The two compartment tracer minimal model provides glucose effectiveness ( $S_G^{2*}$ ), insulin sensitivity ( $S_I^{2*}$ ) and plasma clearance rate (*PCR*). The parameter $S_G^{2*}$ is defined as the ability of glucose to promote its own disposal and is given by:

$$S_G^{2*} = \frac{\partial[dG_1^*(t)/dt]}{\partial C_G^*} = V_1(k_P + \frac{k_{21}k_{02}}{k_{02}+k_{12}}) \quad \text{Eq. 2.52}$$

$S_I^{2*}$ is defined as the ability of insulin per se to stimulate the glucose promoted glucose disposal and is given by:

$$S_I^{2*} = \frac{\partial^2[dG_1^*(t)/dt]}{\partial C_G^* \partial I(t)} = V_1 s_k + \frac{k_{21}k_{12}}{(k_{02}+k_{12})^2} \quad \text{Eq. 2.53}$$

where $s_k=k_a k_c/k_b$. The steady state PCR is defined as

$$PCR = V_1(k_p + + \frac{R_{d,0}}{V_1 C_{G_b}} \frac{k_{21}k_{02}}{k_{02}+k_{12}}) \quad \text{Eq. 2.54}$$

**2.2 Modeling of insulin secretion**

Precise and timely delivery of insulin from the pancreas is required for the maintenance of the glucose level in the normal range. Thus, understanding the glucose-insulin system requires a quantitative evaluation of the insulin secretion rate (ISR) under basal and stimulated states, which is crucial for understanding the progression from normal glucose tolerance to diabetes.

Mathematical modeling of the beta-cell function is aimed at capturing the physiological properties of its secretory process in response to glucose. In 1980, Toffolo *et al.* (55) proposed a one-compartment model called the ‘minimal model’ because of its simplicity in describing insulin dynamics in response to IVGTT. However, the limitation of this model is that it does not describe first-phase insulin secretion and only reflects post-hepatic insulin delivery information.

A number of models described from this minimal model have been developed to overcome these problems by modeling pancreatic insulin secretion with CP data since CP

is co-secreted with insulin without liver extraction. Two-compartment modeling of CP kinetics (79, 114) with the deconvolution technique has been used to reconstruct the prehepatic insulin secretion time course under various protocols, but it requires an extra experiment to determine individual CP parameters. Alternatively, a combined model (115) describing CP and insulin co-secreted kinetics can estimate insulin secretion by fitting CP and insulin data from the same procedure simultaneously. Recently, a minimal model with an additional delay (98) between insulin's prevision and its release has been proposed to provide indices for the assessment of insulin secretion and extraction. Considerable effort (116, 117) has been devoted to assess beta-cell function from an OGTT which is an experimentally simple method for large studies and physiologically close to an 'after-meal' state. Gupta *et al.* (97, 118) proposed a mechanism-based model to detect the existence of the prediabetic condition in biphasic insulin secretion.

Overall, models for assessing beta-cell function are fairly new and are mainly descriptive, not mechanistic. Further work is necessary in order to evaluate the accuracy and reliability of model-derived indices for beta-cell function. More mechanistically- and physiologically-based models are needed to provide a better understanding of the glucose-insulin interaction and to improve early diagnosis of diabetes.

### *2.2.1 Minimal model of insulin kinetics*

The model is called 'minimal' because its design uses the least complex mathematical model to account for the observed dynamic relationship between insulin and glucose disappearance. The strategy was used to define a mathematical representation of the quantitative measure of pancreatic sensitivity in insulin secretion in response to a well-defined glucose perturbation, such as the IVGTT.

The structure of the minimal model of insulin kinetics (55) is illustrated in Figure 2.5. A single compartment is used to describe plasma insulin dynamics observed in IVGTT:

$$\frac{dC_I(t)}{dt} = IDR(t) - nC_I(t) \qquad \text{Eq. 2.55}$$

where $C_I(t)$ is the plasma insulin concentration above the final 60-120 min basal level, $IDR(t)$ denotes insulin delivery rate after the first-pass extraction by liver and $n$ is a first-order disappearance rate constant. The model assumes that insulin secretion is stimulated and proportional to both the time elapsed after glucose administration and the extent to which the glucose concentration exceeds the specific threshold $h$. The $IDR(t)$ is given by:

$$IDR(t) = \begin{cases} \gamma [C_G(t) - h]\, t & \text{if } C_G(t) > h \\ 0 & \text{otherwise} \end{cases} \qquad \text{Eq. 2.56}$$

where $C_G(t)$ is the plasma glucose concentration that is used as a 'forcing function', $t$ is time and $\gamma$ is a constant parameter.

In addition to $IDR(t)$, the model allows to estimate two indices for the assessment of pancreatic response to glucose from the model-derived parameters, namely the first-phase sensitivity $\phi_1$ and second-phase sensitivity to glucose $\phi_2$. The parameter $\phi_1$ is estimated by assuming that the glucose injection causes insulin to enter the plasma immediately during the first-phase in an amount of $P_1$. The $P_1$ is given by:

$$P_1 = \int_0^\infty C_{I_0} e^{-nt} dt = \frac{C_{I_0}}{n} \qquad \text{Eq. 2.57}$$

where $C_{I_0}$ is the initial insulin concentration relative to steady state baseline. The first-phase sensitivity to glucose is defined as insulin amount secreted during the first-phase divided by the incremental change in plasma glucose ($\Delta C_G$), which is:

$$\phi_1 = \frac{P_1}{\Delta C_G} = \frac{C_{I_0}}{n \Delta C_G} \qquad \text{Eq. 2.58}$$

Assuming that the $IDR(t)$ is associated with second-phase insulin secretion, the second-phase sensitivity to glucose is defined as the dependence on glucose of the rate of rise of the second-phase:

$$\phi_2 = \frac{\partial^2 IDR(t)}{\partial C_G \partial t} = \gamma \qquad \text{Eq. 2.59}$$

The major limitation of this model is that it does not reflect insulin secretion accurately, ignoring the early first-phase (Figure 2.6) which is an important aspect of beta-cell function and important in the study of the development of T2D.

### *2.2.2 Two-compartment C-peptide model*

C-peptide (CP) kinetics have been validated to be linear and time-invariant over a wide range of concentrations (77, 78). Thus, it is possible to estimate prehepatic insulin secretion from CP dynamics based on the feature that C-peptides are secreted in equimolar amounts from the beta-cell with insulin and does not experience first-pass extraction by liver.

Eaton *et al.* (79) introduced a mathematical operation called deconvolution to reconstruct insulin secretion from CP dynamics. In order to perform deconvolution, CP disposition kinetics must be known. The majority of models describing CP kinetics are two-compartmental model (79, 114) as represented in Figure 2.7. The two-compartment model of CP kinetics is described by:

$$\frac{dC_{P_1}}{dt} = -(K_{01} + K_{12})C_{P_1}(t) + K_{21}C_{P_2}(t) + CPSR(t) \qquad \text{Eq. 2.60}$$

$$\frac{dC_{P_2}}{dt} = K_{12}C_{P_1}(t) - K_{21}C_{P_2}(t) \qquad \text{Eq. 2.61}$$

where *CPSR(t)* is the CP secretion rate which is equal to the prehepatic insulin secretion (ISR) rate, $C_{P_1}$ and $C_{P_2}$ are CP concentration in compartment 1 (plasma) and compartment 2 (extravascular tissues), $K_{12}$ and $K_{21}$ are transfer rate parameters between compartments and $K_{01}$ describes the metabolized rate of CP from plasma. Mathematically, the CP secretion rate which is equal to the ISR can be derived from deconvolution procedure as follows:

$$CPSR(t) = -e^{-K_{21}t}[K_{21}C_{P_2}(t_0)e^{K_{21}t_0} + K_{12}K_{21}\int_{t_0}^{t} e^{k_{21}s}C_{P_1}(s)ds] + \frac{d}{dt}C_{P_1}(t) + (K_{12} + K_{01})C_{P_1}(t)$$

Eq. 2.62

where $t_0$ is the initial moment at which CP reaches to equilibrium between the two-compartments. The variable $C_{P_2}(t_0)$ in equation Eq. 2.62 can be substituted by $C_{P_1}(t_0)$ according to the relationship $K_{21}C_{P_2}(t_0) = K_{12}C_{P_1}(t_0)$, then Eq. 2.62 is given by:

$$CPSR(t) = -e^{-K_{21}t}[K_{12}C_{P_1}(t_0)e^{K_{21}t_0} + K_{12}K_{21}\int_{t_0}^{t} e^{k_{21}s}C_{P_1}(s)ds] + \frac{d}{dt}C_{P_1}(t) + (K_{12} + K_{01})C_{P_1}(t)$$

Eq. 2.63

Eq. 2.63 is used to reconstruct pancreatic CP secretion or insulin secretion under IVGTT, OGTT, or other protocols. However, CP kinetics, $K_{12}$, $K_{21}$, $K_{01}$ must be known. In Ethon's approach (79), CP kinetics was determined by bolus injection of biosynthetic CP in each individual whereas endogenous insulin secretion is suppressed by somatostatin.

In a later study, Cauter *et al.* (80) analyzed 200 curves of biosynthetic CP after IV bolus injection and showed that it is possible to estimated insulin secretion using population-based standard CP kinetic parameters calculated from a regression model without significant loss of accuracy (80, 119). The regression model takes into account body surface area (BSA), degree of obesity, status of diabetes, sex, and age, thus circumvents the need to perform an extra experiment. This approach has made wide application of the CP deconvolution method possible and has been included into a computer-based program ISEC (120), but it introduces errors into the results because of the approximations used.

### *2.2.3 Extended combined model of insulin and C-peptide dynamics*

The combined model developed by Volund *et al.* (115, 121) can estimate prehepatic ISR using the insulin and CP measurements acquired from the same procedure.

Unlike the deconvolution method that requires an extra experiment to acquire CP kinetics, the advantage of the extended combined model is that it is independent of prior knowledge of CP kinetics. An extra experiment to acquire CP kinetics is thus unnecessary. In the original combined model, one single compartment is used to describe both insulin and CP kinetics. However, the single compartment assumption of CP kinetics is not appropriate in term of accuracy under intravenous glucose administration (80, 122). An extended combined model (Figure 2.8) is proposed (96, 123) to overcome this problem which has a similar model structure, but employs two-compartmental CP kinetics.

In the model, insulin and CP are released at equimolar secretion rates which is denoted as *R(t)*, and liver extraction of insulin is assumed to be constant and with no extraction of the CP. The extended model is described by the following differential equations:

$$V_I \frac{dC_I(t)}{dt} = FR(t) - K_I(t)V_I \qquad \text{Eq. 2.64}$$

$$V_{P_1} \frac{dC_{P_1}(t)}{dt} = R(t) - (K_{12} + K_{01})C_{P_1}(t)V_{P_1} + K_{21}C_{P_2}(t)V_{P_2} \qquad \text{Eq. 2.65}$$

$$V_{P_2} \frac{dC_{P_2}(t)}{dt} = K_{12}C_{P_2}(t)V_{P_1} - K_{21}C_{P_1}(t)V_{P_2} \qquad \text{Eq. 2.66}$$

where $C_I(t)$ is plasma insulin concentration, $C_{P_1}(t)$ represents plasma CP concentration , $C_{P_2}(t)$ is the extravascular CP concentration; $K_I$ represents the disappearance rates of insulin from plasma; $F$ is the ratio of insulin not extracted by liver; $K_{12}$, $K_{21}$ and $K_{01}$ are the kinetic parameters for CP kinetics; $V_I$ is the distribution volume for insulin in plasma, and $V_{P_1}$ and $V_{P_2}$ CP are distribution volumes for CP in plasma and extravascular tissues, respectively.

By making the following substitutions:

$$r(t) = \frac{R(t)}{V_{P_1}} \quad \text{Eq. 2.67}$$

$$f = F\frac{V_{C_1}}{V_I} \quad \text{Eq. 2.68}$$

the extended model become:

$$\frac{dC_I(t)}{dt} = f\, r(t) - K_I I(t) \quad \text{Eq. 2.69}$$

$$\frac{dC_{P_1}(t)}{dt} = r(t) - (K_{12} + K_{10})C_{P_1}(t) + K_{21}C_{P_2}(t) \quad \text{Eq. 2.70}$$

$$\frac{dC_{P_2}(t)}{dt} = K_{12}C_{P_1}(t) - K_{21}C_{P_2}(t) \quad \text{Eq. 2.71}$$

where insulin secretion, *r(t)*, is now estimated in term of per unit distribution volume of CP in plasma.

Compared to the deconvolution technique, the extended model accurately estimates prehepatic insulin secretion (124, 125). By analyzing insulin and CP profiles under infusions of insulin and CP via simulating an OGTT, the average insulin extraction ratio was determined to be 45% in healthy subjects and 20% in T2D patients (124, 125). However, the combined model was not superior to the deconvolution method using standard CP kinetic parameters in terms of accuracy in estimation of prehepatic insulin secretion (80, 126).

### *2.2.4 C-peptide minimal model of hepatic extraction*

The liver removes a significant fraction (around 50%) of beta-cell secreted insulin and this fraction is altered at various physiological and pathological conditions. Therefore, a reliable estimation of the hepatic insulin extraction is a crucial part in analyzing the glucose-insulin system. The molar ratio of insulin to CP has been used to estimate hepatic insulin extraction. However, this method is not adequate in dealing with a highly dynamic process, such as IVGTT, since CP has a slower elimination from plasma than

insulin. Pacini and Cobelli (127) proposed a solution to this problem by applying a new model to account for CP dynamics during an IVGTT. The model (Figure 2.9) describes the insulin delivery rate (*IDR(t)*) and CP secretion rate from beta-cell (*CPSR(t)*) separately using similar equations, but with different parameters. The extraction ratio was then estimated by the difference between *IDR(t)* and *CPSR(t)* (127).

CP kinetics in the model have a similar structure to that already used in the minimal model for insulin delivery to blood and disappearance from blood under the IVGTT. The first-phase $CPSR^{I}(t)$ is described as a process in which a bolus release of CP occurs immediately following glucose injection:

$$CPSR^{I}(t) = CP_0\delta(t) \qquad \text{Eq. 2.72}$$

where $CP_0$ is the CP concentration above the basal level and $\delta(t)$ is a Dirac function. The second-phase secretion rate $CPSR^{II}(t)$ is time-variant and proportional to the degree of exceeding a threshold of glucose:

$$CPSR^{II}(t) = \gamma_{CP}[C_G(t) - h]\,t \qquad \text{Eq. 2.73}$$

where $\gamma_{CP}$ is a proportional constant and *h* is the glucose threshold which is the same as that used to describe insulin kinetics. Therefore, the sum of first- and second-phase CP secretion over basal secretion level is the incremental secretion rate, $CPSR(t)$, and given by:

$$CPSR(t) = CPSR^{I}(t) + CPSR(t)^{II} \qquad \text{Eq. 2.74}$$

CP kinetics is described by a two-compartment structure:

$$\frac{dC_{P_1}(t)}{dt} = -(K_{01} + K_{12})C_{P_1}(t) + K_{21}C_{P_2}(t) + CPSR(t) \qquad CP_1(0) = 0 \qquad \text{Eq. 2.75}$$

$$\frac{dC_{P_2}(t)}{dt} = -K_{21}C_{P_2}(t) + K_{12}C_{P_1}(t) \qquad CP_2(0) = 0 \qquad \text{Eq. 2.76}$$

where $C_{P_1}(t)$ and $C_{P_2}(t)$ are CP concentrations above the basal level in compartment 1 (plasma) and compartment 2 (extravascular tissues) respectively, $K_{12}$, and $K_{21}$ are transfer rate parameters between compartments, and $K_{01}$ is the disappearance rate of CP from plasma.

Eq. 2.74 gives the incremental CP secretion rate, while the basal CP secretion rate ($CPSR_b$) can be derived from Eq. 2.75 and 2.76 at the fasting steady state and computed as:

$$CPSR_b = K_{01} CP_b \qquad \text{Eq. 2.77}$$

where $CP_b$ is fasting level of CP. The total insulin secretion ($CPSR^T$) which equal to ISR is the combination of basal secretion rate and incremental secretion rate:

$$CPSR^T(t) = CPSR(t) + CPSR_b \qquad \text{Eq. 2.78}$$

The prehepatic insulin secretion profile can be obtained by integrating of Eq. 2.78 over time. With the model, it is possible to quantify the pancreas' ability to release insulin in terms of the sensitivity to glucose stimulation. During the IVGTT, the model treats the first-phase insulin release as a bolus input of CP in response to glucose. Without a second-phase, the secreted amount of CP above the basal level is $CP_0/K_{01}$. The first-phase sensitivity to glucose, $\phi_{1C}$, is thus defined as the amount of secreted CP divided by the incremental change in plasma glucose ($C_G$):

$$\phi_{1C} = \frac{CP_0}{K_{01}\Delta C_G} \qquad \text{Eq. 2.79}$$

The second-phase sensitivity to glucose is defined as the dependence on glucose of the rate of rise of the second-phase CP secretion and given by:

$$\phi_{2C} = \frac{\partial^2 CPSR^{II}(t)}{\partial C_G \partial t} = \gamma_{CP} \qquad \text{Eq. 2.80}$$

The proposed model describes insulin secretion delivery rate, *IDR(t)*, with a similar expression used for *CPSR(t)* (Eq. 2.72-2.74), but with different parameters. The

posthepatic delivery rate of insulin has first and second-phase components and is described by:

$$IDR(t) = IDR^{I}(t) + IDR^{II}(t) \qquad \text{Eq. 2.81}$$

$$IDR^{I} = I_0\delta(t) \qquad \text{Eq. 2.82}$$

$$IDR^{II}(t) = \gamma_I[C_G(t) - h]t \qquad \text{Eq. 2.83}$$

The kinetics of insulin is described by the single compartment minimal model (Chapter 2.2.1):

$$\frac{dC_I}{dt} = -n_I C_I(t) + IDR(t) \qquad C_I(0) = 0 \qquad \text{Eq. 2.84}$$

The basal insulin delivery rate is:

$$IDR_b = n_I C_{I_b} \qquad \text{Eq. 2.85}$$

Since the CP secretion rate is equal to the prehepatic insulin secretion rate, and CP undergoes negligible hepatic extraction, the profile of the hepatic insulin extraction ratio, *H(t)*, can be calculated by the difference between the delivery rate of CP and insulin divided by CP secretion rate:

$$H(t) = \frac{CPSR^{T}(t) - IDR^{T}(t)}{CPSR^{T}(t)} \qquad \text{Eq. 2.86}$$

where $IDR(t)^{T}$ represents insulin posthepatic insulin delivery rate including basal, first- and second-phase insulin secretion.

The method described here provides a way for simultaneously describing the time course of beta-cell secretion, evaluating beta-cell sensitivity to glucose both in the first- and the second-phase and measuring the hepatic insulin extraction using glucose, insulin and CP data. However, like the insulin minimal model, the CP minimal model is not accurate in quantifying the first-phase insulin secretion as discussed by the authors.

### *2.2.5 C-peptide minimal model with a delay compartment*

Although insulin or CP minimal models have been provided to assess the insulin secretion during IVGTT, these models do not describe biphasic secretion pattern well. To represent insulin's biphasic secretion more accurately than the insulin minimal model, a mathematical model with CP data has been formulated by Toffolo *et al.* (98) as shown in Figure 2.10. The model assumes that the first-phase is derived from promptly releasable insulin granules in the beta-cells, which is rapidly secreted when glucose is increased above its basal value. The second-phase is due to the provision process allowing a delay between provision and insulin release.

A two-compartment CP kinetics was also used in the proposed model, and the endogenous CP secretion over basal secretion level entering the system in response to IV glucose stimulation is described by:

$$isr(t) = ISR^{I}(t) + ISR^{II}(t) \qquad \text{Eq. 2.87}$$

where *isr(t)* is the pancreatic CP/insulin secretion over basal secretion level, which consists of first-phase $ISR^{I}(t)$ and second-phase $ISR^{II}(t)$ release to accommodate the biphasic pattern of CP secretion during IVGTT.

The model allows a delay between the provision *Y* and secretion *ISR(t)* via a new variable *Z* representing the readily releasable insulin in the beta-cells. CP is released at a first-order rate:

$$isr(t) = mZ(t) \qquad \text{Eq. 2.88}$$

and *Z* can be 'refilled' through *Y*:

$$\frac{dZ(t)}{dt} = -mZ(t) + Y(t) \qquad Z(0) = Z_0 \qquad \text{Eq. 2.89}$$

where *m* is a rate constant, $Z_0$ is the amount of CP stored in the beta-cells before the glucose stimulus, which is responsible for the first-phase secretion over basal secretion level. The first-phase is described as a one exponential decay:

$$ISR^{I}(t) = mZ_0 e^{-mt}$$ Eq. 2.90

The second-phase is equal to *Y* representing the newly formed insulin in the beta-cell:

$$ISR^{II}(t) = Y(t) = \beta[C_G(t) - h)]$$ Eq. 2.91

When glucose concentration exceeds the threshold level *h*, *Y* is stimulated via parameter $\beta$ and decays with a rate constant $\alpha$. The rate change in Y is:

$$\frac{dY(t)}{dt} = -\alpha\{Y(t) - \beta[C_G(t) - h]\} \qquad Y(0) = 0$$ Eq. 2.92

Finally, the insulin secretion profile was obtained and described by:

$$\begin{aligned} ISR(t) &= [isr(t) + SR_b]V_C \\ &= [mZ(t) + K_{01}CP_{1_b}]V_C \end{aligned}$$ Eq. 2.93

where $SR_b$ is the basal insulin secretion rate and $V_C$ is the distribution volume of the accessible compartment.

CP kinetics was described by the two-compartment model with the endogenous secretion over basal secretion level during IVGTT. Briefly, the CP kinetics and basal secretion rate are represented by the following equations:

$$\frac{dC_{P_1}(t)}{dt} = -(K_{12} + K_{10})C_{P_1}(t) + K_{21}C_{P_2}(t) + isr(t) \qquad C_{P_1}(0) = 0$$ Eq. 2.94

$$\frac{dC_{P_2}(t)}{dt} = K_{12}C_{P_1}(t) - K_{21}C_{P_2}(t) \qquad C_{P_2}(0) = 0$$ Eq. 2.95

$$SR_b = K_{01}C_{P_{1b}}$$ Eq. 2.96

The model defines three indices ($\phi_{1C}, \phi_{2C}$ and $\phi_b$) to characterize the beta-cell sensitivity to glucose in first-phase, second-phase and basal release, respectively:

$$\phi_{1C} = \frac{Z_0}{\Delta C_G}$$ Eq. 2.97

$$\phi_{2C} = \beta$$ Eq. 2.98

$$\phi_b = K_{01} CP_{1b} / C_{G_b} \qquad \text{Eq. 2.99}$$

where $C_{G_b}$ is the end-test steady-state glucose concentration.

In a later study (128), this model was introduced to assess hepatic insulin extraction during an IVGTT by estimating insulin secretion from CP data and insulin delivery rate from insulin data and to provide information for hepatic insulin extraction. The insulin secretion rate, *ISR(t)*, can be calculated according to Eq. 2.93. For insulin delivery rate *idr(t)* over basal secretion level, it is described by the similar function expressed for *isr(t)*, but with different parameters:

$$idr(t) = m^{IDR} Z^{IDR}(t) \qquad \text{Eq. 2.100}$$

$$\frac{dZ^{IDR}(t)}{dt} = -m^{IDR} Z^{IDR}(t) + Y^{IDR}(t) \qquad Z^{IDR}(0) = 0 \qquad \text{Eq. 2.101}$$

$$\frac{dY^{IDR}(t)}{dt} = -\alpha^{IDR}\{Y^{IDR}(t) - \beta^{IDR}[C_G(t) - h]\} \qquad Y^{IDR}(0) = 0 \qquad \text{Eq. 2.102}$$

where parameters and variables are labeled ‘IDR’ to refer to insulin delivery rate.

The insulin delivery rate, *IDR(t)*, is then calculated as the sum of *idr(t)* and basal insulin delivery rate as:

$$\begin{aligned} IDR(t) &= [idr(t) + nC_{I_b}]V_I \\ &= [m^{IDR} Z^{IDR}(t) + nC_{I_b}]V_I \end{aligned} \qquad \text{Eq. 2.103}$$

where $V_I$ and $n$ is insulin kinetics parameters defined as the distribution volume of insulin and first-order rate constant of insulin cleared from plasma.

To reliably estimate insulin kinetic parameters, an insulin-modified IVGTT (IM-IVGTT) was performed. An intravenous injection of glucose was followed by an insulin infusion 20 to 25 min after. Insulin kinetic parameters are identified from the decay curve of IM-IVGTT. The insulin kinetics during the IM-IVGTT is described by the following minimal model:

$$\frac{dC_I(t)}{dt} = -nC_I(t) + idr(t) + U(t)/V_I \qquad C_I(0) = 0 \qquad \text{Eq. 2.104}$$

where *U(t)* is the exogenous insulin infusion rate.

Indices of the first-phase, second-phase and basal insulin delivery rate ($\phi_{1C}^{IDR}$, $\phi_{2C}^{IDR}$ and $\phi_b^{IDR}$, respectively ) are derived to characterize the beta-cell sensitivity to glucose:

$$\phi_1^{IDR} = \frac{Z_0^{IDR}}{\Delta C_G} \qquad \text{Eq. 2.105}$$

$$\phi_2^{IDR} = \beta^{IDR} \qquad \text{Eq. 2.106}$$

$$\phi_b^{IDR} = \frac{IDR_b}{\Delta C_G} = \frac{nC_{I_b}}{C_{G_b}} \qquad \text{Eq. 2.107}$$

Hepatic insulin extraction ratio *H(t*) can be reconstructed from *ISR(t)* and *IDR(t)* profiles by:

$$H(t) = \frac{ISR(t) - IDR(t)}{ISR(t)} = 1 - \frac{IDR(t)}{ISR(t)} \qquad \text{Eq. 2.108}$$

Two hepatic extraction indices during IVGTT and in the basal state are derived as:

$$H(t) = \frac{\int_0^T ISR(t)dt - \int_0^T IDR(t)dt}{\int_0^T ISR(t)} = 1 - \frac{(\phi_b^{IDR} + \phi_1^{IDR}A_1 + \phi_2^{IDR}A_2)V_1}{(\phi_b + \phi_1 A_1 + \phi_2 A_2)V_C} \qquad \text{Eq. 2.109}$$

$$H_b = \frac{ISR_bV_C - IDR_bV_1}{ISR_bV_C} = 1 - \frac{\phi_b^{IDR}V_1}{\phi_b V_C} \qquad \text{Eq. 2.110}$$

$$A_1 = \frac{\Delta C_G}{TG_b} \qquad \text{Eq. 2.111}$$

$$A_2 = \frac{\int_0^T [C_G(t) - h]dt}{TC_{G_b}} \qquad \text{Eq. 2.112}$$

where *T* is the time at which insulin, CP and glucose reach their steady-state after the IV glucose perturbation. Toffolo *et al.* (128) evaluated hepatic extraction in 20 normal

subjects by using the proposed model with insulin and CP data from IVGTT. In the study, CP kinetics were fixed to standard population values, while insulin kinetics was identified using IM-IVGTT by which a reliable estimation of insulin disappearance rate constant ($n$) and distribution volume ($V_I$) in each individual was acquired. The results indicated that about 54% insulin is removed during IM-IVGTT, and 70% at the basal state.

The delay component between provision of the CP and secretion improves the description. It is possible to reproduce secretion processes in situations different from the IVGTT, such as the IM-IVGTT and graded glucose infusion (129). However, the model failed to describe the OGTT (117) since functional description of insulin delivery would not provide a reasonable description of the insulin response. The insulin model with an *IDR(t)* structured similar to that for the ISR in the oral CP model is thus not appropriate for interpreting the secretion of insulin.

### *2.2.6 C-peptide minimal model under graded up and down glucose infusion*

It is obvious that the evaluation of beta-cell function is essential in the study of the etiology of T2D. The C-peptide (CP) minimal model has been successful applied to estimate insulin secretion and assess the beta-cell response to glucose under an IVGTT. Toffolo and his colleagues (116) developed a new version of the CP minimal model that characterizes beta-cell function during a graded-up and -down regulation of the glucose infusion rate. One advantage of the grade glucose infusion is its ability to characterize glucose and insulin responses under a physiological-like perturbation.

The model was formulated according to the physiological assumptions that glucose stimulates pancreatic insulin secretion by static control (i.e., proportional to its concentration) and dynamic control (i.e., proportional to its rate of change). The model

also assumes that the insulin secretion rate is equal to the rate of new insulin production from provision.

The model describes beta-cell secretory response on the basis of CP data. Insulin secretion is integrated into a two-compartment CP kinetics model as normally used in the evaluation of pancreatic insulin secretion. The proposed model describes the CP kinetics by the following equations:

$$\frac{dC_{P_1}(t)}{dt} = -(K_{12} + K_{10})C_{P_1}(t) + K_{21}C_{P_2}(t) + SR(t) \qquad C_{P_1}(0) = 0 \qquad \text{Eq. 2.113}$$

$$\frac{dC_{P_2}(t)}{dt} = K_{12}C_{P_1}(t) - K_{21}C_{P_2}(t) \qquad C_{P_2}(0) = 0 \qquad \text{Eq. 2.114}$$

*SR(t)* is the pancreatic secretion above basal level and normalized to the CP volume of distribution in compartment 1. Pancreatic insulin secretion rate has two components that reflect functional relationship between insulin secretion and plasma glucose concentration, including a static secretion $SR_s(t)$ controlled by glucose concentration and a dynamic secretion $SR_d(t)$ controlled by the rate of change of glucose concentration:

$$SR(t) = SR_s(t) + SR_d(t) \qquad \text{Eq. 2.115}$$

When plasma glucose concentration increases, insulin is produced and secreted from beta-cells. The model assumes $SR_s(t)$ is equal to production rate of insulin from provision Y:

$$SR_s(t) = Y(t) \qquad \text{Eq. 2.116}$$

, which is controlled by glucose according to the following equation:

$$\frac{dY(t)}{dt} = -\alpha\left\{Y(t) - \beta[C_G(t) - C_{G_b}]\right\} \qquad Y(0) = 0 \qquad \text{Eq. 2.117}$$

where parameter $\beta$ is a constant related to the static control of glucose on beta-cells.

$SR_d(t)$ is derived from the insulin stored in the beta-cells in a labile insulin pool. It was assumed that the labile insulin is not homogeneous in terms of glucose stimulation. The size of glucose-stimulated labile insulin depends on the intensity of stimulus. The amount of released insulin ($dQ$) in response to an increase in glucose level is express by the following increase:

$$dQ = k_d\, dC_G \qquad \text{Eq. 2.118}$$

The dynamic secretion rate, $SR_d$, is then proportional to the derivative of glucose:

$$SR_d(t) = \frac{dQ}{dt} = k(C_G)\frac{dC_G}{dt} = k_d\left(1 - \frac{C_G(t) - G_b}{C_{G_t} - C_{G_b}}\right)\frac{dC_G}{dt}$$

$$\text{if } \frac{dC_G(t)}{dy} > 0 \quad \text{and} \quad C_{G_b} < C_G(t) < C_{G_t} \qquad \text{Eq 2.119}$$

$$= 0 \qquad \text{otherwise}$$

According to the Eq. 2.119, the parameter $k$ is allowed to vary with changes in glucose concentration. It characterizes the dynamic control of glucose on insulin secretion and the dynamic control reached a maximum when glucose levels increase just above its basal value. The insulin secretion, $ISR(t)$, during the up- and down-graded infusions is then described by:

$$ISR(t) = [SR_b + SR(t)]\, V_1$$

$$= \left\{ k_{01} C_{P_{1b}} + Y(t) + k_d\left[1 - \frac{C_G(t) - C_{G_b}}{C_{G_t} - C_{G_b}}\right]\frac{dC_G}{dt} \right\} V_1$$

$$\text{if } \frac{dC_G(t)}{dy} > 0 \quad \text{and} \quad C_{G_b} < C_G(t) < C_{G_t} \qquad \text{Eq. 2.120}$$

$$= \left\{ k_{01} C_{P_{1b}} + Y(t) \right\} V_1 \qquad \text{otherwise}$$

where $SR_b$ is insulin secretion rate at the basal state, and $V_1$ is the CP volume of distribution in compartment 1.

The static sensitivity to glucose ($\phi_s$) measures the stimulatory effect of a glucose stimulus on beta-cell secretion at steady state:

$$\phi_s = \beta \qquad \text{Eq. 2.121}$$

The dynamic sensitivity to glucose measures the stimulatory effect of the rate of change in glucose on secretion of stored insulin $Z_0$ which is expressed as:

$$Z_0 = \int_{C_{G_b}}^{C_{G_{\max}}} k(C_G)dC_G = k_d\left[1 - \frac{C_{G_{\max}} - C_{G_b}}{2(C_{G_t} - C_{G_b})}\right](C_{G_{\max}} - C_{G_b}) \qquad \text{Eq. 2.122}$$

where $C_{G_{max}}$ is the maximum glucose concentration during the experiment. If $C_{G_t} < C_{G_{max}}$, $Z_0$ becomes:

$$Z_0 = \int_{C_{G_b}}^{C_{G_t}} k(C_G)dC_G = k_d(C_{G_{\max}} - C_{G_b})/2 \qquad \text{Eq. 2.123}$$

The dynamic sensitivity to glucose ($\phi_d$) is derived by normalizing $Z_0$ to the glucose increase as follows:

$$\phi_d = \frac{Z_0}{C_{G_{\max}} - C_{G_b}} \qquad \text{Eq. 2.124}$$

The index of basal sensitivity ($\phi_b$) has the same expression as that under IVGTT:

$$\phi_b = \frac{SR_b}{C_{G_b}} = \frac{k_{01}C_{P_{1b}}}{C_{G_b}} \qquad \text{Eq. 2.125}$$

This study shows that the proposed model can describe dynamic insulin secretory responses to a physiological-like up- and down-graded regulation of glucose concentration and gives indices to characterize basal, statistic ($\phi_s$), and dynamic ($\phi_d$) insulin secretory responses. The indices, $\phi_s$ and $\phi_d$, can be compared with their IVGTT counterparts, the second-phase sensitivity ($\phi_2$), and first-phase sensitivity ($\phi_1$). Its application to various pathological states may provide insight into the role of insulin secretion in the development of glucose intolerance. However, further work is needed to verify the accuracy of these indices before they can be routinely used in clinical and epidemiological investigations.

### *2.2.7 The Gupta et al. PK/PD model*

Gupta *et al.* (97, 118) proposed a model that accounts for insulin secretion based on physiological processes of insulin inside beta-cells. The model was developed in order to differentiate the responsiveness of beta-cells to IV glucose stimulation between lean and obese children. Additionally, it was used to detect a defect in the first-phase of insulin secretion. The model is formulated at the beta-cell level. It includes five kinetic variables to describe glucose-insulin regulation and the movement of insulin from the interior of the cell to the membrane, involving cellular glucose ($G_C$), proinsulin ($I_P$), reserve insulin ($I_R$), docked insulin ($I_D$) and readily releasable insulin ($I_{RR}$).

Figure 2.11 schematically describes the model. Once glucose concentration in plasma ($C_G$) is higher than in beta-cells ( $C_{G_C}$ ), glucose enters the cell at a rate proportional to the difference between $C_G$ and $C_{G_C}$ :

$$\frac{dC_{G_C}(t)}{dt} = k_1[C_G(t) - C_{G_C}(t)] - k_2 \qquad C_{G_C}(0) = C_G(0) - k_2/k_1 \qquad \text{Eq. 2.126}$$

where $k_1$ is the rate constant for the transportation of glucose into the beta-cell and $k_2$ is the utilization rate of glucose by the beta-cell.

The cellular glucose levels affect the production of proinsulin which is the insulin precursor. Proinsulin converts to insulin and then is stored in the $I_R$ and $I_D$ pool at the first-order manner. The rate of change in the $I_P$ pool is given by:

$$\frac{dI_P(t)}{dt} = k_3 C_{G_C}(t) - (k_4 + k_5) I_P(t) \qquad I_P(0) = \frac{k_3 C_{G_C}(0)}{(k_4 + k_5)} \qquad \text{Eq. 2.127}$$

where $k_3$ is the rate constant for proinsulin production and $k_4$ and $k_5$ denote transport of insulin to $I_R$ and $I_D$.

It is assumed that the transfer of insulin granules from $I_R$ to $I_D$ is regulated by a first-order process. The $I_D$ pool are insulin granules that are docked on the membrane. Subsequently, the docked granules are primed (prepared) and translocated to $I_{RR}$ for

release. This process is also affected by the cellular glucose concentration, $C_{G_C}$, as in Eq. 2.129. The rates of change in $I_R$ and $I_D$ are:

$$\frac{dI_R(t)}{dt} = k_4 I_P(t) - k_6 I_R(t) \qquad I_R(0) = \frac{k_3 k_4 C_{G_C}(0)}{k_6(k_4 + k_5)} \qquad \text{Eq. 2.128}$$

$$\frac{dI_D(t)}{dt} = k_5 I_P(t) + k_6 I_R(t) - k_7 C_{G_C}(t) I_D(t) \qquad I_D(0) = \frac{k_3}{k_7} \qquad \text{Eq. 2.129}$$

where $k_4$, $k_5$, $k_6$ and $k_7$ are the first-order rate constants.

In this model, the initial burst of release is attributed to $I_{RR}$ and is controlled by the parameter $k_8$. The rate change in $I_{RR}$ is given by the following differential equation

$$\frac{dI_{RR}(t)}{dt} = k_7 C_{G_C} I_D(t) - k_8 I_{RR}(t) \qquad I_{RR}(0) = \frac{k_3 C_{G_C}(0)}{k_8} \qquad \text{Eq. 2.130}$$

The fraction of insulin removed by liver the ($E$) can be estimated by this model. The parameter $k_e$ represents the elimination rate of insulin from the plasma. Thus, the rate change in plasma insulin concentration is described as:

$$\frac{dI(t)}{dt} = k_9 I_{RR}(t) - k_e I(t) \qquad I(0) = \frac{k_3 k_9 C_{G_C}(0)}{k_e k_8} \qquad k_9 = (1 - E) k_8 \qquad \text{Eq. 2.131}$$

The model has the potential to detect a prediabetic condition. However, it is not clear how to associate the prediabetic condition to the first-phase and the second-phase secretion.

**2.3 Models of insulin-glucose system**

A central characteristic of the dynamic relationship between glucose and its controlling hormone is the feedback loop. Glucose stimulates the secretion of insulin, and insulin stimulates the utilization of glucose while at the same time suppresses the production of glucose. The models discussed above only describe insulin and glucose kinetics separately; they do not include their mutual interaction. An integrated model has been developed and has provided additional knowledge based on upon physiological and

pharmacological phenomenon, such as the oscillation of insulin concentration, effects of drugs on the insulin-glucose system, and the progression to T2D (99, 102).

Mathematical models for diabetes research have focused on the dynamics of blood glucose or insulin levels for measuring insulin sensitivity and beta-cell function. Neither of these efforts considered the beta-cell mass dynamics as developed by Topp *et al.* (101)

In PK/PD modeling, the family of indirect physiological response models constitutes a useful basis for the development of mechanism-based PK/PD models, which can be extended to describe complex time dependent physiological mechanisms and disease process. In this manner, a T2D progressing analysis (100) has been proposed where the influence of antidiabetic drugs' effect on the change of T2D status over time is characterized. The disease model is helpful for developing new drugs specifically designed to modify the processes and progression of T2D.

### *2.3.1 Dynamic model*

The minimal model includes two parts: one part describes glucose kinetics treating insulin plasma concentration as a known forcing function and the other component uses a single differential equation to describe the time course of plasma insulin by treating glucose plasma concentration as a known forcing function. De Gaetano and Arino (99) tried to couple the two parts, but they discovered it was difficult to simultaneously fit glucose and insulin data from the IVGTT. In order to overcome the difficulties of the coupled minimal model, they proposed a 'dynamic model' employing the delay differential equation.

The proposed model for glucose kinetics is based on the same assumptions as proposed in the minimal model (99). It is assumed that the disappearance of glucose is partly dependent on insulin concentration and partly dependent on glucose itself. The rate of insulin clearance from plasma is a first-order process and a delay term is used for

pancreatic insulin secretion (i.e., the effective pancreatic secretion at time *t* is considered to be proportional to the average value of glucose level in the $b_5$ minutes preceding time *t)*. The model describes the glucose and insulin kinetics as the following:

$$\frac{dC_G(t)}{dt} = -b_1 C_G(t) - b_4 C_I(t) + b_7$$
$$C_G(t) \equiv C_{G_b} \ \forall t \in [-b_5, 0), \qquad C_G(0) = C_{G_b} + b_0 \qquad \text{Eq. 2.132}$$

$$\frac{dC_I(t)}{dt} = -b_2 C_I(t) + \frac{b_6}{b_5} \int_{t-b_s}^{t} C_G(s)ds, \qquad C_I(0) = C_{I_b} + b_3 b_0 \qquad \text{Eq. 2.133}$$

where $b_1$ is the glucose first-order disappearance rate constant, $b_2$ is the insulin first-order disappearance, $b_3$ is the first-phase insulin concentration increase per increase in the concentration of glucose at time 0 due to the bolus injection, $b_4$ is the constant representing insulin-dependent glucose disappearance, $b_5$ is the length of the past period whose plasma glucose concentration influence the current pancreatic insulin secretion; $b_6$ is the constant amount of second-phase insulin release rate per of average plasma glucose concentration throughout the previous $b_5$ minutes and $b_7$ is the rate constant of basal insulin secretion rate.

The advantage of this model is that glucose and insulin time courses were described simultaneously and account for the glucose-insulin feedback relationship. The model has been used to deal with data from IVGTT and showed good agreement with experimental data. However, the description of first-phase fitting is not good. The model can also be used for protocols other that IVGTT according to the authors.

### *2.3.2 Disease progression model for type 2 diabetes*

Type 2 diabetes (T2D) is a chronic disease progressing over a long time period. Several efforts have been made in developing new antidiabetic drugs that can alter disease progression. Therefore, it is particularly important to consider disease progression in the PK/PD model for long-term studies of drug effects and disease progression.

De Winter *et al.* (100) developed a disease progression model and utilized it to compare the long-terms effect of three antidiabetic agents, pioglitazone, metformin and gliclazide, against the progression of T2D. The study originated from the fact that some conventional anti-hyperglycemic agents, such as insulin, various sulfonylureas, and metformin do not affect the progression of T2D, despite being efficacious for glycemic control over the short term. These findings point to the need for agents with long-term disease-modifying properties. The authors modeled the homeostatic feedback relationships between glucose and insulin, and described the disease as a disturbance of homeostasis based on an indirect response model in which $k_{in}$ and $k_{out}$ were changed by the disease.

Pioglitazone, metformin and gliclazide are anti-hyperglycemic agents working with different physiological mechanism. Pioglitazone is a novel member of the thiazolidinedione class of insulin sentilizer, increasing insulin sensitivity in liver, muscle and adipose tissue. Hence, it promotes peripheral glucose uptake as well as reduces hepatic glucose production. Metformin is also an insulin sensitizer and acts mainly by suppressing hepatic glucose production. Gliclazide is classified as secretagogue, which stimulates pancreatic insulin secretion.

Glycosylated hemoglobin $A_{1c}$ ($HbA_{1c}$) is used as the primary biomarker in this study. As the average amount of plasma glucose increases, the fraction of glycated hemoglobin increases accordingly. Once a hemoglobin molecule is glycated, it remains this way. Plasma glucose and insulin concentrations fluctuate throughout the day because of food ingestion, while the $HbA_{1c}$ concentration remains stable. The $HbA_{1c}$ measurement reflects the average glucose concentration which the cell has been exposed to during its life cycle of approximately four weeks to three months. Therefore, $HbA_{1c}$ provides reliable information of glycemic control over the long-term period and serves as a marker for average blood glucose levels. Fasting plasma glucose concentration (FPG) and fasting

serum insulin concentration (FSI) are secondary biomarkers, which are more responsive to changes in glycemic control in the short-term period.

The structure of the disease model and the actions of different classes of drugs on the maintaining glycemic control are shown in Figure 2.12. The model includes mechanism-based expressions (Eq. 134-136) for the relationship between FPS and FSI. It was assumed that the production of FSI is proportional to the FPG as FPG exceeds the empirical value of 3.5 mmol/l, and the production of FPG is inversely proportional to the FSI, while the production rate of $HbA_{1c}$ is proportional to the FPG.

$$\frac{dFSI(t)}{dt} = EF_B \cdot B \cdot (FPG(t) - 3.5) \cdot k_{in\,(FSI)} - FSI(t) \cdot k_{out\,(FSI)} \qquad \text{Eq. 2.134}$$

$$\frac{dFPG(t)}{dt} = \frac{k_{in\,(FPG)} FPG(t)}{EF_S \cdot S \cdot FSI(t)} - FPG(t) \cdot k_{out\,(FPG)} \qquad \text{Eq. 2.135}$$

$$\frac{dHbA_{1C}(t)}{dt} = FPG(t) \cdot k_{in(HbA1c)} - HbA_{1c}(t) k_{out\,(HbA1c)} \qquad \text{Eq. 2.136}$$

where $k_{in}$ and $k_{out}$ are influx and efflux rate constants for *FSI(t), FPG(t)* and $Hb_{A1c}(t)$, and $EF_B$ and $EF_S$ are parameters related to treatment effects of drugs on beta-cell function and insulin sensitivity, respectively. Values of $EF_B$ greater than 1 indicates the stimulatory effect of drugs, such as gliclazide on beta-cells, while loss of beta-cell function reflected in values of $EF_B$ is smaller than 1. $EF_S$ reflects insulin sensitivity with value from 0 to 1, representing the suppressing effects of pioglitazone and metformin on hepatic glucose production.

The coefficient *B* and *S* correspond to HOMA-B and HOMA-S of homeostasis model assessment (HOMA). *B* is the fraction of remaining beta-cell function and *S* is the fraction of remaining hepatic insulin sensitivity in diabetic patients relative to the value in healthy persons. During the progression from normal glucose tolerance to T2D, both beta-cell function and insulin sensitivity are gradually lost, thus *B* and *S* should decrease over the range from 1 to 0 as a function of time. *B* and *S* were modeled as following:

$$B = \frac{1}{1+\exp(b_0 + r_B \cdot t)} \quad \text{Eq. 2.137}$$

$$S = \frac{1}{1+\exp(s_0 + r_S \cdot t)} \quad \text{Eq. 2.138}$$

where parameters $r_B$ and $r_S$ determine the rate of change over time in beta-cell function ($B$) and insulin sensitivity ($S$); and $b_0$ and $s_0$ are initial condition of the disease progression curves, calculated according to the HOMA-%B and HOMA-%S.

This disease progression PK/PD model combined with population analysis has shown it has the ability to distinguish the disease-modifying properties of a treatment from its direct short-term impact on hyperglycemia. $EF_B$ and $EF_S$ account for short-term influence of drugs on the disease state, while $r_B$ and $r_S$ are associated with the disease-modifying effects. By this model, it was also found that both metformin and pioglitazone therapy shows a steady improvement in beta-cell function as well as reducing FPG levels immediately as expected from insulin sensitizers. However, the model predicted disease-modifying effects of metformin that stand in contrast with those found from a clinical trial (100). The authors argued that the disease-modifying effect of metformin on beta-cell function is due to the misspecification of metformin's action.

In summary, the model has several advantages. It integrates the interactions of fasting glucose, insulin, HbA1c, insulin sensitivity, and beta-cell function and also the effects of drugs with different mechanisms of action. Disease progression was described as the changes in beta-cell function and insulin sensitivity. Therefore, the model has the promise to be a valuable tool for the evaluation of a drug's disease-modifying effects. However, the authors reported that there is a model misspecification for metformin that leads to a disagreement with the findings from another clinical trial (100).

### *2.3.3 Model of beta-cell mass, insulin, and glucose kinetics pathways to diabetes ( $\beta GI$ model)*

Type 2 diabetes (T2D) is associated with the insulin resistance, reduced insulin secretion and loss of beta-cell mass (130). The relative contribution and interaction of these defects in the onset of T2D remains to be clarified.

Topp and his colleagues (101) formulated a model that describes beta-cell mass, and glucose and insulin dynamics aimed at studying the normal behavior of the glucose regulatory system and the path towards diabetes. The model was formulated based on the assumptions that a moderate increase in glucose concentration results in a growth of a beta-cell mass, while severe and persistent hyperglycemia leads to loss of the beta-cell mass. The equations that describe glucose, insulin, and beta-cell mass dynamics are based on physiological observations from a number of *in vitro* experiments.

A single compartment model was used to describe glucose kinetics. It was found that when glucose concentrations change rapidly, a single compartment model is not adequate. Accordingly, the first-phase is not considered in the minimal model under the IVGTT. However, the focus of this study is an evolution of the fasting glucose concentration. Thus, the glucose dynamics was appropriately modeled with a single compartment model.

Experimentally, the relationship between glucose and insulin can be measured by breaking the feedback loop, such as via the glucose clamp technique at various steady-state blood glucose and insulin levels. Both glucose production and uptake are found to be linearly related to glucose concentration ($C_G$) and the slope is defined as glucose effectiveness ($E$). Hyperinsulinemic clamp studies indicate that glucose effectiveness is proportionally related to insulin concentrations ($C_I$). Based on these findings, the following model was used to describe the rate of change in plasma glucose:

$$\text{Production} = P_0 - (E_{GOP} + S_{IP} C_I)\, C_G \qquad \text{Eq. 2.139}$$

$$\text{Uptake} = U_0 + (E_{GOU} + S_{IU} C_I(t)) C_G(t) \quad \text{Eq. 2.140}$$

$$\begin{aligned} \frac{dG(t)}{dt} &= \text{Production} - \text{Uptake} \\ &= R_0 - (E_{G0} + S_I C_I(t)) C_G(t) \end{aligned} \quad \text{Eq. 2.141}$$

where $P_0$ and $U_0$ are the rate of glucose production and uptake at zero glucose level, $E_{GOP}$ and $E_{GOU}$ denote glucose effectiveness at zero insulin for production and uptake, $S_{IP}$ and $S_{IU}$ are insulin sensitivity for production and uptake, $R_0$ (equal to $P_0$-$U_0$) is the net rate of production, $E_{G0}$ (equal to $E_{GOP}$ +$E_{GOU}$) is defined as the total glucose effectiveness and $S_I$ (equal to $S_{IP}$+$S_{IU}$) is the total insulin sensitivity.

The authors model insulin kinetics with a single compartment. The rate of insulin clearance is a first-order process as used in most studies of insulin kinetics. A Hill function is used to describe pancreatic insulin secretion which depends on glucose concentrations and the beta-cell mass:

$$\text{Secretion} = \frac{\beta(t)\sigma C_G(t)^2}{\alpha + C_G(t)^2} \quad \text{Eq. 2.142}$$

where $\beta$ is the mass of pancreatic beta-cell; $\sigma$ is the insulin secretion rate from beta-cell, which is supposed to be homeostasis throughout the pancreas and release insulin at the same rate; and $\alpha$ is the Hill function parameter. Therefore, the insulin kinetics is described as:

$$\frac{dC_I(t)}{dt} = \frac{\beta\sigma C_G(t)^2}{\alpha + C_G(t)^2} - kC_I(t) \quad \text{Eq. 2.143}$$

The $\beta IG$ model supposes that beta-cell replication and death rate are nonlinear with respect to blood glucose levels. The formation of beta-cell mass increases with the increasing glucose concentrations and reduces at extreme high levels of glucose. The authors use polynomial functions to describe the rate of beta-cells formation and loss as in Eq. 2.144 and 2.145, respectively:

$$\text{Formation} = (r_{1r} C_G(t) - r_{2r} C_G(t)^2)\beta(t) \quad \text{Eq. 2.144}$$

$$Loss = (d_0 - r_{1a}C_G(t) - r_{2a}C_G(t)^2)\beta(t) \quad \text{Eq. 2.145}$$

where $r_{1r}$ and $r_{2r}$ are constant parameters of the polynomial function for beta-cell mass formation, $d_0$ indicates the death rate of the beta-cells at zero glucose, and $r_{1a}$ and $r_{2a}$ are constants of the polynomial function for beta-cell mass loss. The rate of change in beta-cell mass is then written as:

$$\begin{aligned} \frac{d\beta(t)}{dt} &= \text{Formation} - \text{Loss} \\ &= (d_0 - r_{1a}C_G(t) - r_{2a}C_G(t)^2)\beta(t) \end{aligned} \quad \text{Eq. 2.146}$$

where $r_1 = r_{1r} + r_{1a}$ and $r_2 = r_{2r} + r_{2a}$.

Glucose toxicity has been thought to be associated with pancreatic exhaustion for many years. By use of this model, the pathways from normal glucose to the beta-cell mass loss and overt diabetes were simulated. The model provides a tool that explains the adaptation of plasma insulin levels to insulin resistance. The failure of this adaptation is followed by a reduced plasma insulin secretion and hyperglycemia.

The $\beta IG$ model predicts a critical glucose concentrations (>250 mg/dl) at which the beta-cell death rate exceeds formation rate, driving the system towards diabetes. The relationship between the beta-cell mass and insulin sensitivity can also be predicted from the model. If insulin sensitivity is reduced slowly, then the beta-cell mass adapts and maintains mild hyperglycemia. On the other hand, if insulin sensitivity is reduced too quickly, the beta-cell mass adapts for some period of time, but eventually the glucose level become larger than the pathological limit (250 mg/dl), and the beta-cell mass begins to decrease. The $\beta IG$ model may provide theoretical estimation of beta-cell mass which is impossible to experimentally estimate *in vivo*. However, the study did not show model performance with real data.

### *2.3.4 Integrated model for glucose and insulin regulation*

Silber *et al.*(102) developed a model for describing glucose and insulin feedback control of glucose homeostasis. The effect compartments were introduced to account for

feedback regulation without affecting the mass balance. The integrated model shown in Figure 2.13 is based on several types of IVGTT, including an IVGTT with labeled glucose with or without insulin infusion to better identify the relevant kinetic parameters.

Glucose kinetics was described by a two-compartment model. The glucose is eliminated from the central compartment ($G_C$) through insulin-independent and insulin-dependent (influenced by $I_E$) pathway. Endogenous glucose ($G_{PROD}$) enters the central compartment. The glucose model had two effect compartments ($G_{E1}$ and $G_{E2}$) representing the control of endogenous glucose and second-phase insulin secretion, respcetively. The following differential equations were used to describe the kinetics for the central compartment, $G_C$, the peripheral compartment, $G_P$, and the two effect compartments:

$$\frac{dG_C(t)}{dt} = G_{PROD}(t) + \frac{Q}{V_P}G_P(t) - (\frac{CL_G}{V_G} + \frac{CL_{GI}}{V_G}I_E(t) + \frac{Q}{V_G})G_C(t) \qquad G_C(0) = G_{SS} * V_G$$

Eq. 2.147

$$\frac{dG_P(t)}{dt} = \frac{Q}{V_G}G_C(t) + \frac{Q}{V_p})G_p(t) \qquad G_p(0) = G_{SS} * V_p$$

Eq. 2.148

$$\frac{dG_{E1}(t)}{dt} = K_{GE1}\frac{G_C(t)}{V_G} - K_{GE1}G_{E1}(t) \qquad G_{E1}(0) = G_{SS}$$

Eq. 2.149

$$\frac{dG_{E2}(t)}{dt} = K_{GE2}\frac{G_C(t)}{V_G} - K_{GE2}\cdot G_{E2}(t) \qquad G_{E2}(0) = G_{SS}$$

Eq. 2.150

where $V_G$ and $V_P$ are the volumes of distribution of glucose in central and peripheral compartment, respectively; $G_{SS}$ is steady state glucose concentration; $Q$ is the intercompartmental clearance of glucose; $CL_G$ and $CL_{GI}$ are the insulin-independent and insulin-dependent clearance of glucose from the central compartment, respectively; and $K_{GE1}$ and $K_{GE2}$ are rate constants for the effect compartments, respectively.

Endogenous glucose production at steady state ($G_{PROD,0}$) is described by Eq.151. Glucose effect on its production ($G_{CM1}$) is modeled by a power function of the ratio of $G_{E1}$ to $G_{SS}$ as shown in Eq. 2.152 in which the power *GPRG* is an estimated parameter. The endogenous glucose production rate is finally expressed as in Eq. 2.153:

$$G_{PROD,0} = G_{SS}(CL_G + CL_{GI} I_{SS}) \quad \text{Eq. 2.151}$$

$$G_{CM1}(t) = \frac{G_{E1}(t)}{G_{SS}}^{GPRG} \quad \text{Eq. 2.152}$$

$$G_{PROD}(t) = G_{PROD,0} \cdot G_{CM1}(t) \quad \text{Eq. 2.153}$$

First-phase insulin secretion was modeled as a bolus dose which enters the disposition compartment ($I$) through a delay compartment ($I_{FPS}$). Given the rate constant as $K_{IS}$, the rate in change in first-phase insulin secretion is expressed as:

$$\frac{dI_{FPS}(t)}{dt} = -K_{IS} \cdot I_{FPS}(t) \qquad I_{FPS}(0^+) = FPS \quad \text{Eq. 2.154}$$

, where $K_{IS}$ is the rate constant.

Second-phase secretion was modeled with the same type of expression that was used for endogenous glucose production. The basal insulin secretion rate ($I_{SEC,0}$) is equal to the product of the steady state insulin concentration ($I_{SS}$) and the clearance of insulin from the central compartment. A power function was used to describe the regulation of glucose on insulin production ($G_{CM2}$). The insulin model has one effect compartment for the regulation of insulin-dependent glucose elimination. Insulin is eliminated from the plasma by a first-order process. Given the insulin disposition compartment $I$, and effect compartment $I_E$, the first-phase and second-phase insulin release rates are described by following equations:

$$\frac{dI(t)}{dt} = I_{SEC}(t) - \frac{CL_I(t)}{V_I} I(t) \quad I(0) = I_{SS} V_I \quad \text{Eq. 2.155}$$

$$\frac{dI_E(t)}{dt} = K_{IE}\frac{I(t)}{V_I} - K_{IE}\cdot I_E(t) \qquad I_E(0) = I_{SS} \quad \text{Eq. 2.156}$$

$$I_{SEC,0} = I_{SS}\cdot CL_I \quad \text{Eq. 2.157}$$

$$G_{CM2}(t) = \left(\frac{G_{E2}(t)}{G_{SS}}\right)^{IPRG} \quad \text{Eq. 2.158}$$

$$I_{SEC}(t) = I_{SEC,0}G_{CM2}(t) + K_{IS}I_{FPS}(t) \quad \text{Eq. 2.159}$$

where $V_I$ is the insulin volume of distribution, $CL_I$ is the insulin clearance, $K_{IE}$ is the rate constant associated with insulin compartment, $K_{IS}$ is the rate constant describing first-phase insulin secretion and *IPRG* is the parameter of the power function.

The model has shown good performance in simultaneously predicting the dynamics of insulin and glucose under various types of IVGTTs. The model may be used for impact analysis of antidiabetic drugs on diabetes development. However, the model has fifteen parameters, thus it needs intensive data to properly identify the kinetic system.

## 2.4 Conclusions

Our understanding of the glucose and insulin system can be enhanced by kinetic modeling. Numerous PK/PD models have been developed for the assessment of insulin sensitivity and beta-cell function. Minimal model and its variants provide indices that quantify insulin sensitivity, glucose effectiveness and beta-cell function from clinical test (IVGTT, hot IVGTT and OGTT), but these models are mainly descriptive, not mechanistic. In recents days, modeling in this area has progressed to the more mechanism-based models with the goal of improving early diagnosis of diabetes and explanation of the progression to T2D. Thus, it is natural to include current knowledge for the mechanism of insulin biphasic secretion in PK/PD modeling, which will be addressed in this study.

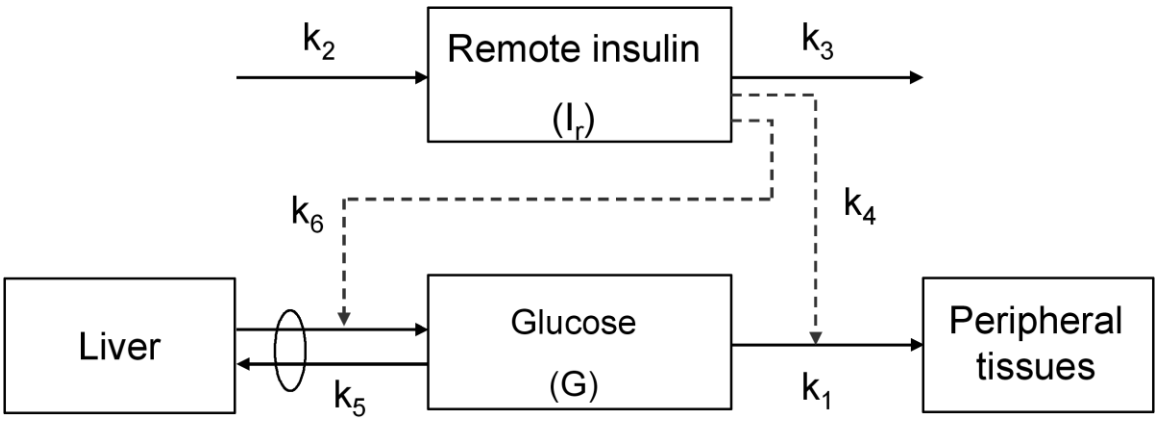


Figure 2.1. Compartmental structure of minimal model of glucose disappearance in response to intravenous glucose tolerance test.

Plasma insulin enters a hypothesized remote insulin compartment ($I_r$) to lower glucose ($G$) level by accelerating its disappearance into peripheral tissues through parameter $k_4$ and suppressing hepatic glucose through parameter $k_6$ (56).

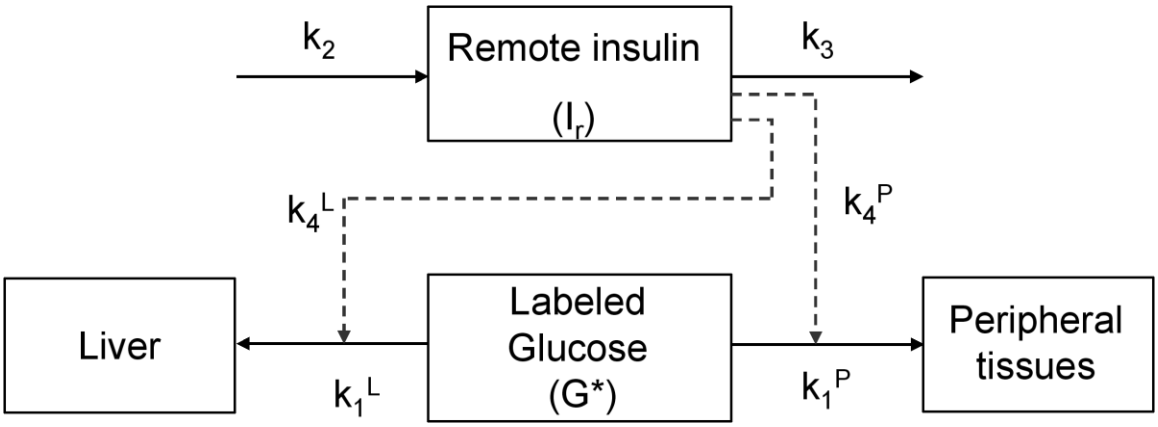


Figure 2.2. Diagram of minimal model of glucose disappearance with labeled IVGTT.

Tracer (*G**) disappears from plasma into liver and peripheral tissues. Insulin acts from a remote compartment ($I_r$) (93).

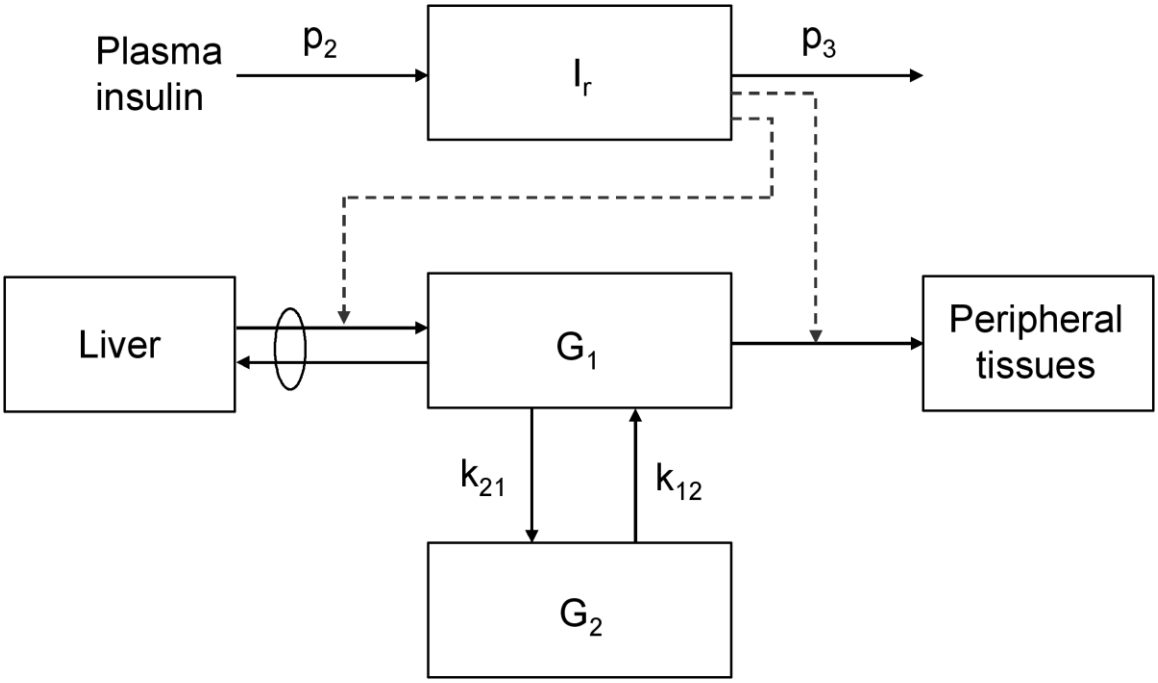


Figure 2.3. Two-compartment minimal model.

$G_1$ and $G_2$ are glucose masses in the accessible (blood) and nonaccessible compartments, respectively; $k_{12}$ and $k_{21}$ are rate parameters describing glucose exchange kinetics (92).

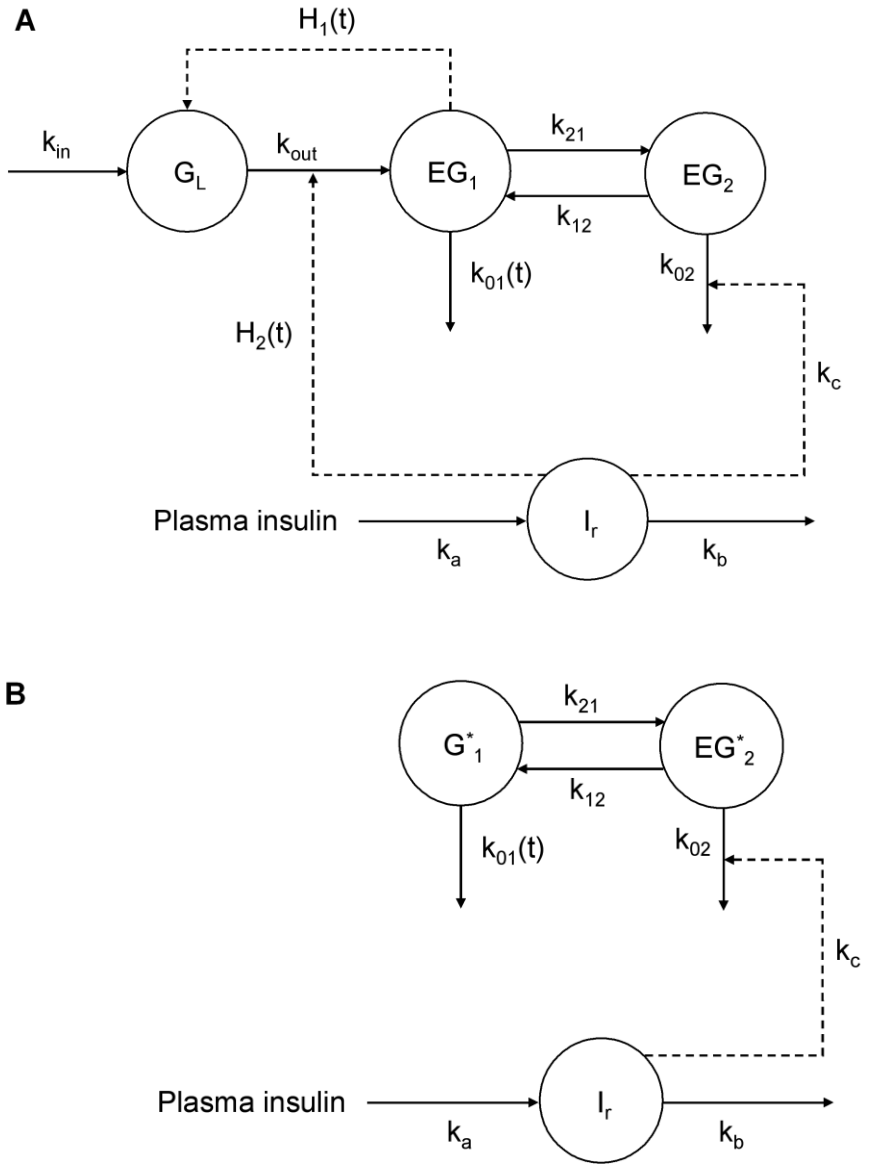


Figure 2.4 Diagram of two-compartment minimal model with endogenous glucose production.

*EG₁* and *EG₂* are endogenous glucose masses in the accessible and nonaccessible compartment, respectively; $G_L$ represents the amount of glucose in the liver; $k_{in}$ is the rate constant of hepatic glucose formation; $k_{out}$ is the rate constant of hepatic glucose secretion; $H_1(t)$ is glucose effect on glucose production; $H_2(t)$ is inhibit effect of remote insulin ($I_r$) on glucose secretion (113).

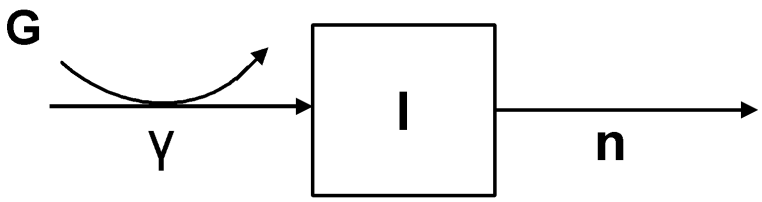


Figure 2.5. Minimal model of insulin kinetics.

A single compartment is used to describe the insulin kinetics. *G* represents glucose that influence the insulin production rate and *I* is insulin, and $\gamma$ and *n* are the rate constants associated with insulin production and elimination; respectively (55).

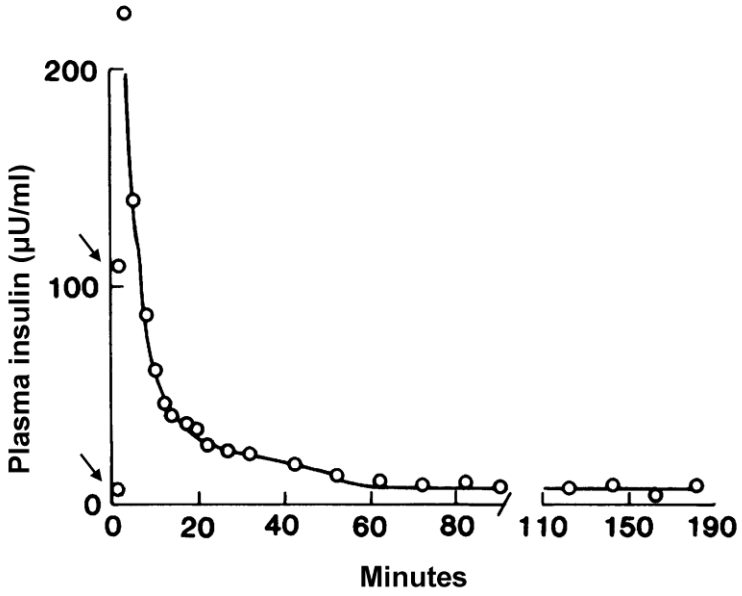


Figure 2.6. Ability of minimal model to describe insulin kinetics during IVGTT.

Observations are represented by open circles and predictions are solid curves. The early first-phase observations indicated by arrows are not used in the analysis using the insulin minimal model (54).

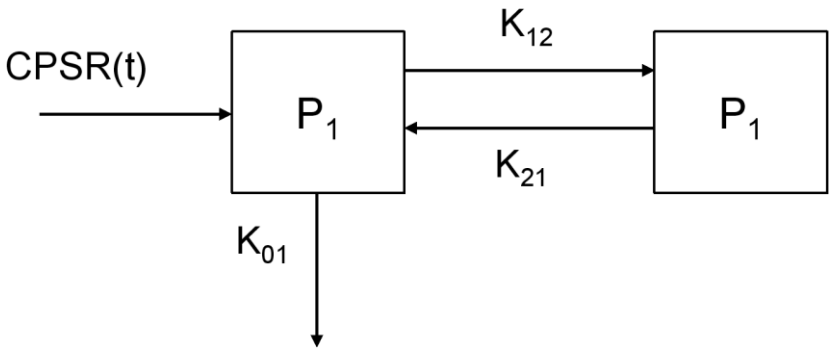


Figure 2.7. Two-compartment model of C-peptide kinetics.

$P_1$ and $P_2$ represent C-peptide in plasma and extravasacular tissues, respectively; *CPSR(t)* is C-peptide secretion rate from pancreas; $K_{12}$, $K_{21}$ and $K_{01}$ are kinetic transfer parameters (79).

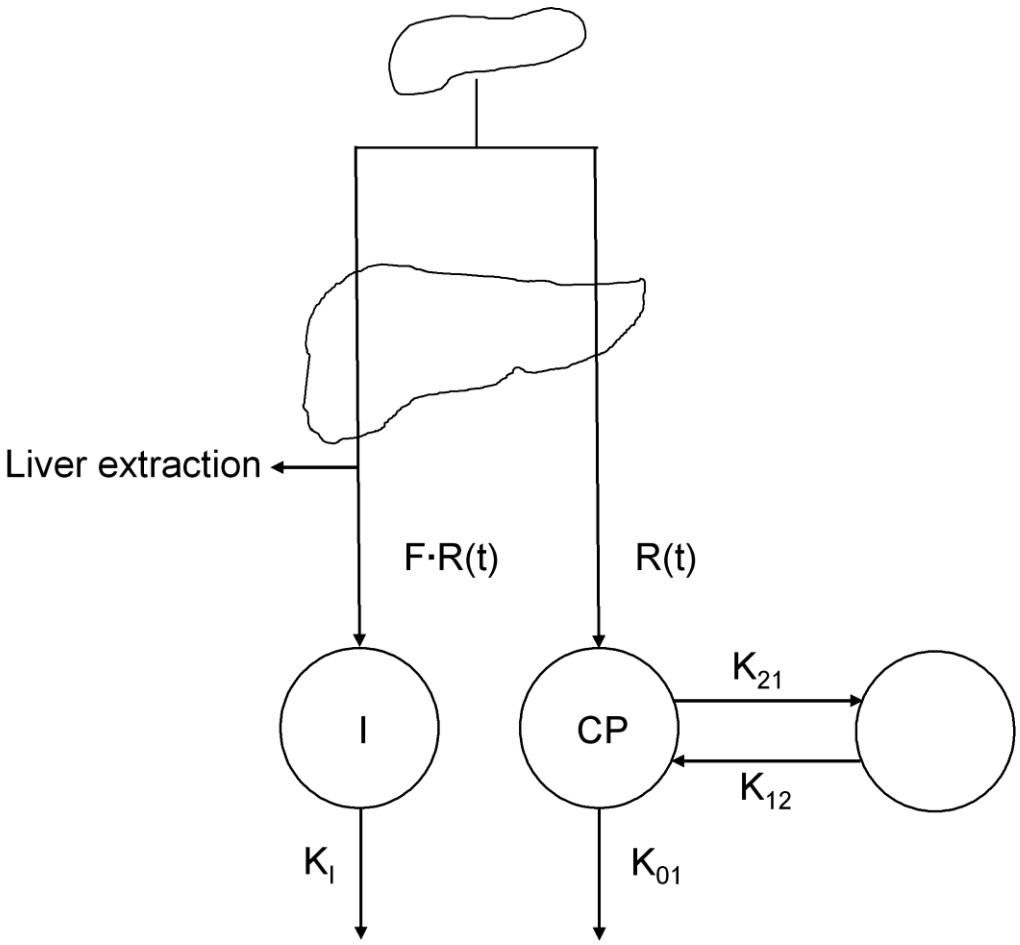


Figure 2.8. Extended combined model of insulin and C-peptide kinetics.

Insulin and C-peptide (CP) are co-secretion from beta-cell at the same rate, *R(t)*. *F·R(t)* denotes the insulin that reach the systemic circulation, and *(1-F)* is the hepatic insulin extraction ratio. The C-peptide kinetics is described by a two-compartment model (124).

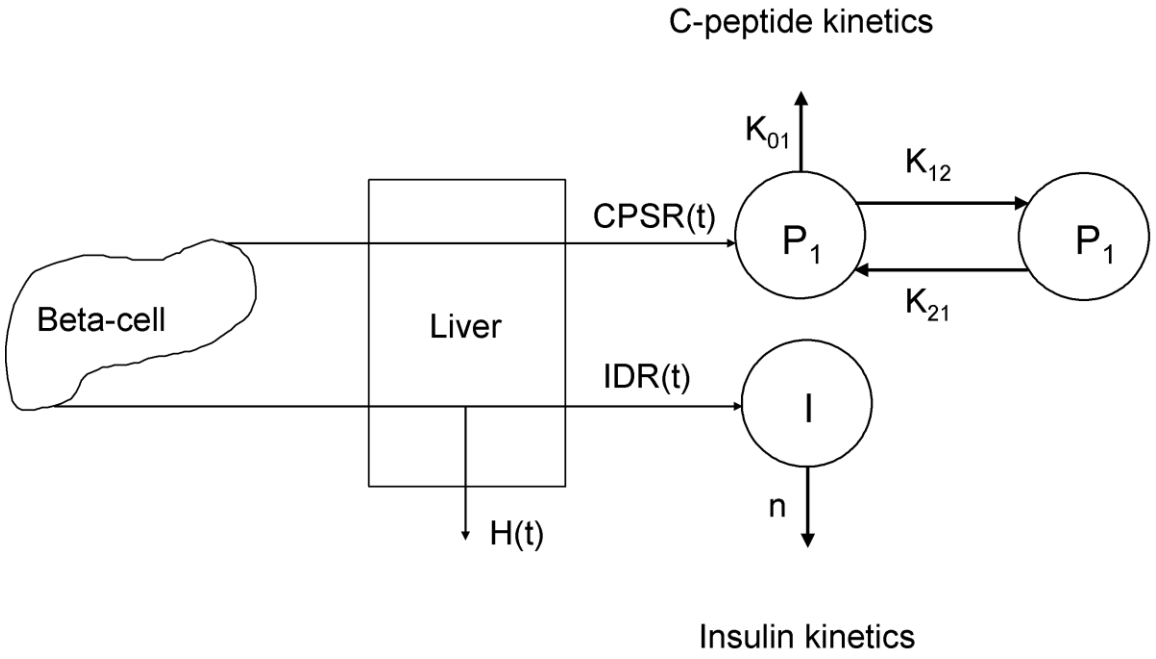


Figure 2.9. Schematic representation of the assessment of hepatic insulin extraction.

Insulin and C-peptide are released from pancreas in response to glucose in equimolar amounts. A fraction of insulin, *H(t)*, is removed by liver with no extraction of C-peptide. A two-compartment model is used to describe the C-peptide kinetics, and a single compartment minimal model to describe the insulin kinetics (127).

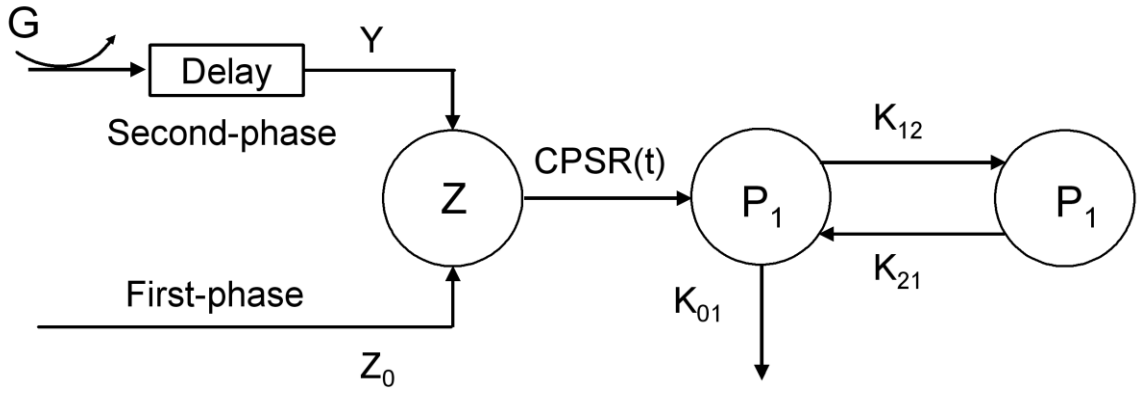


Figure 2.10. Minimal model of C-peptide kinetics with a delayed component.

*G* denotes glucose; *Y* is provision of new insulin; $P_1$ and $P_2$ are C-peptide amount above basal level in plasma and extravascular tissues, respectively; $Z_0$ is the initial amount of releasable insulin in the beta-cell in response to glucose-stimulation and *CPSR(t)* is the insulin secretion rate from beta-cells (98).

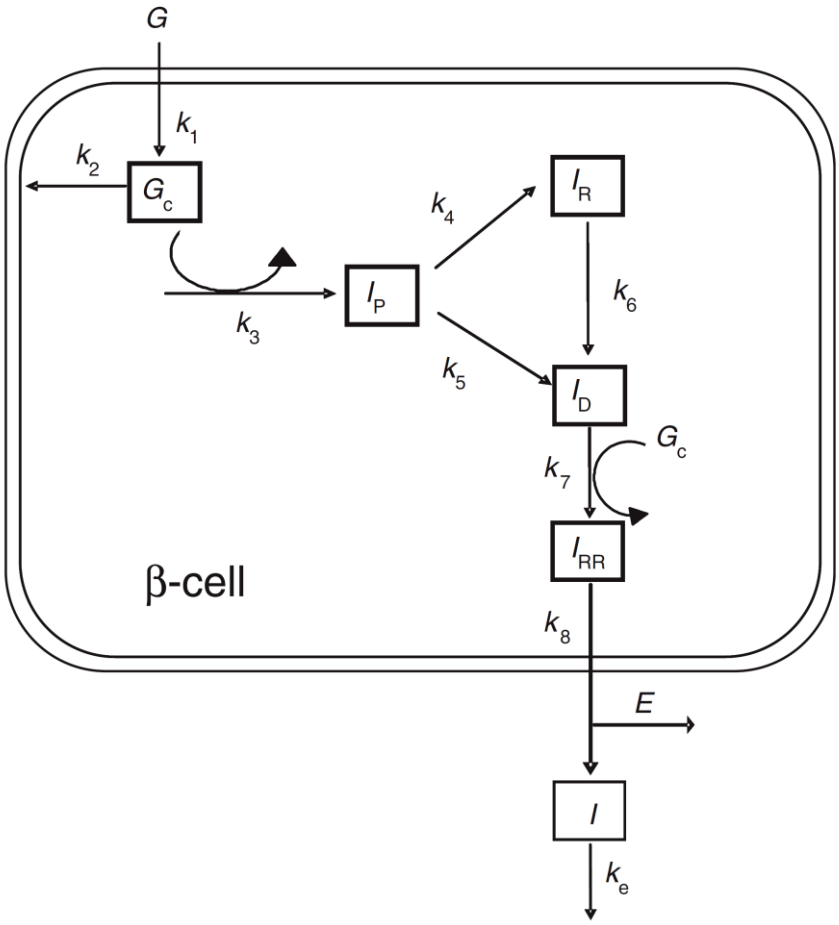


Figure 2.11. Gupta *et al.* model describing insulin physiology in the beta-cell.

$G$ is glucose in plasma; $G_C$ is cellular glucose; $I_P$ is proinsulin pool; $I_R$ is reserved insulin pool; $I_D$ is docked insulin pool; $I_{RR}$ is readily releasable insulin pool; $I$ is insulin in plasma; $E$ is the hepatic extraction ratio and $k_1$ to $k_9$ are rate constants (97, 118).

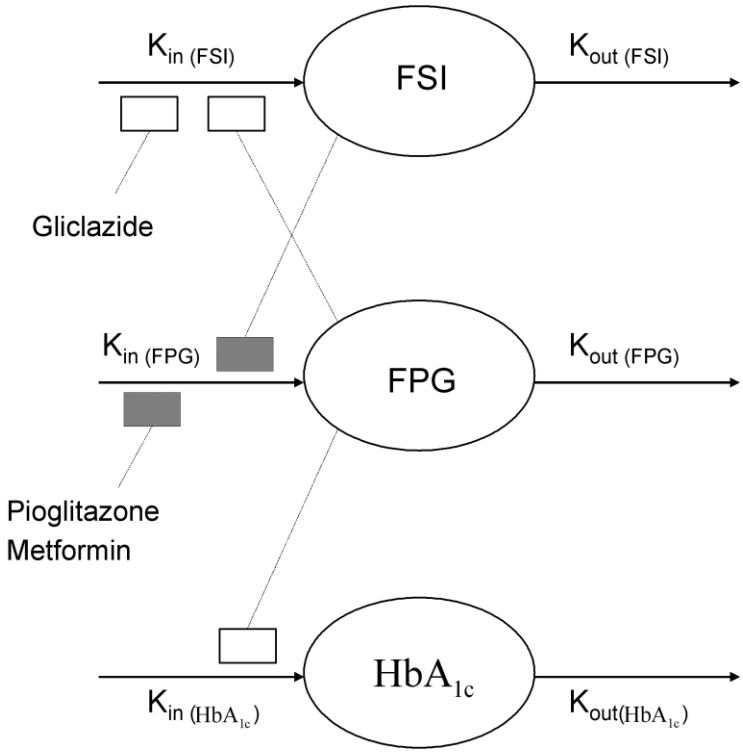


Figure 2.12. Diabetes progression model for long-term effects of antidiabetic drugs.

*FSI*, *FPG* and $HbA_{1C}$ represent fasting serum insulin, fasting plasma glucose and glycosylated haemoglobin, respectively; $k_{in}$ and $k_{out}$ are first-order rate constants (100).

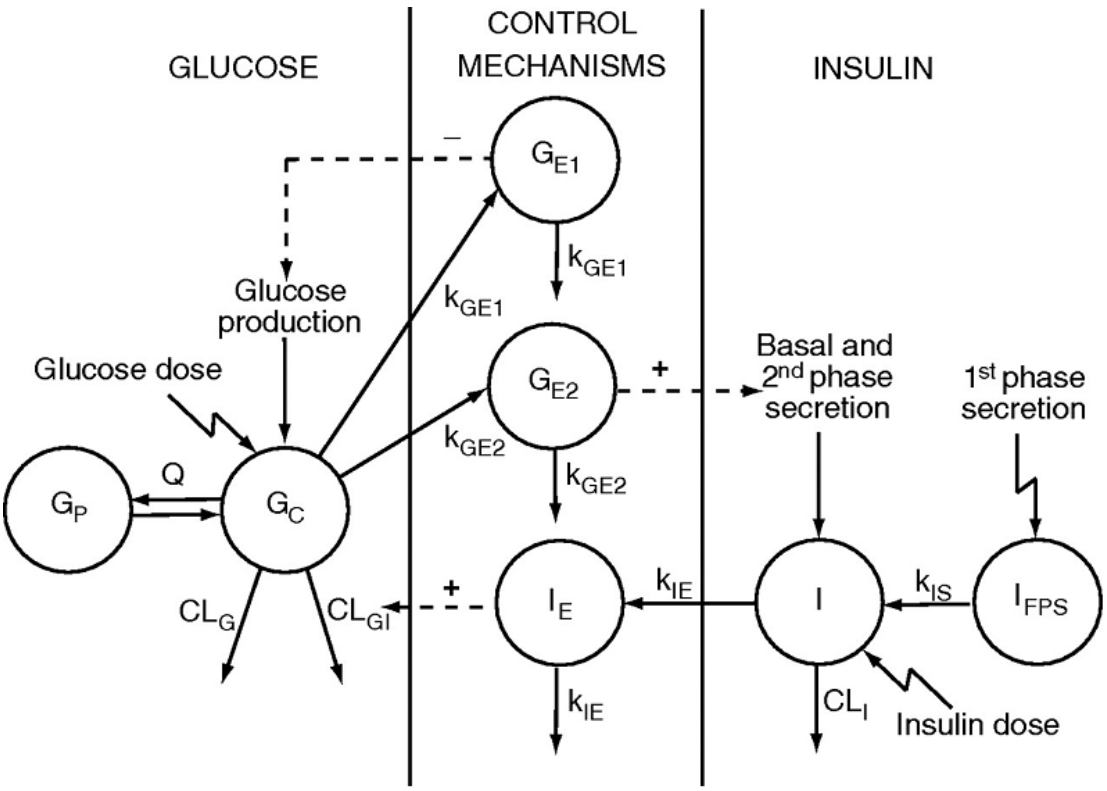


Figrue 2.13. Integrated model including glucose, insulin and regulations of glucose production, glucose elimination and insulin secretion.

Full arrows indicate flows, and broken arrows represent control mechanisms. A two-compartment model is used to describe glucose kinetics, in which $G_C$ and $G_P$ are central and peripheral compartments of glucose, $G_{E1}$ and $G_{E2}$ are effect compartments that control glucose production and insulin secretion, respectively. Insulin kinetics includes a disposition compartment, $I$, a delay compartment, $I_{FPS}$, for first-phase insulin release, and a effect compartment, $I_E$, for control of glucose elimination (102) .

# CHAPTER 3. POPULATION ANALYSIS APPROACH

Lewis B Sheiner and Stuart L Beal inspired and led the earliest work in the development of population pharmacokinetics. They published a series of papers (131-135) in the 1970's and 1980's that described a new approach capable of estimating population-based PK parameters with sparse samples (only 2 or 3 samples) collected from subjects. This approach was recently termed as 'population pharmacokinetics (PK) analysis' and implemented in a software package called NONMEM.

Population PK/PD modeling seeks to integrate various sources of variability, such as intra- and inter-individual variability in drug abortion, disposition, and action into the modeling process. Thus, it provides a valuable tool to quantitatively define typical parameters and their variations in target populations treated with a drug. Population modeling finds its most important uses in direct patient care and drug development. It provides quantitative guidelines for individualized and optimized dose regimens by analyzing the data obtained from clinical monitoring and based on patent-specific covariates (e.g., age, sex, and disease history). In recent years, population methods have played an important role in drug development. Although a non-compartmental approach is still used for many phase I studies, population-based methods are commonly used for phase II and III studies, as well as to analyze combined data from different clinical trials. This approach is helpful in understanding the quantitative relationship between patient characteristics and drug behavior, or explaining variability in a target population.

Population analysis has several important advantages. Firstly, unlike the traditional PK/PD studies which require intensive samplings, population analysis can be done with sparse or intensive data. The population method can give better estimates of variability, such as inter-individual, intra-individual, and interoccation variability, versus biased estimates derived from traditional approaches. The method can also utilize heterogenous types of data from various sources, such as data from several different

trials, study centers or sparse samples. Secondly, population analysis provides not only an opportunity to estimate variability, but also to recognize the sources that may either by explained through identifying factors or remain unexplained. Thirdly, population modeling can incorporate covariates to assess variability caused by factors, such as demographics, or pathophysiologic- and drug-related changes in the behavior of a drug.

The main disadvantages of the population PK/PD method are rooted in its mathematical and statistical complexity. Population analysis requires appropriate modeling of inter- and intra-individual variations and covariates. Additionally, it requires appropriate assumptions for the random- and fixed-effects distribution models.

Over the past few decades, various techniques have been used to perform population analysis, for instance naïve pool data approach, two-stage approach, nonlinear mixed-effects model, Bayesian hierarchical model, and nonparametric maximum likelihood. In this chapter, naïve pool data, two-stage, and nonlinear mixed-effects approaches were discussed.

The following notations are commonly used in population modeling:

$y$: the observation, typically a drug level in plasma;

$x$ : the collection of independent variables other than time, such as age, sex, etc;

$i$: individuals;

$k$: the number of individuals studied, $i$=1,2,3, …$k$;

$j$: an observation;

$n_i$: the number of observations within an individual $j$=1, 2, 3, ….., $n_i$.

### 3.1 Individual data model

A data set and a model are needed in the analysis. The corresponding data model for an individual has an explained portion and an unexplained portion. The explained component is usually a function of certain parameters and covariates. The unexplained part is the residual random error. The individual data model takes the form:

$$y_j = f(\phi, x_j) + \varepsilon_{ij} \quad \text{Eq. 3.1}$$

where $y_j$ is the *j*th observation of the individual; $f(\phi, x_j)$ is a parameterized function describing a response and give a predicted value based on $x_j$ within the individual; $\phi$ is a parameter vector of the PK/PD model reflects the relationship between *x* and *y*; and $\varepsilon_j$ is the residual error.

All the residual errors of observations of an individual, $\varepsilon_1, \varepsilon_2, ...\varepsilon_{ni}$, arise from a normal distribution with a mean of zero and variance $\sigma_j^2$. The value of $\sigma_j^2$ across each observation can be assumed to be constant or modeled into the modeling process if the residual changes with observed values. For example, a log-normal structure is often used in biological system and describe by:

$$y_j = f(\phi, x_j, t_j) \cdot e^{\varepsilon_j} \quad \text{Eq. 3.2}$$

where $\varepsilon_j$ has a normal distribution with median 1 and constant value of variation. This log-normal form error is appropriate when the measurements always are positive and less precision when the value of measurement increases. Other error structures are also used in practice, such as additive, proportional or combination of additive and proportional type. Maximum likelihood estimation (MLE) can be performed if the statistics of $\varepsilon_j$ are known. When all of $\varepsilon_j$ are assumed to be normal with zero mean and uniform variance, maximum likelihood estimation becomes ordinary least-squares estimation.

### 3.2 Population data model

Compared to individual data model, a more elaborate statistical model is required to deal with population data. In the population analysis, the overall variability in the measured PK/PD response in a sample of an individual is attributed to the measurement error and inter-individual variability. The population model can take the following form:

$$y_{ij} = f(\phi + \eta_i, x_{ij}) + \varepsilon_{ij} \quad \text{Eq. 3.3}$$

$$\phi_i = g(x_{ij}) \quad \text{Eq. 3.4}$$

Thus, $y_{ij}$ is the *j*th observation of the *i*th individual, *f* is the PK/PD model that describes the relationship between *x* and *y*, *g* is a function that describes the relationship between the parameters $\phi_i$ and covariates $x_i$, $\eta_i$ is a random variable of parameters of *i*th subject having a normal distribution with mean zero and variance $\omega_i^2$, and $\varepsilon_{ij}$ is the residual error.

Within the *i*th individual, the value of $\varepsilon_j$ is normally distributed and has a mean of zero. The variable $\varepsilon_{ij}$ can be coded in the population model as was previously discussed in the individual data model. The whole population has just one value for each model parameter $\phi$. Individual values of the parameter $\phi_i$ is determined by the random variable $\eta_i$ and covariates $x_i$. The $\eta_i$ is often assumed to be independent and has constant variance across individuals. An $\eta$ is normally distributed with mean of zero and variance $\omega^2$.

## 3.3 Approaches applied to population PK/PD modeling

### *3.3.1 Naïve pooled data approach*

The simplest method to estimate population parameters is the naïve pooled data (NPD) approach. It pools all the data from all individuals as if the data were arising from the same individual. With a least-squares fitting, the parameter vector is calculated by assuming $y_{ij}^*$ is a prediction from the least-square method and minimizing the objective function:

$$O_{NPD}(\phi_i) = \sum_{i=1}^{k}\sum_{j=1}^{n_i}(y_{ij} - y_{ij}^*)^2 \qquad \text{Eq. 3.5}$$

This method does not provide a reasonable estimate of the intersubject variability of the parameters. NPD can easily deal with rich data, sparse data, and a mixture of both. It may perform well when variations between subjects are small. This is occasionally the case in a group with homogeneous PK/PD characteristics, but it is rarely true in humans, especially in the clinical setting. The disadvantage of NPD is that it ignores the differences in parameters between subjects, thus no information is available for

individual parameters. The NPD estimate for the parameter should be considered as a rough approximation of the population parameters of $\phi$. This method is currently rarely used in population analysis.

### *3.3.2 Two-stage method*

The standard two-stage (STS) approach is a well-known and widely-used procedure. With this approach, each individual's parameters are estimated in the first stage through ordinary least square method by individually fitting data from the individual. The first stage is described by:

$$O_{STS}(\phi_i) = \sum_{j=1}^{n_i} (y_{ij} - y_{ij}^*)^2 \qquad \text{Eq. 3.6}$$

where $\phi_i$ is the vector of *i*th individual's parameters of the PK/PD model, $y_{ij}$ is the *j*th observed response in the *i*th individual, and $y_{ij}^*$ is the predict value of $y_{i.}$

At the second stage, the population parameters are estimated as the empirical mean $\hat{\phi}$ (arithmetic or geometric) and variance matrix ($\hat{\Omega}$) of the individual parameter from all the subjects according to the following equations:

$$\hat{\phi} = \frac{\sum_{i=1}^{k} \phi_i}{n} \qquad \text{Eq. 3.7}$$

$$\hat{\Omega} = \frac{\sum_{i=1}^{k} (\phi_i - \hat{\phi})^2}{n} \qquad \text{Eq. 3.8}$$

The advantage of the STS method is its simplicity, but problems arise when the number of observations in individual subjects is small relative to the number of parameters. In that situation, it may be impossible to estimate the individual parameters correctly and these subjects might have to be discarded, even though they contain valuable information about the population parameters. The serious problem is also encountered with the estimate of variance. The variance are likely to be overestimated in

most situations (133, 136) because TST tends to add intra-individual random error of observations to the estimated parameters.

The deficiencies in the STS method have motivated the development of iterative two-stage (IT2S) approach. This method relies on repeated fittings of individual data. An initial guess or a reasonable estimation of population mean and variance of parameters is required to initiate the procedure. The initial estimation may be obtained from the literature, from the NPD approach performed with current study data and a reasonable choice of the parameter variability, or the STS approach. In the first stage, these initially selected population parameters are used as priors for the estimation of the individual parameters from individual data. In the second stage, the population parameters are recalculated with these new individual parameters in order to form the new set of prior values. The iterative process is repeated until the difference between the new and old prior values become negligible. IT2S can be applied to rich data, sparse data, or a mixture of both. This algorithm has been implemented in the software USC*PACK (137) .

### *3.2.3 Nonlinear mixed-effects model*

The nonlinear mixed-effects (NLME) modeling approach is a procedure introduced by Sheiner and Beal (138) and has become the most common procedure for population analysis. As NTD approach, the NLME approach analyzes the data of all individuals simultaneously, but takes the inter-individual random effects structure into account. The variation in each parameter between individuals and the measurement errors are considered in the analysis.

The NLME method provides estimates of population characteristics that define the population distribution of the PK/PD parameters. In the NLME modeling, the population characteristics are composed of population mean values derived from fixed-effects parameters (explanatory variables, such as clearance), their variability within the

population, and variance derived from random-effects parameters (unexplanatory variables, such as measurement error).

The parameters of the NLME model are usually estimated by the MLE approach. The joint probability of the observations under the population model is written as a function of the model parameters, and parameter estimates are chosen to maximize this probability. It is difficult to calculate the likelihood of the data for most PK/PD models because of the nonlinear dependence of the observations on the random parameters $\eta_i$ and probably $\varepsilon_i$. Two widely used algorithms, the First-order (FO) approximation and stochastic approximation version of expectation-maximization (SAEM) method, are described below.

**First-order method.** The first-order estimation of population parameters was first implemented in NONMEM, the first nonlinear mixed-effects modeling computer program for population analysis, to minimize the objective function. In the NONMEM program, an extended least square is used as the objective function, where $\sigma^2$ is the variance of random error $\varepsilon$.

$$O_{FO}(\phi, y_i, \sigma^2) = \sum_{i=1}^{n}\left[\frac{(y_i - f(\phi, x_i))}{\sigma^2} + \ln\sigma^2\right] \qquad \text{Eq.3.9}$$

First-order Taylor series expansion is used to approximate model outcome ($y_{ij}$) with respect to the random effect variables $\eta_i$ and $\varepsilon_{ij}$ around zero and is given by:

$$y_{ij} = f(\phi, x_{ij}) + G_{ij}(\phi, x_{ij})\eta_i + \varepsilon_{ij} \qquad \text{Eq. 3.10}$$

where

$$G_{ij}(\phi, x_{ij}) = \partial f(\phi, x_{ij}, \eta_{ij}, \varepsilon_{ij}) / \eta_i \,|_{\eta_i = 0} \qquad \text{Eq. 3.11}$$

where $G_{ij}(\phi, x_{ij})$ is a matrix of the first derivatives of $f(\phi, x_{ij}, \eta_{ij}, \varepsilon_{ij})$ of $\eta_i$. The random effect $\eta_i$ and $\varepsilon_{ij}$ are assumed to be independent and normally distributed with zero means and variance-covariance $\Omega$ and variance $\sigma^2$, respectively.

Expectation (E) and variance-covariance of all observations for the *i*th individual are given by:

$$E_i = f(\phi, x_{i\,j}) \qquad \text{Eq. 3.12}$$

$$C_i = G_i(\phi, x_i)\Omega G_i(\theta, xi)^T + \sigma 2 I_{nj} \qquad \text{Eq. 3.13}$$

where *I* represents the identity matrix and *T* denotes the transpose, a matrix operator.

The nonlinear model is approximated with a linear model using the FO Taylor series expansion, and then MLE of the population parameters can be obtained by minimizing the objective function which is equal to the minus twice the logarithm of the likelihood of the population model.

**Stochastic approximation of expectation-maximization (SAEM).** One alternative to the linearization approximation methods is the expectation-maximization (EM) algorithm developed for models with missing or non-observed data such as random effects.

EM algorithm stands for 2 steps in each iteration: 1) an E-step, computing a conditional expectation of parameters; 2) a M-step, the maximization of a conditional likelihood, resulting in a set of parameter values which are more likely than those in the previous iteration.

The EM algorithm has found many applications, however practical application of this method may encounters computational difficulties, for instance the E-step is hard or impossible to calculate. To overcome this problem, an extension of the stochastic approximation version of expectation-maximization (SAEM) algorithm (139) was developed. The basic idea is to replace the usual E-step by a stochastic procedure which splits the E-step to a simulation step and an integration step. The simulation step consists of generating realizations of the missing data vector under the posterior distribution. The integration step includes stochastic averaging procedure to update the estimates. Lately, a more powerful algorithm, SAEM coupled with Markov Chain Monte Carlo (SAEM-MCMC) was introduced to improve the simulation step of SAEM, when the conditional

distribution is not in a close form. The SAEM-MCMC procedure has been implemented in the software Monolix (140).

### 3.3 Conclusions

Population approach is aimed at better estimates of variability derived from various sourece. Nonlinear mixed-effects model is the most common procedure for population analysis. Population analysis can be done with sparse or intense data from different trials or studies. In addition, populiaton analysis is a tool to assess the effects of covariates on the parameters of PK/PD model and will be used in Chapter 5 and 6 of the thesis.

# CHAPTER 4. NONCOMPARTMENTAL PHARMACOKINETIC ANALYSIS OF GLUCOSE-STIMULATED INSULIN RESPONSE IN AFRICAN-AMERICAN AND CAUCASIAN YOUTHS

## 4.1 Introduction

Insulin is produced by the beta-cells in the islets of Langerhans of the pancreas. The major functions of insulin are to increase muscular glucose uptake and suppress hepatic glucose production and thus maintain normal plasma glucose levels. Loss of beta-cell function leads to diabetes. Most patients in type 2 diabetes (T2D) are characterized by insulin resistance with subsequent inability of the beta-cells to maintain increased insulin secretion which leads to relative insulin deficiency and hyperglycemia.

In comparison with Americans of other racial groups, African-Americans are at greater risk of obesity (141) and T2D (142), which suggests an inherent difference in glucose and insulin metabolism between these racial groups. Indeed, Chiu *et al.* (95) and Arslanian *et al.* (143) found that African-American children have higher insulin concentration and higher acute insulin response to glucose (AIRg) which reflect racial differences in beta-cell function and sensitivity of peripheral tissue to insulin. Therefore, this study was undertaken to investigate racial differences in insulin secretion after a glucose stimulus between African-Americans and Caucasians at adolescence, a developmental stage with hormonal and body composition changes that may influence insulin secretion (144, 145).

The insulin response to an intravenous glucose challenge is often biphasic, which is defined as an early transient burst of insulin (first-phase) followed by a gradually increasing phase of insulin release (second-phase). The concept of biphasic release is important in understanding of the maintenance of glucose homeostasis (146, 147). It appears that the first-phase release allows prompt inhibition of endogenous glucose production and thereby restraining the rise in plasma glucose (148). In the early stages of

T2D, the first-phase is almost invariably lost despite the enhancement of second-phase secretion (149).

Several methods are currently used to assess beta-cell function and tissue sensitivity to insulin. The minimal model developed by Bergman (56, 58) is a well-accepted method of analyzing the frequently sampled intravenous glucose tolerance test (FSIVGTT). The fitted parameters from this nonlinear model enable estimation of indices of both insulin sensitivity and secretion. However, the major problem of the minimal model is it does not represent the insulin secretion accurately; the first-phase was discarded in the model. Another relatively simple modeling alternative, that has been used in population-based studies (47), is the homeostasis model assessment of insulin resistance (HOMA-IR) for the estimation of insulin resistance. HOMA-IR is calculated from fasting glucose and insulin levels. However, it primarily measures hepatic rather than peripheral insulin sensitivity (150) and thus compared to the minimal model may not be as relevant. Therefore, it appears valuable to analyze the insulin glucose kinetics under dynamic conditions using a nonparametric, noncompartmental approach, which is done in this study.

A more objective analysis should be possible by a nonparametric approach that does not rely on the many underlying kinetic assumption of model-based approaches. Furthermore, the proposed novel, longitudinal analysis provides a more comprehensive analysis than possible by "single point" methods e.g. fasting glucose level. The longitudinal analysis also provides an objective evaluation of where possible differences in the kinetic responses exist in the two groups. This should be particularly valuable because of the different phases of insulin release known to occur in response to a glucose challenge. These phases, that are poorly considered by most known methods, are closely related to the molecular biology of the beta-cells (147, 151). Thus, the proposed analysis is not only providing an initial, comprehensive, exploratory analysis of the two populations, but is also a valuable starting point for a more data-driven model building of

the glucose-insulin system, that considers covariates such as sex, body mass index (BMI) and pubertal status explored in the initial nonparametric analysis. Thus, such an approach can lead to models more suitable for differentiating the kinetics in different patient groups and can lead to better targeted treatment and prevention procedures.

## 4.2 Specific aim and hypothesis

The specific aim is to determine the differences in insulin secretion response after an intravenous glucose stimulation between African-American and Caucasian youths using noncompartmental method.

The specific hypothesis is that quantifiable differences in insulin secretion response to glucose challenge between African-American and Caucasians youths.

## 4.3 Materials and methods

### *4.3.1 Subjects and data collection*

Sixteen African-American (12 males and 4 females) and 22 Caucasian (14 males and 8 females) adolescents were enrolled in the study. All subjects were in good health based on examining medical history and physical examinations. No subjects were taking medications. Pubertal status was determined based on Tanner staging of breasts or genitalia depending on sex by an experienced pediatric endocrinologist. Tanner 1 subjects were considered prepubertal; Tanner 2 to 4 subjects were considered pubertal and Tanner 5 subjects were considered postpubertal. Table 4.1 provides the age, BMI, and pubertal status for each group. The protocol was approved by the Ohio State University Office of Responsible Research. Informed consent was obtained from the legal guardian and informed assent from the subjects.

Subjects received their routine diet for at least 3 days before the glucose tolerance test and then were admitted at 8AM after 10 hours fasting to the General Clinical Research Center (GCRC, Ohio State University). On the morning of the test, a bolus

glucose of 250 mg/kg was administered through an intravenous catheter at time 0. Blood samples were collected at -10, 0, 2, 4, 6, 8, 10, 12, 14, 16, 19, 22, 27, 32, 42, 52, 62, 72, 82, 92, 102, 122, 142,162 and 182 minutes relative to glucose administration at time 0.

Plasma glucose was measured by the YSI model 2300 glucose analyzer (Yellow Springs Instruments, Yellow Springs, OH). The coefficient of variation (CV) of this method is < 2%. Plasma insulin was measured in the CORE laboratory of the GCRC using a double antibody radioimmunoassay (Coat-A-Count kit manufactured by Siemens Medical Solutions Diagnostics). The sensitivity of the insulin assay was 2.5 μU/ml. The intra- and interassay CV were 6% and 10%, respectively.

### *4.3.2 Data analysis*

All statistical analysis was performed with S-Plus enterprise developer version 7.0 for windows (Insightful Corp.). Glucose concentration, insulin concentrations and AIRg were log-transformed according to assumption of log-normality. Two-sample student t-tests based on equal or unequal variance determined by F-test were used for between-group comparisons of mean value. All data were reported as mean and standard error of mean unless otherwise indicated. P-values less than 0.05 were considered statistically significant.

### *4.3.3 Kinetic parameters*

AIRg represents the acute insulin response and is defined as the area under the plasma insulin curve between 0 and 10 min (53, 152):

$$AIR_g = \int_0^{10} [I(t) - I_b]\, dt \qquad \text{Eq. 4.1}$$

where *I(t)* is insulin concentration at time *t* and $I_b$ is the baseline of insulin expressed in μU/ml. AIRg was calculated from a cubic spline fitted to the insulin data according to the general cross validation principle (153).

### *4.3.4 Homeostatic model assessment of insulin resistance (HOMA-IR)*

The HOMA-IR proposed by Matthews *et al.* (47) is calculated as follows:

$$HOMA-IR = \frac{G_b \cdot I_b}{405} \qquad \text{Eq. 4.2}$$

where $G_b$ is the basal glucose plasma concentration expressed in mg/dl, and $I_b$ is the basal insulin level measured in μU/ml.

### *4.3.5 Regression Analysis*

Multiple linear regression analysis was used to assess the effects of sex, BMI and pubertal status on insulin and glucose responses. For the *j*th observation point, the regression model has the form:

$$y_i = \beta_0 + \sum_{k=1}^{3} \beta_k x_{k,\,ij} \qquad \text{Eq. 4.3}$$

where $y_i$ is the value of response variable (glucose or insulin plasma level) for subject *i*, *k* = 1, 2, 3, and $x_{k,ij}$ are explanatory variables *k* for the *i*th subject at *j*th observation. In each linear regression, there are three explanatory variables chosen from sex, BMI, pubertal status and race based on how subjects are grouped. Sex is a factor, race is a factor, BMI is continuous value, and puberty is an integer with prepuberty as -1, puberty as 1 and post-puberty as 2. The regression coefficients, $\beta_0, \beta_1, \beta_2$ and $\beta_3$ were estimated by least-squares.

## 4.4 Results

Demographic data of subjects are shown in Table 4.1. The mean ages of both groups were similar. African-American adolescents had significantly higher BMIs than Caucasian adolescents ($p < 0.05$). Table 4.2 presents the basal insulin and glucose concentration in plasma, β-cell function estimated by AIRg, and HOMA-IR. Two-sample t-tests revealed that mean concentrations of insulin and glucose did not differ at baselines between African-Americans and Caucasians. As expected, African-American adolescents

had significantly higher AIRg compared to Caucasians ($p < 0.05$). No racial difference in $AUC_{glucose}$ /$AUC_{insulin}$ and HOMA-IR were found.

The glucose and insulin profiles obtained using FSIVGTT are shown in Figure 4.1. At each observation point t-tests were used for comparison of between-group difference in glucose and insulin levels and the resulting t-test probabilities were plotted. The plasma insulin concentrations were mainly different in the peak area between African-American and Caucasian children (Figure 4.1A). The African-Americans had significantly higher insulin concentration in the 4-19 minutes interval (all $p < 0.05$). The mean values of plasma glucose concentration (Figure 4.1B) were not significantly different between the two racial groups.

The between-group differences in plasma insulin and glucose concentrations were also examined by the t-test probabilities when grouped in terms of BMI, sex and pubertal status. The resulting probability plots are shown in Figure 4.2, 4.3 and 4.4, respectively. For BMI, the median 23.05 was chosen as the cut-point to get equal number of subjects in the low and high BMI groups. Second-phase (defined as after 20 min) insulin concentrations were significantly different in insulin levels (Figure 4.2A, all $p < 0.05$). In contrast, the differences in glucose were significant only after 100 min, at which time glucose levels approached steady state basal levels (Figure 4.2B, all $p < 0.05$). The between-group differences in insulin were not significant as the subjects were grouped based on sex (Figure 4.3A) and pubertal status (Figure 4.4A). No significant differences in glucose response were found between male and female (Figure 4.3B), but there were significant differences in glucose as the comparisons were performed through pre-puberty vs. post-puberty (Figure 4.4B, all $p < 0.05$ after 100 min).

By the exploratory probability plots resulting from the t-tests we found racial differences in insulin level (Figure 1A) during the first 20 minutes and BMI's differences in glucose level (Figure 1B) after 100 min. To determine the dependence of those differences on other covariates, such as age, sex, pubertal status and BMI, a series of

multiple linear regression analysis were performed using S-Plus. The resulting probabilities for every covariate at each observation were plotted as shown in Figure 4.5 (corresponding to Figure 4.1A) and in Figure 4.6 (corresponding to Figure 4.2B). Figure 4.5A shows that, for Caucasians, insulin concentrations in the first-phase (defined as less than 20 min) were strongly related to BMI (all $p < 0.05$ in the 8-20 min interval), and not related to sex and pubertal status. Figure 4.5B shows that, for African-Americans, insulin concentrations in the first-phase did not appear to depend on sex, pubertal status or BMI (all $p>0.05$ in 4-20 min). For the group with BMI less than 23.05 (Figure 4.6A), we found that glucose concentrations were associated with sex (all $p < 0.05$ after 120 min), but independent of race and pubertal status. For the group with larger BMI (BMI larger than 23.05, Figure 4.6B), pubertal status, sex and race did not show significant effect on the glucose concentrations, although race seems to have a stronger association with glucose concentrations compared to pubertal status and sex.

## 4.5 Discussion

The insulin and glucose responses in the FSIVGTT were analyzed by noncompartmental PK to determine the between-group differences and covariate effects on glucose and insulin. Rather than using a minimal model to derive indices (such as glucose effectiveness and insulin sensitivity), we performed Student's t-tests longitudinal across each observation for comparing between-group differences.

### *4.5.1 Racial effect on insulin, glucose levels, AIRg and HOMA-IR*

The glucose stimulated insulin response is predominantly biphasic. The first-phase insulin response ("acute response") is defined as the initial burst followed by a fall in insulin level, which lasts about 20 minutes in our study. The second-phase starts from the end of first-phase. The rise of the second-phase is more gradual and its magnitude is directly related to the degree and duration of the stimulus. In our FSIVGTT study, about 65% of subjects exhibit an identifiable first- and second-phase insulin release.

Our analyses revealed that African-American youths have higher insulin concentrations in the first-phase compared to Caucasians. This finding is consistent with the study conducted by Arslanian *et al.* (143). AIRg represents a measurement of insulin release and clearance during first-phase. It is a simple measurement for assessing first-phase and beta-cell function (154, 155). The results of our study demonstrate that compared with Caucasians, African-Americans have significantly greater AIRg. These findings are in agreement with other published reports (50, 51, 156, 157). Our study suggested that the calculation of AIRg should be extended to 20 minutes after glucose administration to provide a better differentiation. The racial difference in AIRg is more significant based on the calculation over 20 minutes ($p < 0.0006$) compared to the calculation of AIRg over 10 minutes ($p < 0.001$). The racial difference in AIRg may be caused by either higher insulin secretion, lower clearance or lesser hepatic insulin extraction in African-Americans compared to Caucasians. Although the underlying physiology is not well understood, a study of C-peptide would provide information for better resolving the kinetics.

We did not identify a difference in insulin resistance between African-Americans and Caucasians. This result is consistent with a population-based HOMA-IR investigation by Lee et al (49). However, the difference in insulin resistance between African-American and Caucasian children has been found using both euglycemic clamp (50, 51, 158) and FSIVGTT analysis (159). This discrepancy could be due to the HOMA-IR being calculated from fasting glucose and insulin levels. Furthermore, HOMA-IR primarily measures hepatic rather than peripheral insulin sensitivity (150) and thus is difficult to compare to the clamp studies and the minimal model analysis.

### *4.5.2 BMI's effect on insulin and glucose levels*

African-Americans have been reported to have higher BMI compared to Caucasians (141). Obesity has been demonstrated as a critical factor that affects the

biphasic insulin secretion in adolescents (156). Therefore, comparison of our results with other investigations has to be undertaken with caution, as most subjects in our study are not obese. In our study, the BMI significantly affected the insulin level in the second-phase (all $p < 0.05$, after 20 min, Figure 4.2A), but does not appear to have an effect on the first-phase response. This result is supported by the study presented by Walton *et al.* (160) in individuals with normal BMI. Although only racial difference was found in first-phase, BMI is the major covariate that determined the insulin concentration. Multivariate linear regression analysis indicated that, for Caucasians, insulin concentrations in the first-phase are significantly associated with BMI, and higher BMI leads to higher insulin levels. In contrast, the relationship in African-Americans was not significant. The possible reason may be that the Caucasians have lower BMI compared to African-Americans, higer BMI values mask the association of BMI with insulin concentration.

### *4.5.3 Pubertal effect on insulin*

Previous studies have revealed that puberty is associated with insulin resistance and insulin resistance is compensated by increased insulin secretion, which results in increased serum insulin concentrations (144, 161, 162). The results of our study did not indicate pubertal effect on insulin concentration. The relatively small number of subjects and the racial effect on insulin level may mask the relationship. Although we found differences in glucose concentrations at steady state (>100 min) between groups with different pubertal status (pre-puberty vs. post-puberty), these findings most likely are a reflection of the smaller BMIs in pre-pubertal subjects in this study, in which the means (±SD) of BMI for pre-pubertal and post-pubertal subjects were 18.9±3.58 and 25.6±4.53, respectively.

## 4.6 Conclusions

In summary, our study suggests that African-American youths have higher glucose stimulated insulin response in the first-phase (<20 min) compared to Caucasian

youths and higher AIRg. For the subjects with normal BMI, BMI has significant effect on second-phase insulin secretion. The calculation of AIRg extended to 20 minutes indicates a more significant racial difference compared to the AIRg in 10 minutes. After reaching steady-state (>100 min), subjects with different levels of BMI cause the between-group difference in glucose concentration. During steady state, the glucose levels in subjects with lower BMI are significantly correlated with sex ($p < 0.05$), but large BMI may obscure the gender's effect on glucose concentration.

Table 4.1. Subject demographics

| | African-American | Caucasian |
|---|---|---|
| BMI*‡ ($kg/m^2$) | 25.5±1.10 | 21.8±0.90 |
| Sex | | |
| Male | 12 | 14 |
| Female | 4 | 8 |
| Age‡ (years) | 13.8±0.62 | 13.8±0.57 |
| Pubertal Status | | |
| Pre-puberty | 2 | 6 |
| Puberty | 6 | 9 |
| Post-puberty | 8 | 7 |

*P < 0.05. ‡ Data are mean ±SE

Table 4.2. Measures and estimates of insulin and glucose responses in plasma during FSIVGTT according to race

| | African-American (mean ±SE) | Caucasian (mean ±SE) |
|---|---|---|
| Basal Insulin (μU/ml) | 12.4 ±2.10 | 15.0 ± 4.73 |
| Basal Glucose (mg/dl) | 82.9 ± 1.82 | 83.2 ±1.68 |
| AIRg * (μU·min/ml) | 898±157 | 457 ± 56.2 |
| $AUC_{glucose}$ /$AUC_{insulin}$ | 6.24±0.89 | 8.95±1.31 |
| HOMA-IR | 2.62 ± 0.46 | 3.17 ± 1.00 |

*P < 0.05 denotes significant difference between racial groups.

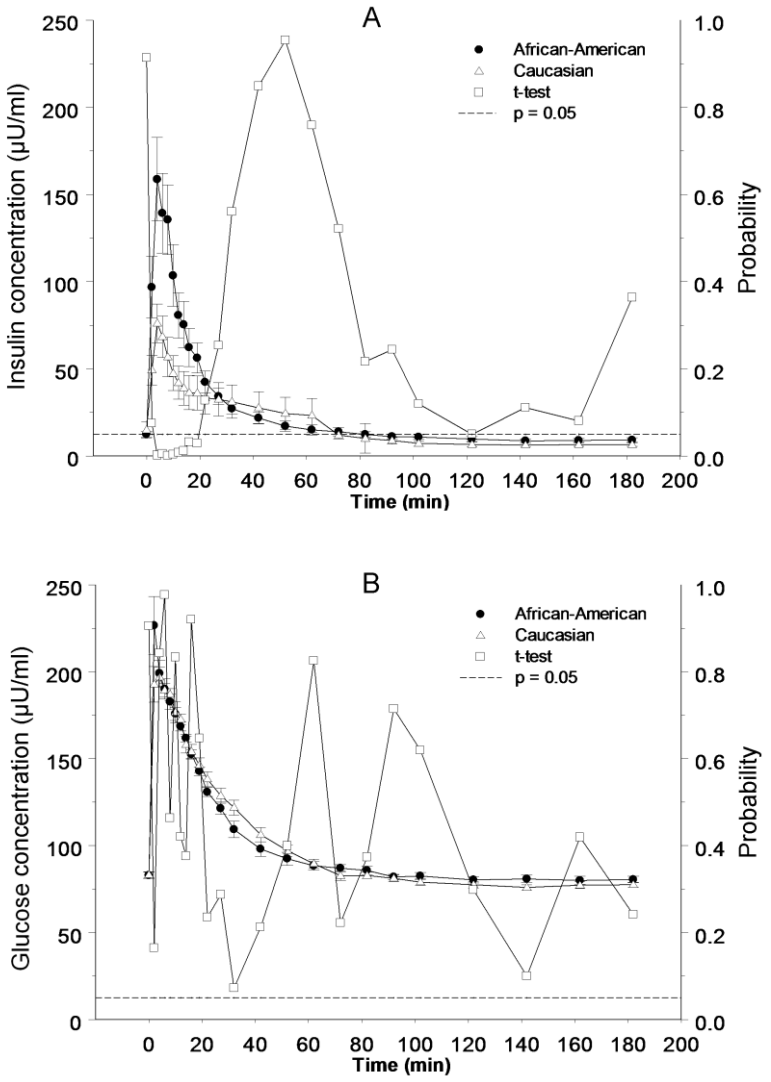


Figure 4.1. Mean (±SE) plasma insulin (A) and glucose (B) concentrations after IV glucose administration in African-American and Caucasian adolescents.

The racial difference in mean concentration at each observation was evaluated using t-test.

\

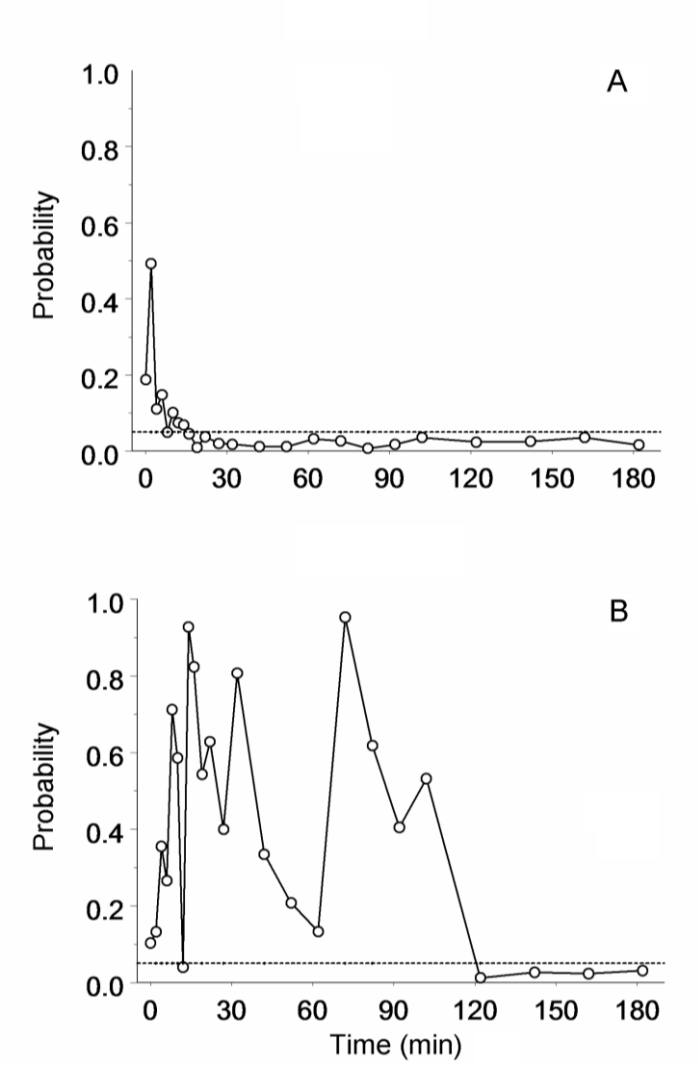


Figure 4.2. P-values of two-sample t-test for between-group differences in mean values of insulin (A) and glucose (B) when subjects were grouped in terms of BMI with cut point equal to median 23.05.

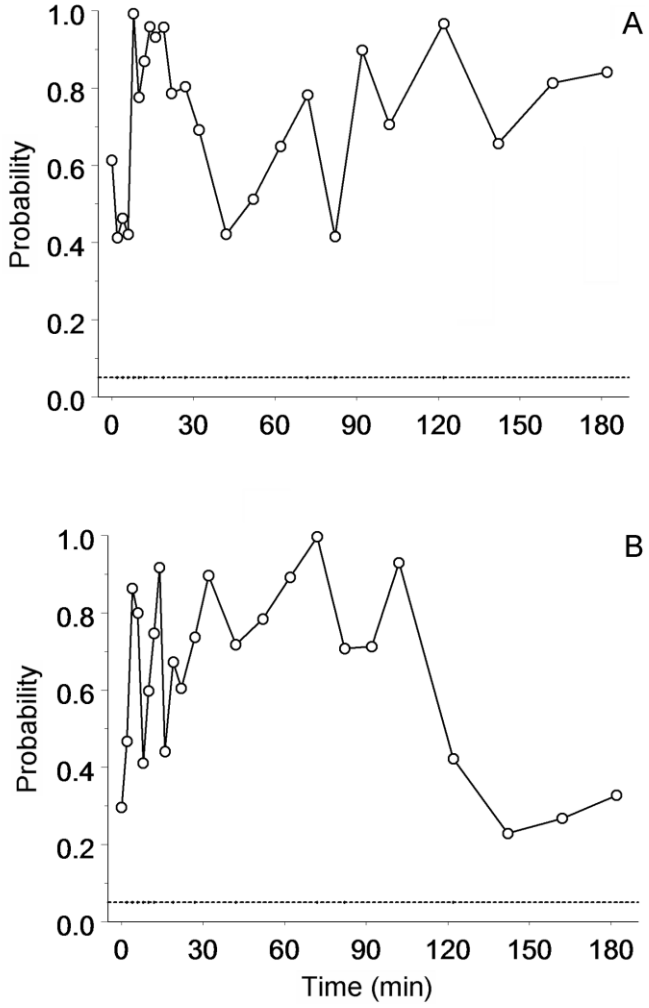


Figure 4.3. P-values of two-sample t-test for between-group differences in mean values of insulin (A) and glucose (B) when subjects were grouped in terms of sex.

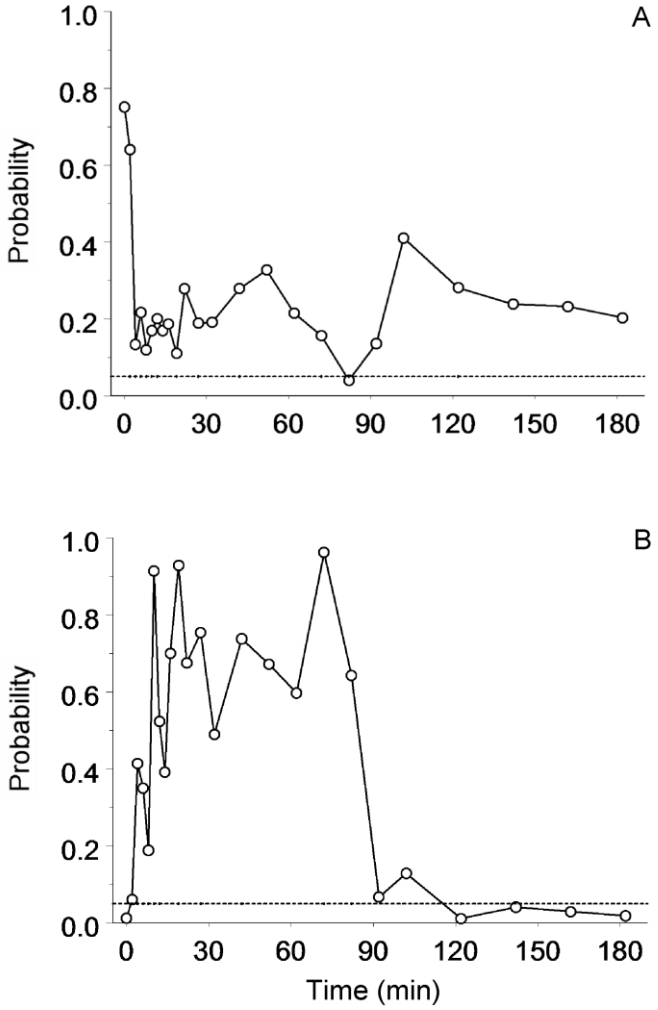


Figure 4.4. P-values of two-sample t-test for between-group differences in mean values of insulin (A) and glucose (B) when subjects were grouped in terms of pubertal status.

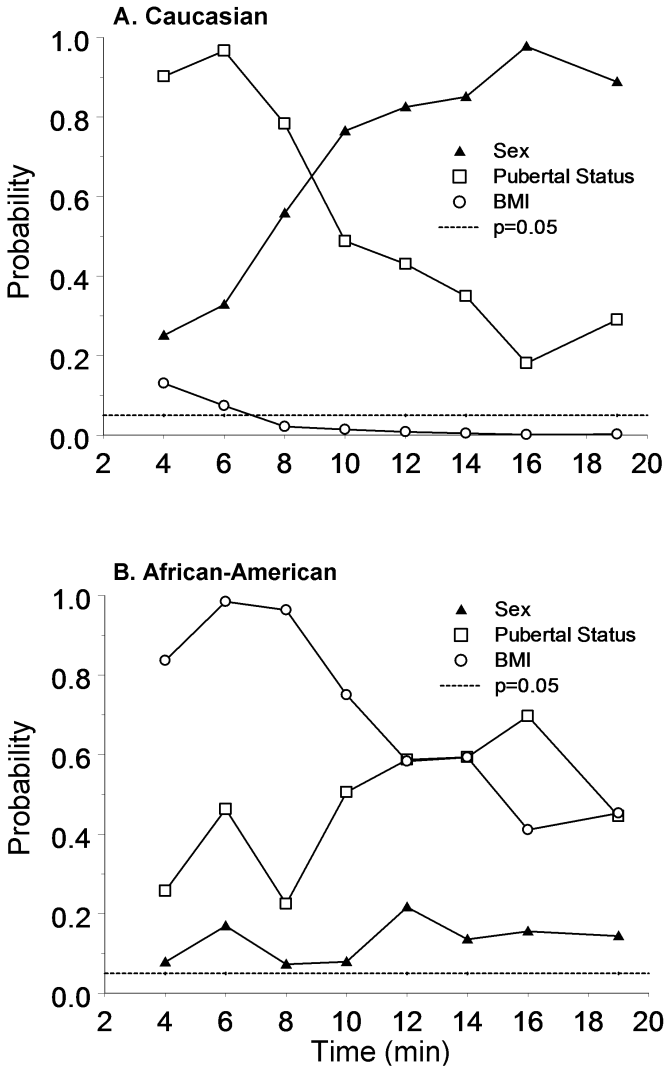


Figure 4.5. Covariate effects on insulin concentration in first 20 minutes following an IV glucose administration in healthy Caucasian (A) and African-American (B) youths.

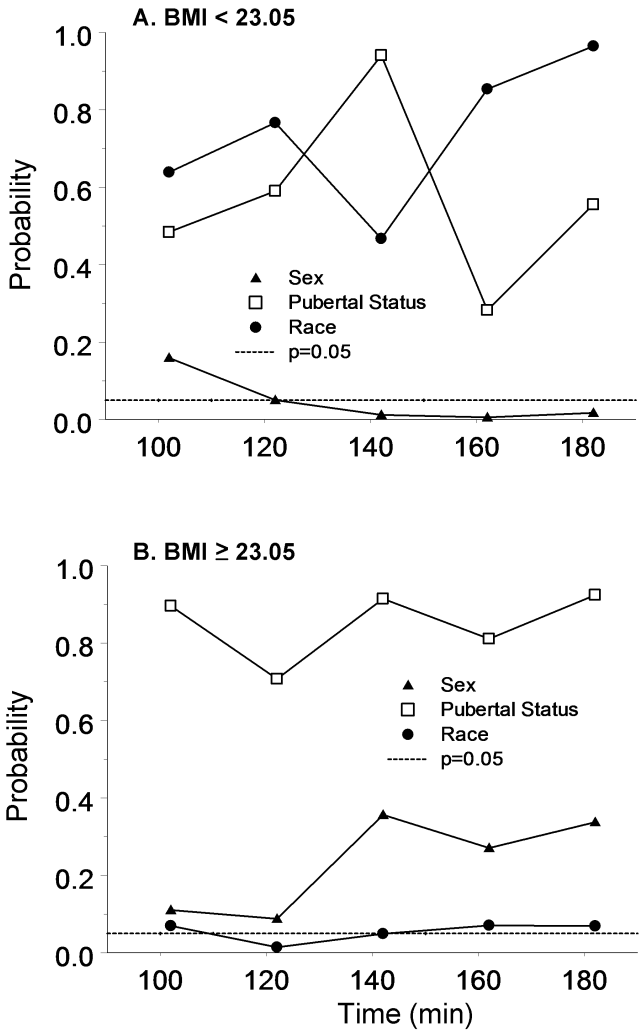


Figure 4.6. Covariate effects on glucose concentration after 100 minutes of glucose IV administration in subjects with lower BMI (A) and higher BMI (B).

# CHAPTER 5. POPULATION ANALYSIS OF ETHNICITY AND FIRST-PHASE INSULIN RELEASE

## 5.1 Introduction

The prevalence of obesity and type 2 diabetes (T2D) among children is increasing in U.S., and this problem is greater in African-American children compared to Caucasian children (141). A number of recent reports have demonstrated that non-diabetic African-Americans have increased insulin resistance (51, 143, 163, 164) which is a risk factor for developing T2D (165, 166). Increased insulin secretion in African-Americans may compensate for or precede the insulin resistance (22, 163, 167, 168). In any event, it appears that there is an inherent difference in glucose and insulin metabolism between these two populations.

In our previous study (25) a nonparametric approach was used to analyze insulin dynamics by means of data from frequently sampled intravenous glucose tolerance tests (FSIVGTT). That study indicated that race, as a major covariate, only affects the insulin concentration in the first-phase for non-obese subjects. As first demonstrated by Cerasi and his colleagues (169) *in vivo*, insulin secretion in response to glucose exhibits a biphasic pattern. Much effort has been devoted to understanding the underlying mechanisms of the biphasic release because of the apparent association between the onset of T2D and the loss of the first-phase (149, 169).

A wide variety of models have been used to study the glucose and insulin dynamics. The often applied minimal model (54) has been used for several decades due to its capability of estimating indices of insulin sensitivity. However, the minimal model does not accurately represent the early insulin secretion. The early first-phase data points are commonly not included in the minimal model analysis. Thus, the minimal model is not suitable for analyzing the early phase release. Only few models have been proposed to describe insulin secretion based on the mechanism of a biphasic insulin secretion.

Grodsky *et al.* modeled multiple insulin pools in beta-cells (170). They studied the phasic insulin secretion both *in vitro* and *in vivo* and suggested a two-compartment model to describe the biphasic secretion. However, the model only successfully simulated the first-phase secretion under certain levels of glucose stimulation. A more elaborate model with a biphasic mechanism of insulin secretion has been proposed by Gupta *et al.* (97). However due to the greater complexity of that model the parameters that relates to first- or second-phase release are difficult to evaluate in a population kinetic framework.

In this work, the physiological mechanism of biphasic secretion is specifically considered in the PK/PD analysis, with a strong structural connection to current knowledge of the beta-cell insulin physiology. Compared to other models that consider a biphasic insulin models, the proposed model is simpler in structure and number of parameters and includes physiologically-based parameters closely related to the important biphasic insulin secretion. Insulin concentrations obtained from FSIVGTT in the two racial groups were simultaneously analyzed in a population modeling framework using the Monolix software (140) according to the proposed mechanistic kinetic model. A specific covariate structure was used in the population analysis enabling the identification of distinct differences in physiologically relevant kinetic parameters between African-American and Caucasian youths.

**5.2 Specific aims and hypotheses**

One specific aim of this chapter is to formulate a novel physiologically based mechanistic PK/PD model aimed at dynamically evaluate the biphasic insulin secretion. The proposed model should be simple and have the ability to relate the kinetic parameters to the important biphasic pattern of insulin secretion. The other aim is to evaluate the impact of ethnicity on insulin secretion kinetics using population modeling approach.

The hypotheses are 1) the plasma insulin concentrations after an IV glucose challenge can be accurately described using a PK/PD model based on the cellular

mechanism of biphasic insulin secretion and 2) the proposed model is able to identify kinetic parameters that cause the difference in the insulin secretion response to IV glucose stimulation between African-American and Caucasian youth using population analysis.

## 5.3 Materials and methods

### *5.3.1 Subjects*

The database used here were the same as the one used in our previous noncompartmenal analysis (25) except 5 subjects were excluded due to missing entire first- or second-phase samples. The FIVGTT analysis involved 15 healthy African-American (3 females and 12 males), age 13.7±2.55 (mean±SD), and 18 healthy Caucasian children (8 females and 10 males), age 14.1±2.90. The BMI of African-Americans is 25.6±4.63, which is significantly ($p < 0.05$) higher comparing to that of 21.5±4.13 of Caucasians. The study was conducted in accordance with the guidelines in The Declaration of Helsinki and the protocol approved by the Ohio State University Office of Responsible Research.

### *5.3.2 Sampling procedure*

Subjects received their routine diet for at least 3 days before the glucose tolerance test and then were admitted at 8 AM after 10 hours fasting to the General Clinical Research Center, Ohio State University. On the morning of the test, a bolus glucose of 250 mg/kg was administered within one minute through an intravenous catheter at time 0. Blood samples were collected at -10, 0, 2, 4, 6, 8, 10, 12, 14, 16, 19, 22, 27, 32, 42, 52, 62, 72, 82, 92, 102, 122, 142,162 and 182 minutes relative to the glucose administration at time 0.

### *5.3.3 Laboratory analysis*

Plasma glucose was measured by the YSI model 2300 glucose analyzer (Yellow Springs Instruments, Yellow Springs, OH). The coefficient of variation (CV) of this method is <2%. Plasma insulin was measured in the CORE laboratory of the GCRC using a double antibody radioimmunoassay (Coat-A-Count kit manufactured by Siemens Medical Solutions Diagnostics, Los Angeles, CA). The sensitivity of the insulin assay was 2.5 μU/ml. The intra- and interassay CV were 6% and 10%, respectively.

### *5.3.4 PK/PD modeling*

A physiologically-based mathematical model was developed to describe plasma insulin concentration in response to an acute glucose challenge during FIVGTT. The model considers the physiologic mechanism of biphasic secretion of insulin at the beta-cell level. The model (Figure. 5.1) includes two insulin pools in the beta-cells, which store the biosynthesized insulin granules and account for the biphasic nature of insulin secretion. One pool, here denoted the reserved insulin pool ($I_R$), governs the second-phase insulin secretion and the other denoted the readily releasable insulin pool ($I_{RR}$) governs the first-phase insulin secretion.

Eq. 5.1 describes the second-phase insulin secretion from the $I_R$ pool. It considers a rate of formation of $I_R$ proportional to the plasma glucose concentration ($C_G$) and a release of insulin empirically described by a sigmoidal Hill equaiton:

$$\frac{dI_R}{dt} = K_G C_G - \frac{E_{\max} C_G{}^{\alpha}}{C_{50}{}^{\alpha} + C_G{}^{\alpha}} I_R \qquad \text{Eq. 5.1}$$
$$I_R(0) = I_R\_0$$

with $K_G$ denoting the first-order formation rate constant, and the $E_{max}$, $C_{50}$ and α the Hill equation parameters, while $I_{R\_0}$ is the estimated initial condition of the $I_R$ pool.

The insulin in the readily releasable pool ($I_{RR}$) has been "primed" (prepared for release) for ready release according to the biphasic secretion mechanism. The readily

releasable insulin can in response to the glucose stimulation be released at a relatively fast rate compared to that in the $I_R$ pool, to form the first-phase. The change in $I_{RR}$ is given by:

$$\frac{dI_{RR}}{dt} = -K_{RR} I_{RR}$$
$$I_{RR}(0) = I_{RR}\_0 \qquad \text{Eq. 5.2}$$

where $K_{RR}$ is a first-order rate constant and $I_{RR}$ *_0* is the estimated initial condition of the $I_{RR}$ pool.

The insulin from the beta-cells ($I_R$ and $I_{RR}$ pools) needs to go through the liver prior to its entry into the circulation. A fraction of insulin described by the extraction ration $E$ is removed by the liver. The plasma is considered as a single compartment for insulin with first-order elimination kinetics. Accordingly, the rate of change in the plasma insulin concentration is described by:

$$\frac{dC_I}{dt} = \left(\frac{1-E}{V_I}\right)\frac{E_{\max} C_G{}^{\alpha}}{C_{50}{}^{\alpha} + C_G{}^{\alpha}} I_R - K_I \frac{I}{V_I} + \left(\frac{1-E}{V_I}\right) K_{RR} I_{RR}$$
$$= P_e \frac{E_{\max} C_G{}^{\alpha}}{C_{50}{}^{\alpha} + C_G{}^{\alpha}} I_R - K_I C_I + P_e K_{RR} I_{RR} \qquad \text{Eq. 5.3}$$
$$C_I(0) = C_I\_0$$

where $C_I$ is the plasma insulin concentration, $C_I$*_0* is the initial plasma insulin concentration, $K_I$ is a first-order elimination rate constant, $V_I$ is the distribution volume of insulin in plasma and $P_e$ has been introduced to represent the expression of *(1-E)/*$V_I$ and avoid identifiability problems.

### *5.3.5 Population PK/PD modeling*

A nonlinear mixed-effects model was used for the population analysis in which the insulin concentration profile is described by the above set of differential equations, and random effects account for variability between- and within-subjects. Let $y_{ij}$ denotes

the *j*-th observed plasma insulin concentration of subject *i* at time $t_{ij}$ ( $i = 1, \ldots, n$, $j = 1, \ldots, k$), then the nonlinear mixed-effects model is written as:

$$y_{ij} = f(\phi_i, t_{ij}) + g(\phi_i, t_{ij}) \cdot \varepsilon_{ij} \qquad \text{Eq. 5.4}$$

where $f$ is the PK/PD model consisting of the solution to the differential equations 1-3, $g$ is the residual error model, $\varepsilon_{ij}$ is the coefficient of the error model following a normal distribution with mean 0 and variance 1.

Various residual error models were investigated for the population analysis and the choice made based on the likelihood ratio test with significant level equal to 0.05 and plots of goodness-of-fit. As possibilities we consider the function $g$ (Eq.5.4) to have the following constant, proportional and combined forms:

Constant $$g(\phi_i, t_{ij}) = a \qquad \text{Eq. 5.5}$$

Proportional $$g(\phi_i, t_{ij}) = bf(\phi_i, t_{ij}) \qquad \text{Eq. 5.6}$$

Combined $$g(\phi_i, t_{ij}) = a + bf(\phi_i, t_{ij}) \qquad \text{Eq. 5.7}$$

with $\phi_i$ being a *p*-dimensional vector of individual parameters for subject *i* assumed to be log-normally distributed, ensuring non-negativity in the estimation. Race was evaluated as a categorical covariate to explain between-subject variability in the kinetic parameters. To describe racial effects, $\phi_i$ was modeled with the following covariate structure:

$$\ln(\phi_i) = \mu + \beta c_i + \eta_i \quad \text{with} \quad \eta_i \sim_{i.i.d} N(0, \Omega) \qquad \text{Eq. 5.8}$$

where $c_i$ is a categorical vector corresponding to the ethnicity of subject *i* (African-American was used as reference class); $\beta$ is a vector of coefficients of size $p$; $\mu$ is a vector of population means for parameters with length *p*; $\eta_i$ represents the random effect assumed to follow a normal distribution with mean of zero and $\Omega$ is a diagonal variance matrix of the random effects. Significance of the racial effect on parameters was evaluated by the Wald test at a significance level of 0.05.

### *5.3.6 Data analysis*

The data from all the subjects were simultaneously analyzed using the open-source free computer software Monolix, standalone version 3.1 developed by INRIA, France (140). The population parameters were estimated based on the maximum likelihood estimation (MLE). A Stochastic Approximation Expectation Maximization (SAEM) algorithm coupled with Markov Chain Monte Carlo (MCMC) (139, 171-173) procedure was used for MLE estimation of the parameters of the population model without the use of approximations in the estimation of the likelihood. We made use of Monolix because its algorithm showed much better convergence properties compared to the software NONMEM VI which failed to converge in our case. The Hastings-Metropolis algorithm was applied to compute conditional means and conditional standard deviations of the individual parameters. The glucose concentrations were represented by a linear spline interpolation.

## 5.4 Results

The residual error in the nonlinear mixed-effects population kinetic analysis was best described with a proportional model . Population estimates of parameters and between-subject variability (standard deviation) are presented in Table 5.1. A visual predictive check (VPC) with 1000 simulated data set was performed. The simulated median and the 95% confidence interval are given in Figure 5.2 together with the observed insulin concentrations. The VPC plot provides good evidence of the adequacy of the model.

In the present investigation race as a covariate was incorporated in the structure of population model (Eq. 5.8). Inclusion or deletion of covariate was determined by a Wald test at a significance level of 0.05. We first applied the covariate of race to all parameters. It was then found that the initial value of the $I_{RR}$ pool ($I_{RR\_0}$) is significantly associated ($p < 0.05$) with race, and racial effect on the rate constant of $K_{RR}$ is close to significant

(p=0.064). If only the parameter $K_{RR}$ or $I_{RR\_0}$ is considered in the covariate structure, then race shows a significant relationship. Accordingly, the derived parameter $K_R I_R = K_{RR} \cdot I_{RR\_0}$, which provides a metric for the initial first-phase insulin secretion from beta-cell, was used in the population analysis. In this way race was found to have a significant effects on $K_R I_R$, resulting in a 63% decrease in $K_R I_R$ for Caucasians compared with African-Americans. The performance of the population model was shown in Figure 5.3. Apart from the high observed plasma insulin, the population predicted insulin concentrations and observations are clustered around the line of identity (Figure 5.3A). Plotting the individual predictions against the observations for insulin (Figure 5.3B) reduces the scattering around the line of identity as indicating that the population kinetic analysis is able to explain the variability in the insulin response. The scatter plot of population weighted residual against predicted concentrations of insulin (Figure 5.3C) indicates that the residuals are randomly distributed. Thus, the population model appears to adequately describe the biphasic insulin dynamics.

## 5.5 Discussion

The current study combines a nonlinear mixed-effects population modeling approach and a physiologically based PK/PD model for analyzing insulin behavior in response to glucose stimulation. The structure of the PK/PD model contains expressions to describe the physiologic mechanism of insulin's biphasic secretion. The population PK/PD modeling with the covariate analysis approach enables identification of parameters specific to the difference found in the first-phase insulin secretion between African-American and Caucasian youths (25).

### *5.5.1 PK/PD modeling rationale*

The insulin release from the beta-cells involves the arrangement of insulin into secretory granules, trafficking of the insulin-containing granules to the plasma membranes and exocytosis from the beta-cell (18). The release of insulin from the β-cells

has been found to follow a biphasic time course consisting of a rapid and transient first-phase followed by a slowly developing and sustained second-phase. The underlying mechanisms of the biphasic pattern is still poorly understood in spite of the fact that biphasic release of insulin has been known for more than 40 years (169). One explanation proposed by a number of studies (30, 37, 170, 174, 175) suggests that the biphasic release is due to the existence of at least two distinct pools of insulin granules in beta-cells. Based on their release competence or proximity to the plasma membrane it is proposed that the granules belonging to the readily releasable pool ($I_{RR}$) can be rapidly discharged without any further modification and thus is responsible for the first-phase insulin secretion; the second-phase release is due to the insulin granules in the reserved pool ($I_R$) which have to be translocated to the membrane and primed before they can be released.

The PK/PD model presented in this work subscribes to this current cellular biology understanding of the kinetic mechanism governing insulin biphasic secretion. Specifically, the $I_{RR}$ and $I_R$ pools of insulin are included in the proposed model (Figure 5.1) to consider this mechanism. Upon glucose stimulation, the granules in the $I_{RR}$ pool are secreted from beta-cells at a faster rate compared to the $I_R$ pool, and thus form the first-phase release.

Glucose is the main physiological regulator of insulin production and secretion in the beta-cells (176-178). Several studies (170, 175, 179) have reported that the magnitude of the peak of the first-phase is varying with the level of glucose, while the shape and the transient nature of the peak remains unchanged. Thus, the size of $I_{RR}$ should be associated with the glucose level. However, we could not estimate the dependence of $I_{RR}$ on the glucose dose since only one level of glucose stimulation was tested in our study subjects. For the effect of glucose on the second-phase, we assume the production rate of insulin in $I_R$ to be proportional to the glucose concentration. The relationship between glucose and insulin release from the $I_R$ pool was analyzed by using several PK/PD relationships, including the Hill function with or without sigmoidicity and a simple linear function. In

order to determine a reasonable empirical structure for the population analysis as a first step, glucose and insulin data were fitted individually using WINFUNFIT which is a Windows version evolved from the FUNFIT program (180). Our analysis suggests that the model using the Hill function with sigmoidicity best describes the insulin dynamics during FSIVGTT based on the Akaike information criteria (AIC) (181) and graphical comparisons of fits.

### *5.5.2 Model parameters*

The extraction ratio parameter $E$ influences the amount of insulin that reaches the systemic circulation. Approximately 50% ($E$=0.5) of insulin secreted from beta-cell is extracted by the liver , but the value of $E$ may change with the glucose level (23). Instead of estimating $E$, which is not possible based on the current data, our PK/PD analysis estimates the $P_e$ parameter, which "encapsulates" the $E$ and $V_I$ parameters ($P_e = (1-E) /V_I$). The average value of $V_I$ has been reported to be 10 liter (182). Thus, the value of $P_e$ calculated according to these references is about 0.05, which is in agreement with the population estimate of $P_e$ based on our model which is 0.0581 with a 95% confidence interval of 0.0436-0.0773 $L^{-1}$. Thus, our results do not indicate a significant change in $P_e$ in response to a glucose challenge.

The $K_I$ has been reported from 0.1 to 0.3 $min^{-1}$ (121, 183). Our population $K_I$ estimate of 0.194 $min^{-1}$ falls into this range, which corresponds to an insulin half-life time of 3.57 min with a 95% confidence interval of 1.33-6.93 min.

In the proposed model, the initial amount of $I_R$ is treated as an estimated parameter and not calculated assuming an initial steady state condition. The rational for this is the fact that the basal insulin level is not a stable parameter because the insulin concentration in blood changes in a pulsatile manner. At the fasting state, the contribution of the pulsatile insulin secretion has been found to be at least at least 75% of the total insulin secretion (184).

Higher insulin concentrations in the first-phase in the African-American subjects were detected compared to Caucasians (25) which may indicate beginning signs of progression towards insulin resistance and a pre-diabetic state in the African-American group. Increased insulin secretion in the African Americans may also compensate for or precede the insulin resistance (22, 163, 167, 168). The increase in insulin level may be caused by an increase in insulin secretion from $I_{RR}$ and/or $I_R$, or a decreased insulin removal *via* the extraction from the liver or elimination from plasma. Our covariate analysis suggests that the difference is due to the insulin secretion from the $I_{RR}$ pool. The significant racial difference ($p < 0.05$) in the initial insulin secretion ($K_R I_R$) from the beta-cells resulted in the difference in the secretion profiles found in the first-phase. Secretion profiles from beta-cell (Figure 5.4) during FSIVGTT can be reconstructed using population parameters and averaged glucose concentrations. No significant association was found between race and the insulin elimination, and race and insulin extraction by liver.

The present analysis has been based on FSIVGTT experiments which are clinically less involved than OGTT experiments. Accordingly, to possibly broaden the applicability of the analysis work is currently in progress to test the applicability of the model for analyzing OGTT data.

### *5.5.3 Other possible factors*

Because most subjects in the study (BMIs of 5 subjects are larger than 30) are non-obese, obesity can not be ruled out as possible alternative explanation for the difference found between the two groups. A better balanced study is needed to investigate that possibility. Possible differences in other factors that have not been determined in this study such as physical activity that was found to be a possible contributor (185), or genetic factors may also need to be considered.

## 5.6 Conclusions

In summary, the proposed mechanistic PK/PD model is able to describe the biphasic release of insulin in response to a glucose challenge. The population analysis allowed an estimation of the variability of the parameters relating to the important biphasic release and enabled the effect of race on the parameters to be evaluated. A significant difference between races was identified in the derived parameter $K_R\ I_R$ that relates to the first-phase insulin release. Our result is supported by our previous exploratory nonparametric analysis of the insulin-glucose kinetics where we found African-Americans to have a higher insulin concentration in the first-phase compared to Caucasians (25). The proposed kinetic model in this work offers an opportunity to quantify the biphasic characteristic of insulin release and provides a mechanistic and quantitative understanding of the first-phase release, which has been found to play an important role in the development of type 2 diabetes.

Table 5.1. Population estimates of the proposed PK/PD model using Monolix

| Parameters | Estimate | RSE(%)* |
|---|---|---|
| $K_G$ ($min^{-1}$) | 0.24 | 21 |
| $E_{max}$ ($min^{-1}$) | 0.0185 | 16 |
| $C_{50}$ (mg/dl) | 73.8 | 6 |
| $P_e$ ($L^{-1}$) | 0.0581 | 25 |
| $K_I$ ($min^{-1}$) | 0.194 | 12 |
| $K_{RR}$ ($min^{-1}$) | 0.499 | 0.2 |
| α | 4.05 | 13 |
| $I_{R\_}0$ (μU) | 4530 | 34 |
| $C_{I\_}0$ (μU/ml) | 8.7 | 12 |
| $K_R \cdot I_R$ (μU/min) ‡ | 1580** | 31 |
| β_ $K_R I_R$ | -0.922 | 27 |
| b | 0.185 | 3 |
| Standard deviation of parameters | | |
| $K_G$ | 0.296 | |
| $E_{max}$ | 0.189 | |
| $C_{50}$ | 0.224 | |
| $P_e$ | 0.146 | |
| $K_I$ | 0.505 | |
| $K_{RR}$ | 0.216 | |
| α | 0.278 | |
| $I_{R\_}0$ | 0.403 | |
| $C_{I\_}0$ | 0.659 | |
| $K_R \cdot I_R$ (African-American) | 0.608 | |
| $K_R \cdot I_R$ (Caucasian) | 0.699 | |

‡ $p = 0.00016$.

** The value is for African-American which is used as reference.

$K_R \cdot I_R$ of Caucasian is calculated as: 1580*exp(-0.922) = 628.

* RSE, relative standard error.

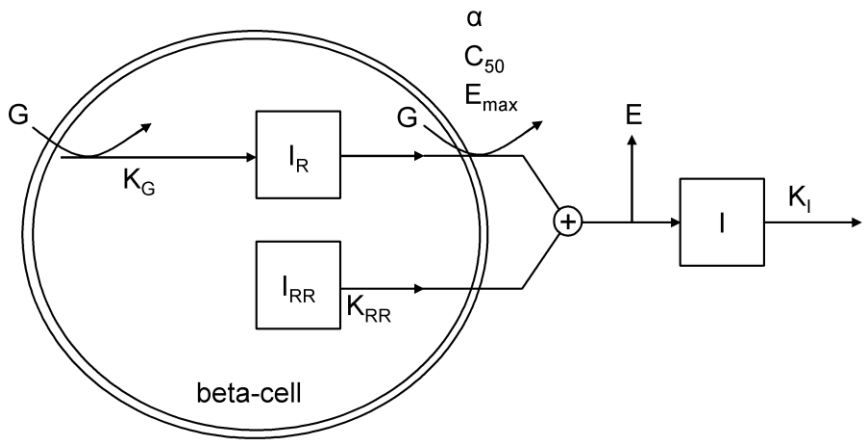


Figure 5.1. Diagram of the proposed PK/PD model.

The proposed model is formulated on the beta-cell level and includes two insulin pools. $I_R$ denotes the reserved insulin that is responsible for the second-phase insulin secretion; $I_{RR}$ denotes the readily releasable insulin that responsible for the first-phase insulin secretion; $G$ represents the glucose; $I$ represents plasma insulin; $E$ denotes the extraction ratio of insulin by liver. $K_G$, $K_I$ and $K_{RR}$ are rate constants; $C_{50,}$ $E_{max}$ and α are the parameters in the Hill equation.

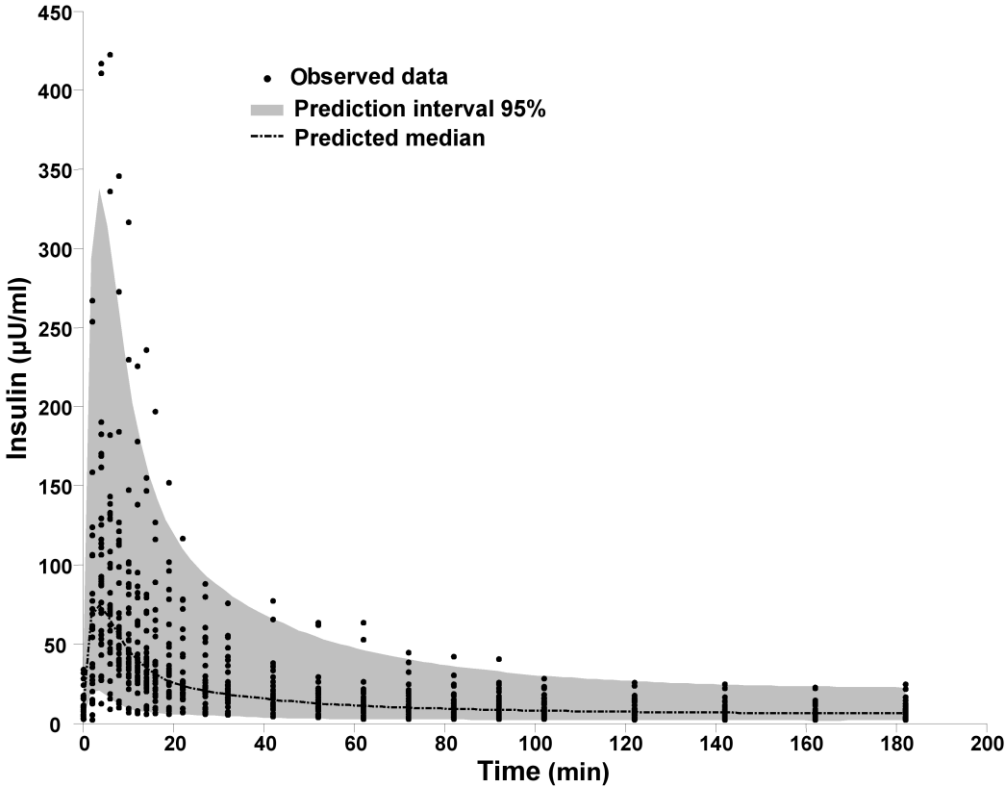


Figure 5.2. Visual predictive check of the population PK/PD model.

Comparison of the observed concentrations with the median and 95% interval predicted for 1000 simulated data sets computed from the estimated population PK/PD model.

.

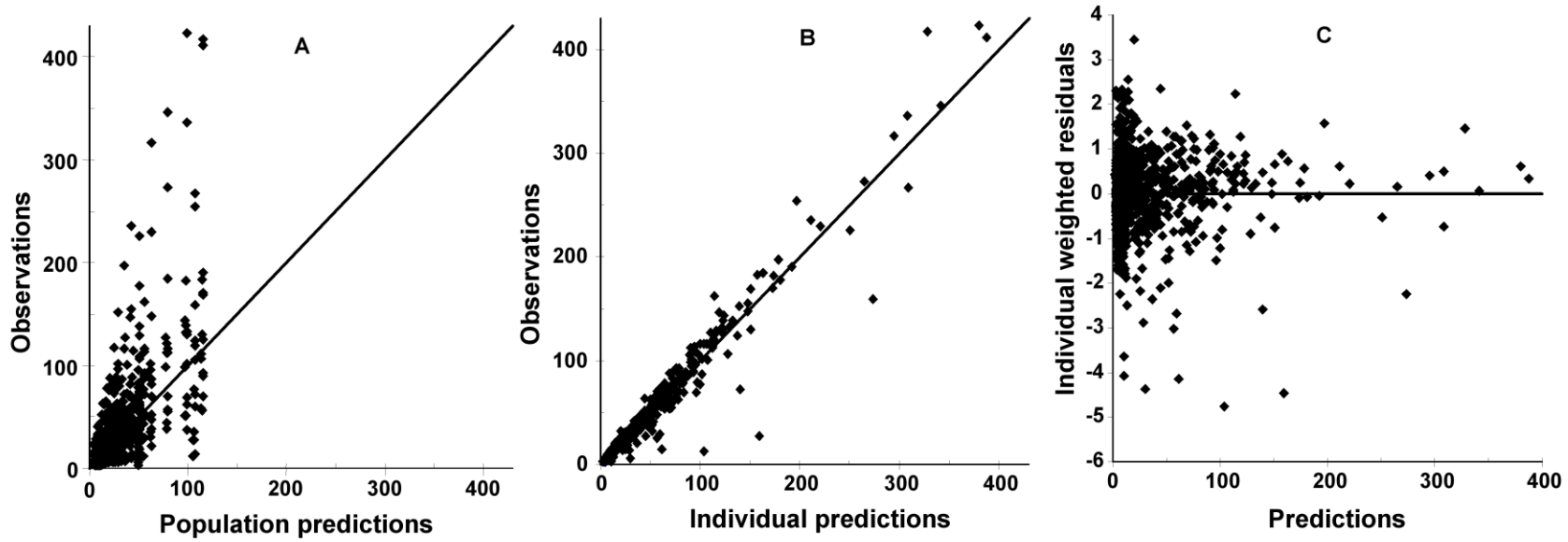


Figure 5.3. Goodness of fit plots of population model. (A) observed insulin concentrations vs. population predictions, (B) observed insulin concentrations vs. individual predictions, and (C) weighted residuals vs. population.

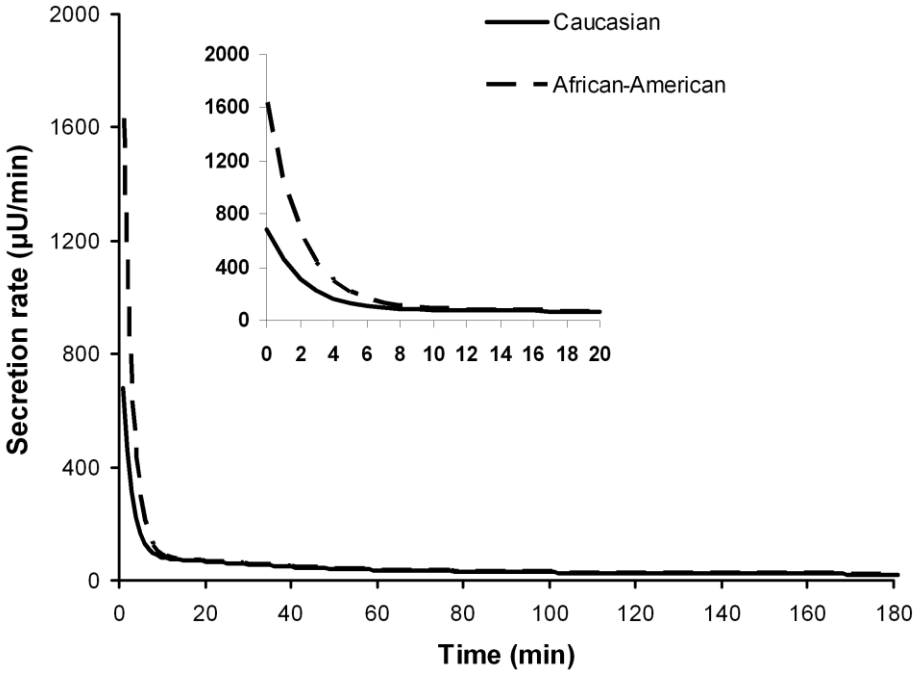


Figure 5.4. Beta-cell secretion profile during FSIVGTT for African-American and Caucasian youth according to population parameters and averaged glucose concentration.

# CHAPTER 6. A POPULATION KINETIC ANALYSIS OF PREHEPATIC INSULIN SECRETION

## 6.1 Introduction

Quantitative estimation of pancreatic insulin release is necessary for the understanding of the pathogenesis of type 2 diabetes (T2D), which is characterized by a progressive loss of beta-cell function (186). However direct measurement of insulin secretion rate (ISR) from beta-cells in human is not feasible because of the need for prehepatic blood sampling. The plasma insulin concentration is accessible *in vivo*, but that only provides information about the posthepatic insulin delivery because insulin released from the beta-cells is partly extracted by the liver before entering the circulation (187). However, the ISR can be quantified indirectly using plasma C-peptide (CP) data based on the fact that CP and insulin are secreted at an equal molar ratio (188). Deconvolution technique (79, 120, 189) can reconstruct ISR from the time course of CP and its disposition kinetics. The required CP kinetics can be acquired in a separate experiment in the same subjects (79), or, alternatively, by using parameter values from population analysis (80). Another choice is the "combined model" (96, 115, 121) that combines insulin and CP data in a single experiment analysis. The advantage of the combined model approach is the combined use of insulin and CP kinetics and not requiring a prior knowledge of CP kinetic parameter. However the combined model does not accurately estimate the second-phase of insulin secretion (126) and does not describe the effect of glucose on insulin secretion. The minimal model of insulin secretion (128, 190, 191) can quantify both the ISR and the glucose effect on ISR. However the minimal model describes insulin and CP kinetics separately, and does not capture the insulin concentration profiles well under oral glucose load (190).

In a previous study (192), we proposed a model for analyzing the insulin kinetics based on an frequently sampled intravenous glucose tolerance test (FSIVGTT). In this

study, the previous model was applied to the oral glucose tolerance test (OGTT) by specifically making use of CP and insulin data based on equimolar co-secretion of insulin and CP, and the impact of covariates on insulin secretion was investigated.

## 6.2 Specific aim and hypothesis

The specific aim of this chapter is to extend the proposed model for the oral glucose administration by making use of the co-secretion kinetics of insulin and glucose and to identify covariates' effects on the prehepatic insulin secretion using a population approach.

The specific hypothesis is the proposed model can simultaneously characterize the insulin and C-peptide secretion responses to an oral glucose load and thus evaluate prehepatic insulin secretion.

## 6.3 Materials and methods

### *6.3.1 Data*

The data used in this study is originated from the published paper by Mari *et al.* (193). The standard 75-g OGTT was performed on 221 subjects who classified as normal glucose tolerance (NGT), impaired glucose tolerance (IGT), or T2D based on the 1997 American Diabetes Association criteria. There are 149 females in NGT group with age 33.1±5.28 (mean±SD) years, BMI 26.1±5.3; 27 females and 2 males in IGT group with age 37.5±5.28 years, BMI 30±4.14 kg/m$^2$; 17 females and 26 males in T2D group with age 53.7±12.7 years, BMI 30.8±4.82 kg/m$^2$. Plasma glucose and insulin concentrations were measured at fasting state (time 0) and 10, 20, 30, 60, 90, 120, 150 and 180 minute after glucose load. Detailed information for subjects and study procedure are described in the original paper (193).

### *6.3.2 PK/PD model*

The proposed model (Figure. 6.1) is adapted for OGTT analysis from the model used in our previous study (192), which was aimed at describing the biphasic character of insulin secretion in response to an IV bolus glucose stimulation. Since the first-phase is not visible from the OGTT data, the insulin pool in the beta-cell that governs the first-phase secretion was not included in the model.

The production rate of insulin in the beta-cell is assumed to be proportional to the plasma glucose concentration ($C_G$), and the release rate of insulin is described by a sigmoidal Hill equation. Let $I_R$ denotes the reserved insulin pool storing the biosynthesized insulin and CP in the beta-cell, then the rate of change of insulin in $I_R$ is given by Eq. 6.1:

$$\frac{dI_R(t)}{dt} = K_G C_G(t) - \frac{E_{\max} C_G(t)^{\alpha}}{C_G(t)^{\alpha} + C_{50}{}^{\alpha}} I_R(t) \qquad \text{Eq. 6.1}$$
$$I_R(0) = I_R\_0$$

where $K_G$ is a first order rate constant, $I_R\_0$ is the estimated initial value of $I_R$ pool, while *Emax*, $C_{50}$ and $\alpha$ are the Hill equation parameters.

A constant extraction fraction, denoted *E*, of insulin secreted from the beta-cells is assumed to be removed by the liver prior to its entry into the circulation. The plasma is treated as a single compartment. Accordingly, the rate change of insulin in the plasma is given by:

$$\frac{dI(t)}{dt} = (1-E)\frac{E_{\max} C_G(t)^{\alpha}}{C_G(t)^{\alpha} + C_{50}{}^{\alpha}} I_R(t) - K_I I(t) \qquad \text{Eq. 6.2}$$
$$C_I(t) = I(t)/V_I \qquad C_I(0) = C_I\_0$$

where $K_I$ is a first-order elimination rate constant for insulin, $C_I$ is the insulin concentration in plasma, $C_I\_0$ is the basal insulin concentration at fasting state and $V_I$ is the distribution volume of insulin in plasma.

The CP secretion rate is equal to the ISR from the beta-cells, which is denotes as R(t):

$$R(t) = \frac{E_{\max} C_G(t)^{\alpha}}{C_G(t)^{\alpha} + C_{50}(t)^{\alpha}} \qquad \text{Eq. 6.3}$$

The CP kinetic is assumed to follow a two-compartmental model (79) described by:

$$\begin{aligned} \frac{dP_1(t)}{dt} &= -(K_P + K_{12})P_1(t) + K_{21}P_2(t) + R(t) \\ \frac{dC_{P_1}}{dt} &= \frac{dP_1(t)/V_P}{dt} \qquad C_{P_1}(0) = C_{P_1}\_0 \end{aligned} \qquad \text{Eq. 6.4}$$

$$\begin{aligned} \frac{dP_2(t)}{dt} &= -K_{21}P_2(t) + K_{12}P_1(t) \\ P_2(0) &= CP_1(0)V_P K_{12}/K_{21} \end{aligned} \qquad \text{Eq. 6.5}$$

where $P_1$ and $P_2$ are amounts of CP in central and peripheral compartments, respectively; $K_{12}$ is the rate constants of CP transferred from the central to the peripheral compartment and $K_{21}$ denotes the reverse transfer rate constant; $K_P$ is the first-order rate constant for CP's elimination from the central compartment; $V_P$ is the volume of distribution for CP in central compartment, and $C_{P_1}\_0$ is the basal plasma CP concentration at fasting state.

### *6.3.3 Population model*

A nonlinear mixed-effects model was applied for the population analysis based on the PK/PD model from which "fixed effect" (parameters) and "random effect" (between-subject variability and within-subject variability) were estimated. The nonlinear mixed-effects model is written as follows:

$$y_{ij} = f(\varphi_i, t_{ij}) + b \cdot f(\varphi_i, t_{ij}) \cdot \varepsilon_{ij} \qquad \text{Eq. 6.6}$$

where $y_{ij}$ is the $j$-th observation of insulin or CP of subject $i$ at time $t_{ij}$ ( $i = 1, \ldots, n$, $j = 1, \ldots, k$), and $f$ is the PK/PD model defined by Eq. 6.1-6.5. Various types of error models including constant, proportional, combined and exponential form were tested and the

error model choice was based on the likelihood ratio test with significant level equal to 0.05 and plots of goodness-of-fit. This resulted in the proportional error model for insulin and CP, consistent with Eq. 6.6, in which *b* is the coefficient and $\varepsilon_{ij}$ is a random variable following a normal distribution with mean 0 and variance 1.

It is assumed that the *p*-dimensional vector $\varphi_i$ which denotes individual parameters for subjects *i* is log-normally distributed, as commonly done in population PK/PD analysis. Accordingly, the individual parameters were modeled with covariates and variability as:

$$\ln(\varphi_i) = \mu + \beta c_i + \eta_i \qquad \text{with} \quad \eta_i \sim_{i.i.d} N(0,\Omega) \qquad \text{Eq. 6.7}$$

where $\mu$ is a vector of population means for parameters of length *p*; $\beta$ is a vector of coefficients of size *p*; $c_i$ is a vector of covariates with size *p*; $\eta_i$ is a random variable assumed to be a normal distribution with mean 0 and a diagonal variance matrix $\Omega$. The significance of $\beta$ was evaluated by Wald test at an alpha error level of 0.05.

### *6.3.4 Data analysis*

The population modeling was executed using Monolix, standalone version 3.1, an open-source free computer software developed by INRIA, France (140). The population parameters were estimated using Stochastic Approximation Expectation Maximization (SAEM) algorithm coupled with Markov Chain Monte Carlo procedure (171, 194-196). The conditional means and conditional standard deviations of individual parameters were calculated using Hastings-Metropolis algorithm. We did not model the glucose time course in this study; instead the glucose concentrations were represented as an "influence function" by a linear spline function interpolating the glucose data. Individual CP kinetic parameters were calculated according to the formula described by Van Cauter et.al. (80) and fixed in the population analysis.

**6.4 Results**

The proposed model is able to simultaneously capture the insulin and CP dynamics well both in the individual and population estimations in response to the oral glucose stimulation. Figure 6.2 shows representative individual fittings of insulin and CP data for the NGT, IGT and T2D groups. The fittings were done using WINFUNFIT (180). Figure 6.3 shows the performance of the population model. The predictions of insulin and CP (left panels of Figure 6.3) calculated based on individual parameter estimates were in good agreement with the observations. The scatter plots of weighted residuals against predicted insulin and CP concentrations (right panels of Figure 6.3) showed that both were randomly distributed around the null ordinate, although three weighted residuals fall out of ± 3 units.

The glucose tolerance (NGT, IGT and T2D), obesity and gender were evaluated as categorical covariates in the population analysis. Age, which could have an effect on insulin and CP secretion, was not considered because all T2D patients are older compared to healthy and IGT subjects (193). Inclusion or exclusion of covariates in the structure of the population model (Eq. 6.7) was determined by Wald test at an alpha significance level of 0.05. Population estimates of parameters, between-subject variability (standard deviation) and covariates'effect ($\beta$) on parameters are summarized in Table 6.1. Compared with female nonobese NGT subjects, obese subjects were found to have higher (p=0.00013) insulin production rate ($K_G$), while IGT, T2D and male subjects have lower (all $p < 0.005$) insulin production rate in response to glucose stimulation. The Hill function parameters ($E_{max}$, $C_{50}$, $\alpha$) and initial size of $I_R$ pool ($I_R\_0$) are the parameters controlling the insulin release from the beta-cells. There are no differences in those parameters between female and male subjects. The IGT and T2D were detected to have significant effects on $E_{max}$ (both $p < 0.00001$), $C_{50}$ (both $p < 0.05$) and $I_R\_0$ ($p < 0.00001$), while obesity only significantly affects $E_{max}$ (p=0.011). Figure 6.4 shows the prehepatic ISR profiles, normalized to body surface area, calculated based on the parameters for the

NGT, IGT and T2D subjects respectively. There are no differences in liver extraction ($E$) between groups. The estimated insulin elimination from plasma ($K_I$) is 0.106 $min^{-1}$ which corresponds to a 6.5 min half-life for female nonobese subject with normal NGT. Male subjects have shorter insulin half-life (5.3 min, p=0.00074) than females, while obese subject has longer insulin half-life of 7.3 min (p=0.016) than subjects with normal weight subjects. IGT and T2D have no significant impact on insulin elimination from plasma. Obesity, IGT, T2D were found to have a positive effect on basal insulin (all $p < 0.05$) and CP (all $p < 0.05$) concentrations, while males have higher basal plasma insulin (p=0.00075) concentrations than females.

**6.5 Discussion**

Model-base approaches are restricted to the experimental protocol and the type of data available. It is recognized that an analysis of the effect of glucose on the production and release of insulin from beta-cell is best served by a model specifically developed to simultaneously describe the plasma insulin and CP time courses and utilizing the fact that insulin and CP are secreted form the beta-cells in a one-to-one molar ratio. Our proposed model adheres to this analysis paradigm. Our study represents an important extension of our prior PK/PD model. It shows that the model is applicable both to IVGTT and OGTT tests. The applicability to the OGTT is particularly important since this test more closely relates to the physiological conditions after a meal compared to the IV glucose challenge.

Both a one- or two-compartment model have been suggested for CP kinetics (79, 197, 198). The one-compartmental kinetics is simple and leads to simpler parameter estimation, but may not provide as good an agreement with the data as the two-compartment model (96). Since in this study the covariate analysis focus on the parameters controlling the insulin kinetics and not the CP kinetics, it was appropriate to fix the CP kinetic parameters according to values calculated based on subject's sex, age, weight and glucose tolerance (80).

Gender was found to affect the production and clearance of insulin in the study. However, the results may be somewhat inaccurate because the distribution of gender between groups is biased. The regulation of insulin secretion is more complex in the case of OGTT compared to IVGTT. In addition to glucose's effects on insulin production and release (176, 178), gastrointestinal hormones also influence the insulin response. For example, the important function of incretin GLP-1 is to increase insulin secretion (199-202). The kinetic modeling based on the present data can not distinguish the action of such hormones. The parameters describing the effect of glucose on insulin production ($K_G$) and secretion ($E_{max}$, $C_{50}$ and $\alpha$) reflect the overall effects of glucose and the gastrointestinal hormones.

The differences in insulin production and insulin secretion during the OGTT between various glucose and obesity groups are identified by our proposed population kinetic analysis. In response to the same glucose level, the production rate of insulin in the obese group was found to be 25% higher than that in NGT with normal weight, while the production rate of insulin is reduced by 22% in IGT and 62% in T2D. Glucose tolerance has effects on parameters that control the insulin release ($E_{max}$, $C_{50}$ , and $I_{R\_}0$). Figure 6.7 shows effects which are consistent with the estimations of prehepatic ISR using a deconvolution approach (193). Compared to the NGT subjects the following 3 effects were observed: 1) a delayed response in the early stage (~80min); 2) an increased secretion after early stage in IGT, and, 3) a delayed and reduced response in T2D in spite of the abnormal hyperglycaemia.

The hepatic extraction fraction ($E$) was estimated as an average value during the OGTT, and was not found to be different between subjects with various glucose tolerance and obesity status. However $E$ is dynamically changing during OGTT. Campioni and his colleages (190) provide an approach to estimate a time variant $E$ by modeling it as a piecewise linear function between break points. We also estimated the dynamic changes in $E$ using a piecewise linear spline function. The following method was used to estimate

the time variant liver extraction: first, the insulin release kinetic parameters were calculated using CP data only and Eq.6.3-6.5; subsequently, the *E*s were estimated using insulin data only and Eq. 6.1-6.2 with known insulin kinetic parameters; the dynamic of *E* in the NGT group is shown in Figure 6.5. Furthermore, covariates analysis on *E* at fasting state indicates that the extraction of insulin is lower in obese, IGT and T2D subjects (all $p < 0.05$) than nonobese NGT group.

### 6.6 Conclusions

In summary, a new combined model has been developed to estimate prehepatic insulin secretion and to investigate the effects of various covariates on insulin secretion using a population kinetic approach. We extended the PK/PD model for IVGTT to estimate insulin secretion *in vivo* and investigated the effects of the BMI and glucose tolerance on insulin secretion using the population kinetic approach. The model makes use of the co-secretion kinetics and is able to adequately capture the insulin and CP plasma concentration profiles simultaneously. The prehepatic insulin secretions obtained using this method agree with previous results calculated using a deconvolution approach (193). There is no significant impact glucose tolerance on the clearance of insulin from the plasma and extraction by liver during OGTT. Therefore, the differences in insulin concentration between groups with various status of obesity and glucose tolerance are mainly cause by insulin secretion during OGTT. Obesity leads to a higher insulin production rate and lower elimination rate from the plasma than normal weight subjects. Whereas T2D and IGT reduce insulin production rate and have delayed insulin secretion by affecting the parameters ($E_{max}$, $C_{50}$ and $I_R\_0$) which control the insulin release from the beta-cells.

Although the precise mechanism by which obesity contributes to insulin resistance and T2D has not yet been defined, it is likely related to the production of

various factors derived from the adipocyte that act on fat, liver, or muscle to impair insulin action.

Table 6.1. Population estimates of the proposed model parameters

| Model parameters | | | |
|---|---|---|---|
| | Mean | RSE% [a] | SD [b] |
| $K_G$ ($min^{-1}$) | 98.5 | 4 | 0.373 |
| $E_{max}$ ($min^{-1}$) | 0.0316 | 10 | 0.317 |
| $C_{50}$ (pmol/l) | 6.07 | 2 | 0.134 |
| A | 4.43 | 5 | 0.388 |
| E | 0.0784 | 64 | 0.612 |
| $K_I$ ($min^{-1}$) | 0.106 | 4 | 0.229 |
| $I_{R\_}0$ (pmol) | 27900 | 11 | 0.424 |
| $C_{L\_}0$ (pmol/l) | 47.2 | 4 | 0.35 |
| $V_I$ (l) | 18.7 | 7 | 0.146 |
| $C_{P_1\_}0$ (pmol/l) | 513 | 3 | 0.344 |
| Coefficient of random structure | | | |
| | Mean | RSE% [a] | |
| b (insulin) | 0.262 | 2 | |
| b (C-peptide) | 0.115 | 2 | |

[a] RSE% denotes relative standard error.

[b] Standard deviation of log(parameter).

Table 6.1. Continued

| Covariate's effect on model parameters | | | |
|---|---|---|---|
| | Mean | RSE%[a] | Significance[c] |
| $\beta\_K_G$ (Male) | -0.728 | 15 | S |
| $\beta\_K_G$ (IGT) | -0.241 | 33 | S |
| $\beta\_K_G$ (T2D) | -0.966 | 10 | S |
| $\beta\_K_G$ (OBE) | 0.222 | 26 | S |
| $\beta\_E_{max}$ (IGT) | 0.999 | 24 | S |
| $\beta\_E_{max}$ (T2D) | 1 | 20 | S |
| $\beta\_E_{max}$ (OBE) | 0.21 | 40 | S |
| $\beta\_C_{50}$ (IGT) | -0.105 | 45 | S |
| $\beta\_C_{50}$ (T2D) | 0.158 | 39 | S |
| $\beta\_K_L\_0$ (Male) | 0.257 | 25 | S |
| $\beta\_K_L\_0$ (OBE) | -0.106 | 42 | S |
| $\beta\_I_R\_0$ (IGT) | -1.79 | 17 | S |
| $\beta\_I_R\_0$ (T2D) | -1.98 | 11 | S |
| $\beta\_C_L\_0$ (Male) | -0.419 | 30 | S |
| $\beta\_C_L\_0$ (IGT) | 0.163 | 56 | NS |
| $\beta\_C_L\_0$ (T2D) | 0.224 | 47 | S |
| $\beta\_C_L\_0$ (OBE) | 0.539 | 13 | S |
| $\beta\_C_{P_1}\_0$ (IGT) | 0.156 | 48 | S |
| $\beta\_C_{P_1}\_0$ (T2D) | 0.144 | 45 | S |
| $\beta\_C_{P_1}\_0$ (OBE) | 0.352 | 16 | S |

[a] RSE% denotes relative standard error.

[c] S denotes significance and NS denotes Non-significance based on the significance level of p=0.05; subject with NGT and non-obesity as reference group.

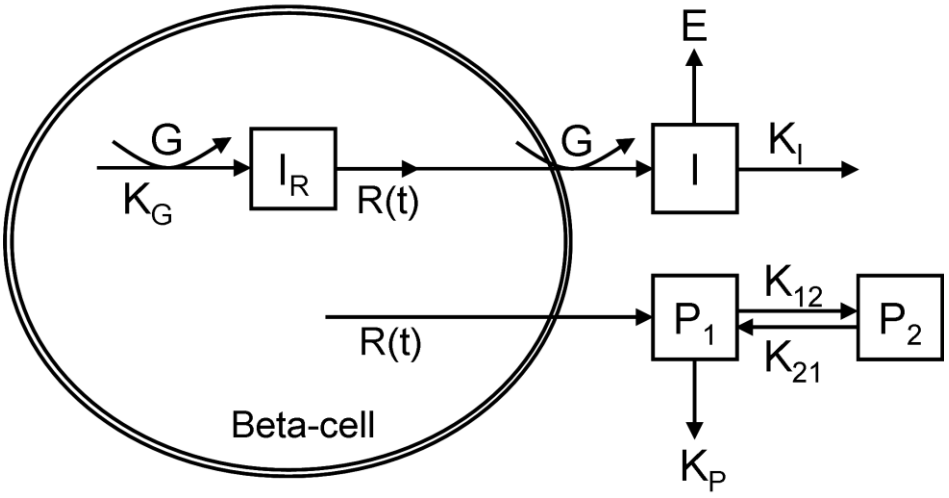


Figure 6.1. Proposed model of insulin and C-peptide dynamics.

*I* denotes insulin in plasma; $P_1$ and $P_2$ are C-peptide in the central and peripheral compartments; $I_R$ is reserved insulin in the beta-cell; *G* is glucose; *R(t)* is the prehepatic insulin or C-peptide secretion rate.

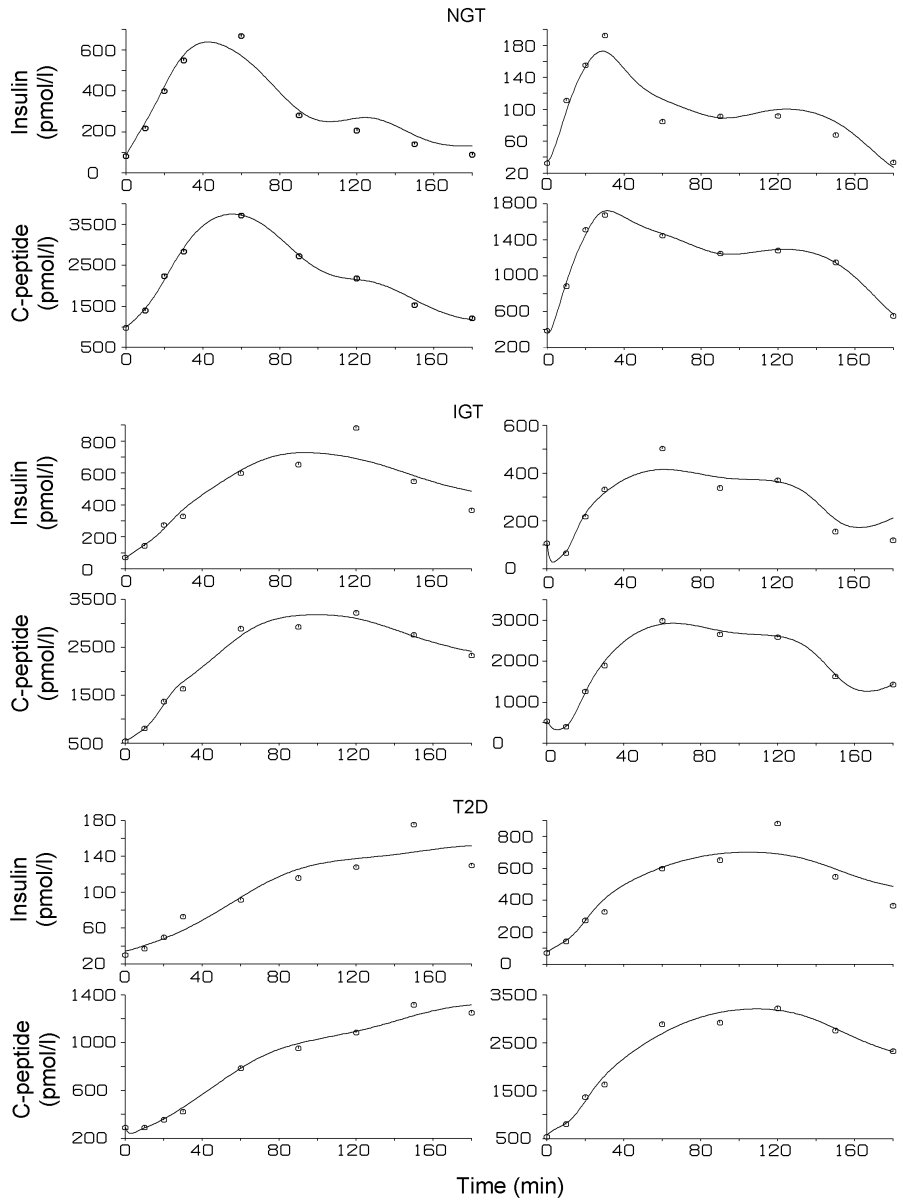


Figure 6.2. Representative plots of the proposed model by simultaneously fitting insulin and C-peptide data in OGTT from subjects with various levels of glucose tolerance.

NGT, IGT and T2D denote normal glucose tolerance, impaired glucose tolerance and type 2 diabetes, respectively. Circles denote observations and lines show the fitting.

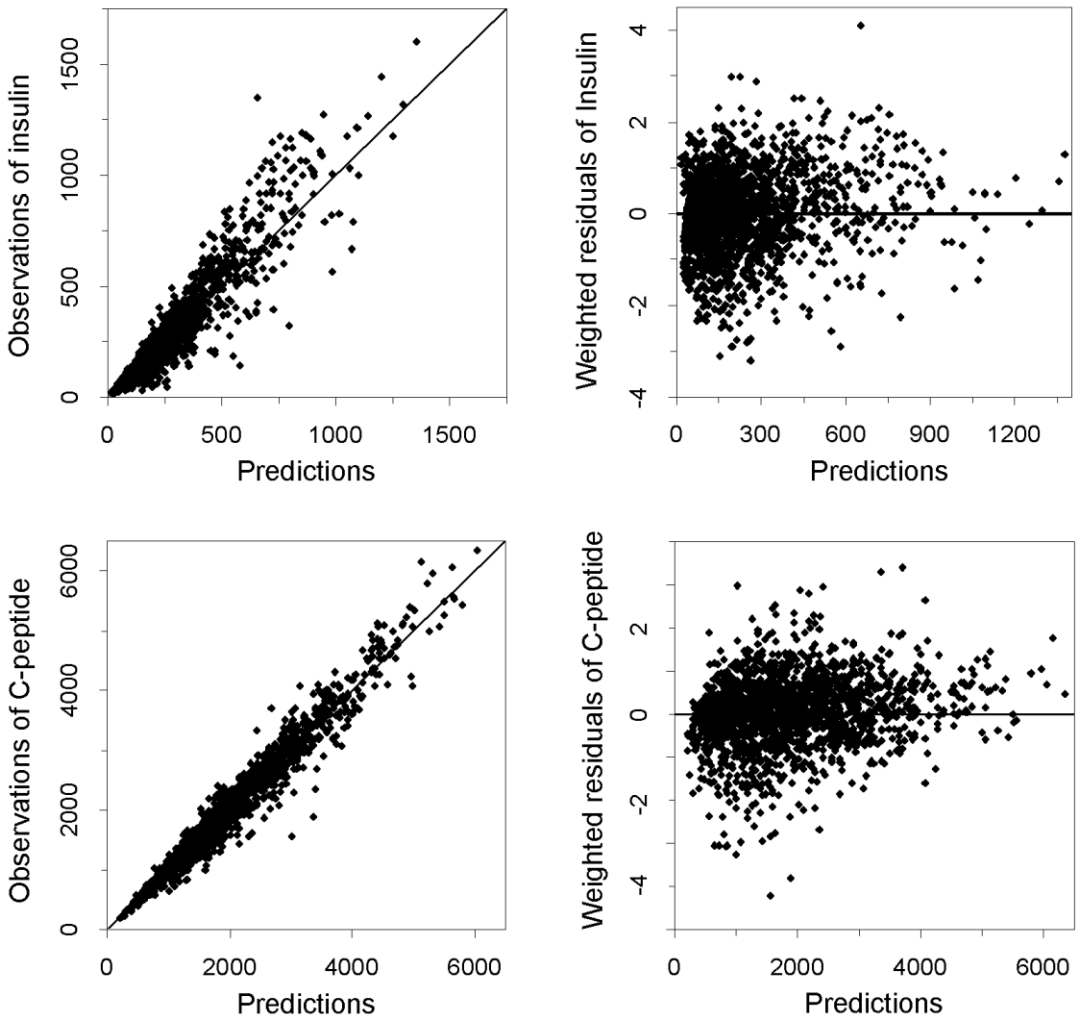


Figure 6.3. Scatter plots of observations versus individual predictions (left panels) and weighted residuals versus individual predictions (right panels) during OGTT.

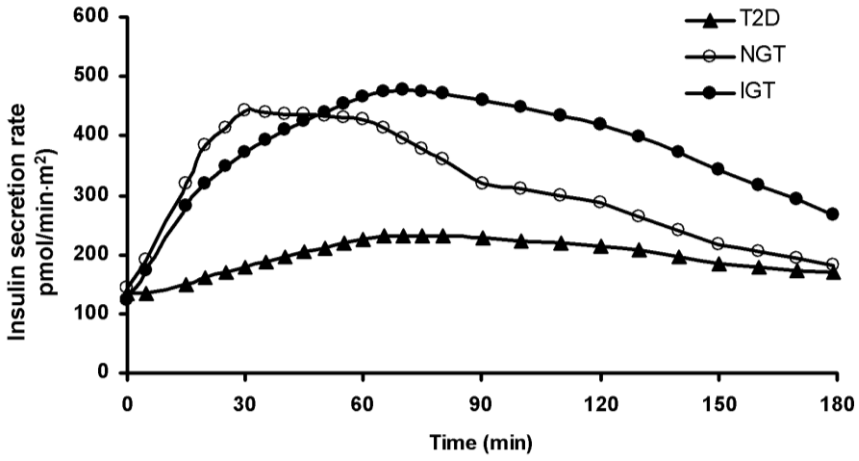


Figure 6.4. Simulated prehepatic insulin secretion rate during OGTT for subjects with various levels of glucose tolerance using population estimates of parameters and mean concentrations of insulin and glucose.

T2D, NGT and IGT denote type 2 diabetes, normal glucose and impaired glucose tolerance, respectively.

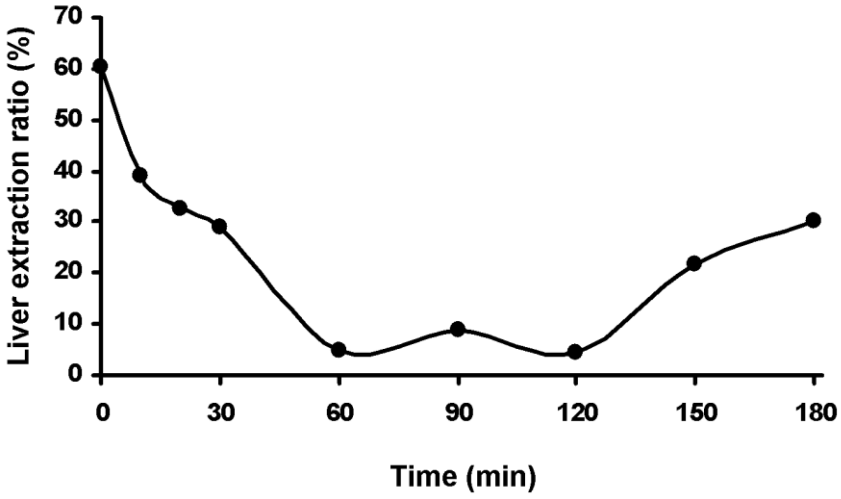


Figure 6.5. The ratio of insulin extracted by liver during OGTT in female subjects with normal glucose tolerance.

# CHAPTER 7. FUTURE WORKS

The study of beta-cell function can benefit from the research which has been undertaken for this thesis. The proposed model is able to describe beta-cell secretory responses to IV or oral glucose stimulation and identify the factors that affect parameters of insulin kinetics, such as first-phase and second-phase insulin secretion, insulin production and elimination of insulin from plasma. However, there are also several additional areas for further development and applications for.

The first potential area that might be highlighted by the study of the thesis is the early diagnosis of type 2 diabetes (T2D). The parameters that quantify first- and second-phase insulin secretion provided by the proposed model, together with other factors such as family history, fating insulin and glucose concentration, could be used for improving early diagnosis of T2D or prevention of development of T2D.

The second possible application is for drug development. It has been gradually realized that insulin secretion should be not only at right amount but also at right time. The importance of biphasic insulin secretion has particularly been addressed in Chapter 1.5. Numerous efforts have been devoted by pharmaceutical companies to develop insulin formulations that closely mimic the kinetics of this complex insulin secretion pattern. The proposed model provides a valuable tool to simulate insulin concentrations under designed formulations. Also for those drugs designed for restoring or increasing first-phase insulin secretion, the effects of those drugs on first-phase can be quantified by the proposed model.

The research presented in this thesis seems to have left questions that need to be answered. For example, the effect of glomerular filtration on insulin clearance. The liver and kidneys are the main sites of insulin degradation. The liver removes approximately 50% of insulin released from the pancreas (21, 22). The kidneys are the major sites that remove insulin from the systemic circulation, removing 50% of peripheral insulin via

glomerular. One of long-term effect of T2D is dysfunction of kidneys. Therefore, creatinine clearance rate (CrCl) reflecting the ability of glomerular filtration should be measured and considered as an important factor that may affects insulin clearance.

The dependency of insulin secretion on glucose concentration is other line that not addressed in the thesis. Several studies (170, 175, 179) have reported that the magnitude of the peak of the first-phase is varying with the level of glucose, while the shape and the transient nature of the peak remains unchanged. Thus, the size of insulin pool ($I_{RR}$) that governs the first-phase insulin secretion according to the proposed model should be associated with the glucose level. However, we could not estimate the dependence of $I_{RR}$ on the glucose dose since only one level of glucose stimulation was tested in our study subjects. The dependency is able to determine by performing multiple glucose dose in the future study.

The model considers the insulin dynamics only. Future work may incorporate glucose dynamic to reflect the feedback system of glucose and insulin, thus develop a model for the progression of T2D.

## APPENDIX A. FORTRAN PROGRAM FOR CHAPTER 4

****Begin prologue
This FORTRAN calculates the first-phase insulin secretion index, AIRg, which is defined as the area under the plasma insulin curve over the basal insulin level between 1 and 10 minutes during an intravenous glucose tolerance test (IVGTT):

$$AIR_g = \int_0^{10} [I(t) - I_b]\, dt \qquad \text{Eq. 4.1}$$

The program runs under a computer-based program WINFUNFIT. The analysis involves 6 files in CD:
(1). program files: \fortran\AIRg.F90
\fortran\GCV.FOR
(2). WINFUNFIT files: \fortran\ALLWINFUNFIT
\fortran\FUNFIT_RESOURCES.res
(3). data file: \fortran\AIRg*.DAT (for example 3MAA_PP@INS.DAT )
(4). output file:\fortran\AIRg\AIR_10.DAT
****End prologue

```
PROGRAM AIRg
IMPLICIT NONE
INTEGER, PARAMETER :: NPT=6000
INTEGER NOBS,J,II,LUN,NN,V, LFile
REAL*8 TOBS(NPT), COBS(NPT),CLN(NPT)
REAL*8 LNG
REAL*8 TSP(NPT),GSP(NPT), TIME_STEP1,TIME_STEP2, G_STEP1, G_STEP2
REAL*8 GGS(NPT),GGL(NPT),TTS(NPT)
LOGICAL SHOWIT
CHARACTER*256 ID,DATAFILENAME,File, FLAG,F
REAL*8 TIME,S

  FLAG='Y'

  DO WHILE((FLAG .EQ. 'Y') .OR. (FLAG .EQ. 'y'))
    NOBS=NPT
    CALL XY_DATA_FOR_SPLIN_FROM_FUNFIT_FILE(TOBS,COBS, NOBS,F)
    CLN(1:NOBS)=DLOG(COBS(1:NOBS))

    V=40
    TIME_STEP1=(TOBS(2)-TOBS(1))/V
    TIME_STEP2=(TOBS(3)-TOBS(2))/V
    G_STEP1=(CLN(2)-CLN(1))/V
    G_STEP2=(CLN(3)-CLN(2))/V

    DO J=1,V+1
      TSP(J)=TOBS(1)+(J-1)*TIME_STEP1
      GSP(J)=CLN(1)+(J-1)*G_STEP1
    END DO

    DO J=V+2,2*V+1
    TSP(J)=TOBS(2)+(J-11)*TIME_STEP2
    GSP(J)=CLN(2)+(J-11)*G_STEP2
    END DO
```

```
    DO J=4,NOBS
      II=2*V-2+J
      TSP(II)=TOBS(J)
      GSP(II)=CLN(J)
    END DO

    NN=NOBS+2*V-2
!   WRITE (*,*) (TOBS(II),COBS(II),CLN(II), II=1,NOBS)
!   WRITE (*,*) 'DONE'
!   READ *
    CALL CUBIC_GCV_FIT(TSP,GSP,NN)

    DO J=1,NOBS
      TTS(J)=TOBS(J)
      CALL CUBIC_GCV(TTS(J),GGL(J))
      GGS(J)=DEXP(GGL(J))
    END DO

    OPEN (10, FILE = 'AIR_10.DAT ')
    V=4000
    TIME=10.0D0/V
    DO J=1, V+1
      TTS(J)=(J-1)*TIME
      CALL CUBIC_GCV(TTS(J), GGL(J))
      GGS(J)=DEXP(GGL(J))
    END DO

    S=0D0
    DO J=1, V
      S=S+ (GGS(J)+GGS(J+1))*TIME/2.0D0
    END DO

    S=S-COBS(1)*10.0D0

    WRITE (10,'(A15,F12.4)') F, S
    WRITE(*,*) ''
    WRITE(*,*) 'AIRg =', S
    WRITE(*,*) 'CONTINUE (Y OR N)'
    READ(*,*) FLAG
  END DO


!**
CONTAINS
SUBROUTINE XY_DATA_FOR_SPLIN_FROM_FUNFIT_FILE (X,Y,N,F)
IMPLICIT NONE
INTEGER, INTENT (INOUT) :: N
REAL*8,  INTENT (INOUT) :: X(*), Y(*)
CHARACTER (LEN=256), INTENT(OUT)  :: F
INTEGER, PARAMETER :: MAXLINES = 10000, LENSTRING = 80
INTEGER :: J, JS, K, NN, IERR
CHARACTER (LEN=256) :: DATAFILENAME
CHARACTER (LEN=LENSTRING) :: STRING

  PRINT*," NEXT SELECT THE FILE CONTAINING THE BLOOD INSULIN C-T DATA "
  CALL FILESELECT("DAT", DATAFILENAME, J)
  PRINT*, 'This is the *.DAT file selcted:', DATAFILENAME

  OPEN(UNIT=101, FILE=DATAFILENAME, STATUS='OLD', IOSTAT = IERR)
  IF(IERR /= 0) STOP ' XY_DATA_FOR_SPLIN_FROM_FUNFIT_FILE: &
                       ERROR IN OPENING DATA FILE'
  NN = 0
  F=DATAFILENAME
```

```
  DO J= 1, MAXLINES
    JS = J
    STRING(1:LENSTRING) = ''
    READ (101,"(A)", END = 10, IOSTAT = IERR) STRING
    IF(IERR /= 0) STOP 'GET_XY_DATA_FROM_FUNFIT_FILE:  &
                        ERROR IN READING DATA FILE'
    K = LEN_TRIM(ADJUSTL(STRING))
    IF(STRING(1:1) == 'C' .OR. STRING(1:1) == 'c' .OR. &
       STRING(1:1) == '' .OR. K <= 2) CYCLE
    NN = NN + 1

    IF(NN > N) STOP ' XY_DATA_FOR_SPLIN_FROM_FUNFIT_FILE:  &
                     ASSIGNED DIMENSION OF X, Y TOO SMALL'
    READ(STRING,*, IOSTAT = IERR) X(NN), Y(NN)

    IF(IERR /= 0) STOP ' XY_DATA_FOR_SPLIN_FROM_FUNFIT_FILE:  &
                        ERROR IN DATA FILE LIKELY, PLEASE CHECK'
  ENDDO

  10 IF (JS == MAXLINES) STOP ' XY_DATA_FOR_SPLIN_FROM_FUNFIT_FILE: &
                       DATA FILE CONTAINS TOO MANY LINES (RECORDS)'
  N = NN
  CLOSE (101,STATUS='SAVE')
END SUBROUTINE XY_DATA_FOR_SPLIN_FROM_FUNFIT_FILE

END PROGRAM
!------------------------END-------------------------------
```

****Begin prologue
This FORTRAN program calculates the AUC which is defined as the area under the curve over the basal insulin or glucose concentration during an IVGTT:

$$AUC_{insulin} = \int_{0}^{182} [I(t) - I_b]\, dt$$

$$AUC_{glucose} = \int_{0}^{182} [G(t) - G_b]\, dt$$

The program runs under a computer-based program WINFUNFIT. The analysis involves 7 files in CD:
(1). program files: \fortran\AUC.F90
\fortran\GCV.FOR
(2). WINFUNFIT files: \fortran\ALLWINFUNFIT
\fortran\FUNFIT_RESOURCES.res
(3). data file: \fortran\AUC*.DAT (for example 3MAA_PP@GLU.DAT )
(4). output file: \fortran\AUC\AUC_GLU.DAT
: \fortran\AUC\AUC_INS.DAT
****End prologue

```
PROGRAM AUC
IMPLICIT NONE
INTEGER, PARAMETER :: NPT=6000
INTEGER NOBS,J,II,LUN,NN,V, LFile
REAL*8 TOBS(NPT), COBS(NPT),CLN(NPT)
REAL*8 LNG
REAL*8 TSP(NPT),GSP(NPT), TIME_STEP1,TIME_STEP2, G_STEP1, G_STEP2
REAL*8 GGS(NPT),GGL(NPT),TTS(NPT)
LOGICAL SHOWIT
CHARACTER*256 ID,DATAFILENAME,File, FLAG,F
REAL*8 TIME,S

  FLAG='Y'

  DO WHILE((FLAG .EQ. 'Y') .OR. (FLAG .EQ. 'y'))
    NOBS=NPT

    CALL XY_DATA_FOR_SPLIN_FROM_FUNFIT_FILE(TOBS,COBS, NOBS,F)
    CLN(1:NOBS)=DLOG(COBS(1:NOBS))

    V=40
    TIME_STEP1=(TOBS(2)-TOBS(1))/V
    TIME_STEP2=(TOBS(3)-TOBS(2))/V
    G_STEP1=(CLN(2)-CLN(1))/V
    G_STEP2=(CLN(3)-CLN(2))/V

    DO J=1,V+1
      TSP(J)=TOBS(1)+(J-1)*TIME_STEP1
      GSP(J)=CLN(1)+(J-1)*G_STEP1
    END DO

    DO J=V+2,2*V+1
      TSP(J)=TOBS(2)+(J-11)*TIME_STEP2
```

```
      GSP(J)=CLN(2)+(J-11)*G_STEP2
    END DO

    DO J=4,NOBS
      II=2*V-2+J
      TSP(II)=TOBS(J)
      GSP(II)=CLN(J)
    END DO

    NN=NOBS+2*V-2
!   WRITE (*,*) (TOBS(II),COBS(II),CLN(II), II=1,NOBS)
!   WRITE (*,*) 'DONE'
!   READ *
    CALL CUBIC_GCV_FIT(TSP,GSP,NN)

    DO J=1,NOBS
      TTS(J)=TOBS(J)
      CALL CUBIC_GCV(TTS(J),GGL(J))
      GGS(J)=DEXP(GGL(J))
    END DO

    OPEN (10, FILE = 'AIR_10.DAT ')
    V=4000
    TIME=182.0D0/V
    DO J=1, V+1
      TTS(J)=(J-1)*TIME
        CALL CUBIC_GCV(TTS(J), GGL(J))
        GGS(J)=DEXP(GGL(J))
    END DO

    S=0D0
    DO J=1, V
      S=S+ (GGS(J)+GGS(J+1))*TIME/2.0D0
    END DO

    S=S-COBS(1)*182.0D0

    WRITE (10,'(A15,F12.4)') F, S
!   WRITE(*,*) 'AUC_GLU', S
    WRITE(*,*) 'AUC_INS', S

    WRITE(*,*) ''
    WRITE(*,*) 'CONTINUE (Y OR N)'
    READ(*,*) FLAG

  END DO


!**
CONTAINS
SUBROUTINE XY_DATA_FOR_SPLIN_FROM_FUNFIT_FILE (X,Y,N)
IMPLICIT NONE
INTEGER, INTENT (INOUT) :: N
REAL*8,  INTENT (INOUT) :: X(*), Y(*)
CHARACTER (LEN=256), INTENT(OUT)  :: F
INTEGER, PARAMETER :: MAXLINES = 10000, LENSTRING = 80
INTEGER :: J, JS, K, NN, IERR
CHARACTER (LEN=256) :: DATAFILENAME
CHARACTER (LEN=LENSTRING) :: STRING

  PRINT*," NEXT SELECT THE FILE CONTAINING THE BLOOD INSULIN C-T DATA "
  CALL FILESELECT("DAT", DATAFILENAME, J)
  PRINT*, 'This is the *.DAT file selcted:', DATAFILENAME
```

```
  OPEN(UNIT=101, FILE=DATAFILENAME, STATUS='OLD', IOSTAT = IERR)
  IF(IERR /= 0) STOP ' XY_DATA_FOR_SPLIN_FROM_FUNFIT_FILE: &
                       ERROR IN OPENING DATA FILE'
  NN = 0
  F=DATAFILENAME
  DO J= 1, MAXLINES
    JS = J
    STRING(1:LENSTRING) = ''
    READ (101,"(A)", END = 10, IOSTAT = IERR) STRING
    IF(IERR /= 0) STOP 'GET_XY_DATA_FROM_FUNFIT_FILE:  &
                        ERROR IN READING DATA FILE'
    K = LEN_TRIM(ADJUSTL(STRING))
    IF(STRING(1:1) == 'C' .OR. STRING(1:1) == 'c' .OR. &
       STRING(1:1) == '' .OR. K <= 2) CYCLE
    NN = NN + 1

    IF(NN > N) STOP ' XY_DATA_FOR_SPLIN_FROM_FUNFIT_FILE:  &
                     ASSIGNED DIMENSION OF X, Y TOO SMALL'
    READ(STRING,*, IOSTAT = IERR) X(NN), Y(NN)

    IF(IERR /= 0) STOP ' XY_DATA_FOR_SPLIN_FROM_FUNFIT_FILE:  &
                        ERROR IN DATA FILE LIKELY, PLEASE CHECK'
  ENDDO

  10 IF (JS == MAXLINES) STOP ' XY_DATA_FOR_SPLIN_FROM_FUNFIT_FILE: &
                       DATA FILE CONTAINS TOO MANY LINES (RECORDS)'
  N = NN
  CLOSE (101,STATUS='SAVE')
END SUBROUTINE XY_DATA_FOR_SPLIN_FROM_FUNFIT_FILE

END PROGRAM
!------------------------END-----------------------------
```

## APPENDIX B. MONOLIX SCRIPT AND FORTRAN PROGRAM

## FOR CHAPTER 5

****Begin prologue
This Monolix script yields population statistics of the proposed PK/PD model in Chapter 5 (Eq. 5.1 -5.3). A nonlinear mixed-effects model was used for the population analysis and ethnicity as a covariate was included in the population model. The population model is described by:

$$y_{ij} = f(\phi_i, t_{ij}) + g(\phi_i, t_{ij}) \cdot \varepsilon_{ij} \qquad \text{Eq. 5.4}$$

Proportional residual error $g(\phi_i, t_{ij}) = bf(\phi_i, t_{ij})$ Eq. 5.6

Covariate structure $\ln(\phi_i) = \mu + \beta c_i + \eta_i$ with $\eta_i \sim_{i.i.d} N(0, \Omega)$ Eq. 5.8

where *f* is the proposed PK/PD model described by the ordinary differential equations Eq. 5.1 -5.3.

The program runs under a computer-based program Monolix, standalone version 3.1. The analysis involves 3 files in CD:
(1). Monolix script: \monolix\AA_C_MODEL.TXT
(2). data file: \monolix\AA_C_2Y.TXT
(3). output file: \IV
****End prologue

```
$PROBLEM IVGTT RACIAL IMPACT ON INSULIN BI-PHASIC RELEASE

$MODEL
    COMP=(CI)
    COMP=(IR)
    COMP=(IRR)

$PSI KG EMAX C50 PE KI KRR ALPHA IRB IB KRIR

$REG t_start g_start t_end  g_end

$PK

    PEKR=PE*KRR

    if (T < 182)
      C = g_start + (T - t_start)*(g_end - g_start)/(t_end-t_start)
    else
      C = g_end
    end

$ODE

    CI_0=IB
    IR_0=IRB
    IRR_0=KRIR/KRR

    DDT_CI = PE*IR*EMAX*(C^ALPHA)/(C^ALPHA+C50^ALPHA)-KI*CI + PEKR*IRR
```

```
    DDT_IR = KG*C - IR*EMAX*(C^ALPHA)/(C^ALPHA+C50^ALPHA)
    DDT_IRR = -KRR*IRR


$OUTPUT
    OUTPUT1=CI
;   OUTPUT2=C
```

****Begin prologue
This FORTRAN program simulates the first-phase and second-phase insulin secretion during IVGTT using the proposed PK/PD model in Chapter 5 and population estimates of parameters from Monolix. The PK/PD model is described by:

$$\frac{dI_R}{dt} = K_G C_G - \frac{E_{\max} C_G{}^{\alpha}}{C_{50}{}^{\alpha} + C_G{}^{\alpha}} I_R \qquad I_R(0) = I_R\_0 \qquad \text{Eq. 5.1}$$

$$\frac{dI_{RR}}{dt} = -K_{RR} I_{RR} \qquad I_{RR}(0) = I_{RR}\_0 \qquad \text{Eq.5.2}$$

$$\frac{dC_I}{dt} = \left(\frac{1-E}{V_I}\right)\frac{E_{\max} C_G{}^{\alpha}}{C_{50}{}^{\alpha} + C_G{}^{\alpha}} I_R - K_I \frac{I}{V_I} + \left(\frac{1-E}{V_I}\right) K_{RR} I_{RR}$$

$$= P_e \frac{E_{\max} C_G{}^{\alpha}}{C_{50}{}^{\alpha} + C_G{}^{\alpha}} I_R - K_e C_I + P_e K_{RR} I_{RR} \qquad \text{Eq. 5.3}$$

$$C_I(0) = C_I\_0$$

The program runs under a computer-based program WINFUNFIT. The analysis involves 9 files in CD:
(1). program files: \fortran\ISR_RACE.F90
\fortran\LinearSpline2Step.for
\fortran\dlsode.for
(2). WINFUNFIT files: \fortran\ALLWINFUNFIT
\fortran\FUNFIT_RESOURCES.res
(3). data file: \fortran\AIRg\ISR_RACE\insulin.DAT (e.g. IV_INS_AA.DAT)
\fortran\AIRg\ISR_RACE\glucose.DAT (e.g. IV_GLU_AA.DAT)
\fortran\AIRg\ISR_RACE\par.PAR (e.g. par_AA.PAR)
(4). output file:\fortran\AIRg\ISR_RACE\RATE_AA.TXT
****End prologue

```
SUBROUTINE USERMODEL_ODE(T,Y,YPRIME,P,NP,IFUN)
IMPLICIT NONE
INTEGER NP,IFUN
REAL*8 T, YPRIME(*),Y(*),P(*)
REAL*8 KG,EMAX,C50,PE,KE,KRR, ALPHA
REAL*8 G,LNG,I2,I,IRR,RT1,RT2,NET_RT1,NET_RT2
REAL*8 I2_ZERO,I_ZERO,IRR_ZERO
REAL*8 I1_PRIME,I2_PRIME,I_PRIME, IRR_PRIME,RT1_PRIME
REAL*8 RT2_PRIME, NET_RT1_PRIME, NET_RT2_PRIME

  IF(IFUN == 1 ) THEN
    CALL LIN_SPLIN_EVALUATE(T,G)
    I = Y(1)           ! PLASMA INSULIN CONC.
    I2 = Y(2)              ! RESERVED INSULIN
    IRR = Y(3)       ! READILY RELEASABLE INSULIN
    RT1=Y(4)               ! PREHEPATIC FIRST-PHASE SECRETION RATE
    RT2=Y(5)           ! PREHEPATIC SECOND-PHASE SECRETION RATE
    NET_RT1=Y(6)
    NET_RT2=Y(7)
```

```
    KG=P(1)
    EMAX =P(2)
    C50=P(3)
    PE = P(4)
    KE = P(5)
    KRR=P(6)
    ALPHA=P(7)
    I2_ZERO =P(8)
    I_ZERO = P(9)
    IRR_ZERO=P(10)

    I_PRIME = PE*I2*EMAX*(G**ALPHA)/(C50**ALPHA + G**ALPHA) &
            - KE*I + PE*KRR*IRR
    I2_PRIME = KG*G - I2*EMAX*(G**ALPHA)/(C50**ALPHA + G**ALPHA)
    IRR_PRIME = -KRR*IRR
    RT1_PRIME=PE*I2*EMAX*(G**ALPHA)/(C50**ALPHA + G**ALPHA)
    RT2_PRIME=KRR*IRR*PE
    NET_RT1_PRIME=PE*I2*EMAX*(G**ALPHA)/(C50**ALPHA   &
                + G**ALPHA)- KE*NET_RT1
    NET_RT2_PRIME=PE*KRR*IRR-KE*NET_RT2

    YPRIME(1) = I_PRIME
    YPRIME(2) = I2_PRIME
    YPRIME(3) = IRR_PRIME
    YPRIME(4)=RT1_PRIME
    YPRIME(5)=RT2_PRIME
    YPRIME(6)=NET_RT1_PRIME
    YPRIME(7)=NET_RT2_PRIME

  END IF

END SUBROUTINE USERMODEL_ODE


SUBROUTINE USERMODEL_ODE_JACOBIAN(T,Y,DFDT,DFDY,N,P,NP,IFUN)
IMPLICIT NONE
INTEGER, INTENT(IN) :: N, NP, IFUN
DOUBLE PRECISION, INTENT(IN) ::T
DOUBLE PRECISION, DIMENSION(N), INTENT(IN) ::Y
DOUBLE PRECISION, DIMENSION(N),INTENT(OUT) ::DFDT
DOUBLE PRECISION, DIMENSION(N,N), INTENT(OUT) :: DFDY
DOUBLE PRECISION, DIMENSION(NP), INTENT(IN) ::P
END SUBROUTINE USERMODEL_ODE_JACOBIAN


SUBROUTINE USERMODEL(T,C,P,NP,IFUN)
IMPLICIT NONE
INTEGER NP,IFUN
REAL*8 T,C,P(*)
INTEGER, PARAMETER :: NEQN =7,NPT=150
INTEGER NOBS,J,JY,NUM,LUN,NN, II
REAL*8 TOBS(NPT), COBS(NPT),CLN(NPT)
REAL*8 KG,K1,K2,KRR,PE,KE,ALPHA, EMAX, C50
REAL*8 I1,I2,I3,I
REAL*8 DT, LNG, GG
REAL*8 G_ZERO,I2_ZERO,IRR_ZERO, I_ZERO
REAL*8 Y(NEQN),YZERO(NEQN) , LG(100)
REAL*8 D,XEND
REAL*8 GGS(NPT),TTS(NPT),TTSP(NPT),GGSP(NPT)
LOGICAL SHOWIT
CHARACTER*256 ID,DATAFILENAME
CHARACTER*512 File
REAL*8 ::TZERO
DATA  TZERO/0.0D0/
```

```
EXTERNAL FEX, JEX
INTEGER IOPT, IOUT, ISTATE, ITASK, ITOL,IWORK(28),LIW, LRW,MF,NEQ
DOUBLE PRECISION ATOL(8), RTOL,RWORK(134),  TOUT, YY(7),TT
DOUBLE PRECISION CI(2000),CI1(2000),CI2(2000),CIRR(2000)
DOUBLE PRECISION CR1(2000),CR2(2000),TC(2000)
DOUBLE PRECISION CNR1(2000),CNR2(2000),POP_I2(2000)
DOUBLE PRECISION POP_IRR(2000), POP_ISR(2000)
INTEGER N
DOUBLE PRECISION PP(10)
COMMON PP

  KG=P(1)
  EMAX =P(2)
  C50=P(3)
  PE = P(4)
  KE = P(5)
  KRR=P(6)
  ALPHA=P(7)
  I2_ZERO =P(8)
  I_ZERO = P(9)
  IRR_ZERO=P(10)

  NEQ=7
  YY(1) = I_ZERO
  YY(2) = I2_ZERO
  YY(3) = IRR_ZERO
  YY(4) = 0.D0
  YY(5) = 0.D0
  YY(6)=I_ZERO
  YY(7)=0.D0
  TT=0.D0
  ITOL=2
  RTOL=1.D-4
  ISTATE=1
  IOPT=0
  LRW=134
  ATOL(1)=1.D-6
  ATOL(2)=1.D-6
  ATOL(3)=1.D-6
  ATOL(4)=1.D-6
  ATOL(5)=1.D-2
  ATOL(6)=1.D-6
  ATOL(7)=1.D-6
  ITASK=1
  LIW=27
  MF=22


  IF(IFUN.EQ.-1000) THEN
    NOBS=NPT
    CALL XY_DATA_FOR_SPLIN_FROM_FUNFIT_FILE(TOBS,COBS,NOBS)

    DO J=1,NOBS
      TTSP(J)=TOBS(J)
      GGSP(J)=COBS(J)
    ENDDO

    CALL LIN_SPLIN_SETUP(TOBS,COBS,NOBS)
    XEND=1.2*TOBS(NOBS)
    D=XEND/FLOAT(NPT-1)

    DO J=1,NPT
      TTS(J) = D*FLOAT(J-1)
```

```
    CALL LIN_SPLIN_EVALUATE(TTS(J),GGS(J))
  END DO

  CALL TITLE('PLOT OF GLUCOSE CONCENTRATION')
  CALL XLABEL('TIME(MIN)')
  CALL ADDPOINTSLEFT_D(TOBS,COBS,NOBS)
  CALL ADDCURVELEFT_D(TTS,GGS,NPT)
  CALL DISPLAYPLOT

  J=6
  CALL SCALE_ABS_ERROR(J,1)

  CALL SetFunfitParameterName(1,"KG")
  CALL SetFunfitParameterName(2,"EMAX")
  CALL SetFunfitParameterName(3,"C50")
  CALL SetFunfitParameterName(4,"PE")
  CALL SetFunfitParameterName(5,"KE")
  CALL SetFunfitParameterName(6,"KRR")
  CALL SetFunfitParameterName(7,"ALPHA")
  CALL SetFunfitParameterName(8,"I2_ZERO")
  CALL SetFunfitParameterName(9,"I_ZERO")
  CALL SetFunfitParameterName(10,"IRR_ZERO")
END IF

IF(IFUN == 1 .OR. IFUN==5 .OR. IFUN == 6) THEN
  YZERO(1) = I_ZERO
  YZERO(2) = I2_ZERO
  YZERO(3) = IRR_ZERO
  YZERO(4) = 0.D0
  YZERO(5) = 0.D0

  JY =IFUN
  CALL INTEGRATE_USERMODEL_ODE(T,C,P,NP,IFUN,TZERO,YZERO,NEQN,JY)
END IF

IF (IFUN.EQ.0) THEN
  PP(1)=P(1)
  PP(2)=P(2)
  PP(3)=P(3)
  PP(4)=P(4)
  PP(5)=P(5)
  PP(6)=P(6)
  PP(7)=P(7)
  PP(8)=P(8)
  PP(9)=P(9)
  PP(10)=P(10)

  TOUT=0.0D0
  DO N=1, 181
    CALL DLSODE(FEX,NEQ,YY,TT,TOUT,ITOL, RTOL, ATOL,      &
                ITASK,ISTATE,IOPT,RWORK,LRW,IWORK,LIW,JEX,MF)

    CI(N)=YY(1)
    CI2(N)=YY(2)
    CIRR(N)=YY(3)
    CR1(N)=YY(4)
    CR2(N)=YY(5)
    CNR1(N)=YY(6)
    CNR2(N)=YY(7)
    TC(N)=TOUT

    CALL LIN_SPLIN_EVALUATE(TOUT,GG)
    POP_I2(N)=PP(2)*CI2(N)*(GG**PP(7))/(PP(3)**PP(7) + GG**PP(7))
    POP_IRR(N)=PP(6)*CIRR(N)
```

```
      POP_ISR(N)=POP_I2(N)+POP_IRR(N)
    END DO

    CALL PROMT(SHOWIT)
    IF(SHOWIT)THEN
      CALL GETDATAFILENAME(DATAFILENAME)
      CALL ADDMARGINTEXT(DATAFILENAME)
      CALL XLABEL('TIME(MIN)')
      CALL LEFTLABEL('INSULIN(MICRO U/ML)')
      CALL ADDOBSERVATIONSLEFT(1)
      CALL ADDFITTEDCURVELEFT(1)
      CALL PLOT_IN_AREA(1,4)

      CALL ADDOBSERVATIONSLEFT(1)
      CALL ADDCURVELEFT_D(TC,CI,181)
      CALL PLOT_IN_AREA(2,4)

      CALL ADDCURVELEFT_D(TC,POP_I2,181)
      CALL BEGINLEFTAT_D(0.0D0)
      CALL LEFT_LABEL("RATET OF ROUTE 1")
      CALL PLOT_IN_AREA(3,4)

      CALL ADDCURVELEFT_D(TC,POP_IRR,181)
      CALL BEGINLEFTAT_D(0.0D0)
      CALL LEFT_LABEL("RATE OF ROUTE 2")
      CALL PLOT_IN_AREA(4,4)

      CALL DISPLAY_PLOT
      CALL GETLUNOUTPUT(LUN)
      CALL RECORDPLOTIFSAVED(LUN)
      CALL RECORDPLOTIFSAVED(3)
    ENDIF
  ENDIF
RETURN


!**
CONTAINS
SUBROUTINE XY_DATA_FOR_SPLIN_FROM_FUNFIT_FILE (X,Y,N)
IMPLICIT NONE
INTEGER, INTENT (INOUT) :: N
REAL*8,  INTENT (INOUT) :: X(*), Y(*)
CHARACTER (LEN=256), INTENT(OUT)  :: F
INTEGER, PARAMETER :: MAXLINES = 10000, LENSTRING = 80
INTEGER :: J, JS, K, NN, IERR
CHARACTER (LEN=256) :: DATAFILENAME
CHARACTER (LEN=LENSTRING) :: STRING

  PRINT*," NEXT SELECT THE FILE CONTAINING THE BLOOD INSULIN C-T DATA "
  CALL FILESELECT("DAT", DATAFILENAME, J)
  PRINT*, 'This is the *.DAT file selcted:', DATAFILENAME

  OPEN(UNIT=101, FILE=DATAFILENAME, STATUS='OLD', IOSTAT = IERR)
  IF(IERR /= 0) STOP ' XY_DATA_FOR_SPLIN_FROM_FUNFIT_FILE: &
                       ERROR IN OPENING DATA FILE'
  NN = 0
  F=DATAFILENAME
  DO J= 1, MAXLINES
    JS = J
    STRING(1:LENSTRING) = ''
    READ (101,"(A)", END = 10, IOSTAT = IERR) STRING
    IF(IERR /= 0) STOP 'GET_XY_DATA_FROM_FUNFIT_FILE:  &
                        ERROR IN READING DATA FILE'
    K = LEN_TRIM(ADJUSTL(STRING))
```

```
    IF(STRING(1:1) == 'C' .OR. STRING(1:1) == 'c' .OR. &
       STRING(1:1) == '' .OR. K <= 2) CYCLE
    NN = NN + 1

    IF(NN > N) STOP ' XY_DATA_FOR_SPLIN_FROM_FUNFIT_FILE:  &
                     ASSIGNED DIMENSION OF X, Y TOO SMALL'
    READ(STRING,*, IOSTAT = IERR) X(NN), Y(NN)

    IF(IERR /= 0) STOP ' XY_DATA_FOR_SPLIN_FROM_FUNFIT_FILE:  &
                        ERROR IN DATA FILE LIKELY, PLEASE CHECK'
  ENDDO

  10 IF (JS == MAXLINES) STOP ' XY_DATA_FOR_SPLIN_FROM_FUNFIT_FILE: &
                       DATA FILE CONTAINS TOO MANY LINES (RECORDS)'
  N = NN
  CLOSE (101,STATUS='SAVE')
END SUBROUTINE XY_DATA_FOR_SPLIN_FROM_FUNFIT_FILE
END SUBROUTINE USERMODEL


SUBROUTINE FEX(NEQ, TT, YY, YDOT)
IMPLICIT NONE
COMMON PP
DOUBLE PRECISION  PP(10)
INTEGER NEQ
DOUBLE PRECISION TT, YY(7), YDOT(7)
DOUBLE PRECISION KG,K1,K2,PE,KE,KRR,IRR_ZERO,G_ZERO, EMAX, C50, ALPHA
DOUBLE PRECISION I_ZERO,I1_ZERO,I2_ZERO,G

  KG = PP(1)
  EMAX = PP(2)
  C50 = PP(3)
  PE = PP(4)
  KE = PP(5)
  KRR=PP(6)
  ALPHA=PP(7)
  I2_ZERO=PP(8)
  I_ZERO=PP(9)
  IRR_ZERO = PP(10)

  CALL LIN_SPLIN_EVALUATE(TT,G)

  YDOT(1) = PE*EMAX*(G**ALPHA)/(C50**ALPHA + G**ALPHA)*YY(2) &
            - KE*YY(1) + PE*KRR*YY(3)
  YDOT(2) = KG*G - EMAX*(G**ALPHA)/(C50**ALPHA + G**ALPHA)*YY(2)
  YDOT(3) = -KRR*YY(3)
  YDOT(4)=EMAX*(G**ALPHA)/(C50**ALPHA + G**ALPHA)*YY(2)*PE
  YDOT(5)=KRR*YY(3)*PE
  YDOT(6)=EMAX*(G**ALPHA)/(C50**ALPHA + G**ALPHA)*YY(2)*PE - KE*YY(6)
  YDOT(7)=KRR*YY(3)*PE-KE*YY(7)

RETURN
!END SUBROUTINE FEX
END
!-----------------------------------------------------------------------
```

## APPENDIX C. MONOLIX SCRIPT AND FORTRAN PROGRAM

## FOR CHAPTER 6

****Begin prologue
This FORTRAN program performs simultaneously individual fits of insulin and glucose data collected from oral glucose tolerance test (OGTT) based on the PK/PD model proposed on Chapter 6. The PK/PD model is given by the following equations:

$$\frac{dI_R(t)}{dt} = K_G C_G(t) - \frac{E_{\max} C_G(t)^{\alpha}}{C_G(t)^{\alpha} + C_{50}{}^{\alpha}} I_R(t) \qquad \text{Eq. 6.1}$$
$$I_R(0) = I_R\_0$$

$$\frac{dI(t)}{dt} = (1-E)\frac{E_{\max} C_G(t)^{\alpha}}{C_G(t)^{\alpha} + C_{50}{}^{\alpha}} I_R(t) - K_I I(t) \qquad \text{Eq. 6.2}$$
$$C_I(t) = I(t)/V_I \qquad C_I(0) = C_I\_0$$

$$R(t) = \frac{E_{\max} C_G(t)^{\alpha}}{C_G(t)^{\alpha} + C_{50}(t)^{\alpha}} \qquad \text{Eq. 6.3}$$

$$\frac{dP_1(t)}{dt} = -(K_P + K_{12})P_1(t) + K_{21}P_2(t) + R(t)$$
$$\frac{dC_{P_1}}{dt} = \frac{dP_1(t)/V_P}{dt} \qquad C_{P_1}(0) = C_{P_1}\_0 \qquad \text{Eq. 6.4}$$

$$\frac{dP_2(t)}{dt} = -K_{21}P_2(t) + K_{12}P_1(t) \qquad \text{Eq. 6.5}$$
$$P_2(0) = CP_1(0)V_P K_{12}/K_{21}$$

The program runs under a computer-based program WINFUNFIT. The analysis involves 8 files in CD:
(1). program files: \fortran\ORAL_ISR.F90
\fortran\GCV.FOR
(2). WINFUNFIT files: \ALLWINFUNFIT
\fortran\FUNFIT_RESOURCES.res
(3). data file: \fortran\ ORAL_2CP\oral.DAT (including all insulin data)
\fortran\ ORAL_2CP\glucose.DAT (e.g. GLU_7_28)
\fortran\ ORAL_2CP\para.PAR
(4). output file: \fortran\ ORAL_2CP\WINFUNFIT_OUTPUT
****End prologue

```
SUBROUTINE USERMODEL_ODE(T,Y,YPRIME,P,NP,IFUN)     !
IMPLICIT NONE

INTEGER NP,IFUN
REAL*8 T, YPRIME(*),Y(*),P(*)
REAL*8 KG,EMAX,C50,ALPHA, KRR,E,VI,VP,KE,KC,K12,K21
REAL*8 G,LNG,IR,IRR,I,CP,CI,CP2
REAL*8 IR_ZERO,IRR_ZERO,CP_ZERO,I_ZERO,CP2_ZERO
REAL*8 IR_PRIME,IRR_PRIME,CP_PRIME,I_PRIME, CP2_PRIME
REAL*8 WEIGHT,RATE
LOGICAL EVENT_IS_ACTIVE

  IF(IFUN == 1 .OR. IFUN==2 .OR. IFUN==3) THEN
    CALL CUBIC_GCV(T,G)
    G=DEXP(G)
    I = Y(1)          ! PLASMA INSULIN CONC.
    CP  = Y(2)        ! c-PEPTIDE IN COMPARTMENT 1
    IR = Y(3)         ! READILY RELEASIBLE INSULIN
    CP2 = Y(4)        ! C-PEPTIDE IN COMPARTMENT 2
    KG = P(1)
    EMAX = P(2)
    C50 = P(3)
    ALPHA = P(4)
    E = P(5)
    VI= P(6)
    KE =P(7)
    KC =P(8)
    VP= P(9)
    K12 = P(13)
    K21 = P(14)


    I_PRIME = (1-E)*(EMAX*(G**ALPHA)*IR/(C50**ALPHA    &
              + G**ALPHA))/VI - KE*I
    CP_PRIME = (EMAX*(G**ALPHA)*IR/(C50**ALPHA     &
               + G**ALPHA))/VP  - KC*CP +K21*CP2/VP -K12*CP
    IR_PRIME = KG*G - EMAX*(G**ALPHA)*IR/(C50**ALPHA + G**ALPHA)
    CP2_PRIME = K12*CP -K21*CP2

    YPRIME(1) = I_PRIME
    YPRIME(2) = CP_PRIME
    YPRIME(3) = IR_PRIME
    YPRIME(4) = CP2_PRIME
  END IF
RETURN


SUBROUTINE USERMODEL(T,C,P,NP,IFUN)
IMPLICIT NONE
INTEGER NP,IFUN
REAL*8 T,C,P(*)
INTEGER, PARAMETER :: NEQN =4,NPT=150
INTEGER NOBS,J,JY,NUM,LUN,NN, II  !NN MODIFED
REAL*8 TOBS(NPT), COBS(NPT),CLN(NPT)
REAL*8 KG,EMAX,C50,ALPHA, KRR,E,VI,KE,KC,VP,K12,K21, WEIGHT
REAL*8 IR,IRR,I,CP, ISR
REAL*8 IR_ZERO,IRR_ZERO,CP_ZERO,I_ZERO,CP2_ZERO
REAL*8 DT, LNG,G
REAL*8 Y(NEQN),YZERO(NEQN) ,LG(100)
REAL*8 TSP(NPT),GSP(NPT), TIME_STEP1,TIME_STEP2,G_STEP1,G_STEP2
REAL*8 GGS(NPT),GGL(NPT),TTS(NPT)
REAL*8 D,XEND
REAL*8 TT, TTT
LOGICAL SHOWIT
```

```
CHARACTER*256 ID,DATAFILENAME
REAL*8 ::TZERO
DATA  TZERO/0.0D0/
INTEGER NEVENTS,n
REAL*8 RATE,T_START, T_STOP

  IF(IFUN.EQ.-1000) THEN
    NOBS=NPT
    CALL XY_DATA_FOR_SPLIN_FROM_FUNFIT_FILE(TOBS,COBS,NOBS)
    CALL LIN_SPLIN_SETUP(TOBS,COBS,NOBS)
    XEND=1.2*TOBS(NOBS)
    D=XEND/FLOAT(NPT-1)

    DO J=1,NPT
      TTS(J) = D*FLOAT(J-1)
      CALL LIN_SPLIN_EVALUATE(TTS(J),GGS(J))
    END DO

    CALL SetFunfitParameterName(1,"KG")
    CALL SetFunfitParameterName(2,"EMAX")
    CALL SetFunfitParameterName(3,"C50")
    CALL SetFunfitParameterName(4,"ALPHA")
    CALL SetFunfitParameterName(5,"E")
    CALL SetFunfitParameterName(6,"VI")
    CALL SetFunfitParameterName(7,"KE")
    CALL SetFunfitParameterName(8,"KC")
    CALL SetFunfitParameterName(9,"VP")
    CALL SetFunfitParameterName(10,"IR_ZERO")
    CALL SetFunfitParameterName(11,"I_ZERO")
    CALL SetFunfitParameterName(12,"CP_ZERO")
    CALL SetFunfitParameterName(13,"K12")
    CALL SetFunfitParameterName(14,"K21")
    CALL SetFunfitParameterName(15,"WEIGHT")
    CALL SetFunfitParameterName(16,"T_START")
    CALL SetFunfitParameterName(17,"T_STOP")
    CALL SetFunfitParameterName(18,"RATE")

    KG = P(1)
    EMAX = P(2)
    C50 = P(3)
    ALPHA = P(4)
    E = P(5)
    VI= P(6)
    KE =P(7)
    KC =P(8)
    VP= P(9)
    IR_ZERO =P(10)
    I_ZERO = P(11)
    CP_ZERO = P(12)
    K12 = P(13)
    K21 = P(14)

    CALL TITLE('LINEAR SPLINE FITTED GLUCOSE')
    CALL XLABEL('TIME(MIN)')
    CALL LEFTLABEL ('GLUCOSE(MMOL/L)')
    CALL ADDPOINTSLEFT_D(TOBS,COBS,NOBS)
    CALL ADDCURVELEFT_D(TTS,GGS,NOBS)
    CALL DISPLAYPLOT
  END IF

  IF(IFUN==1 .OR. IFUN==2) THEN
    JY=IFUN
    YZERO(1) = P(11)   !"I_ZERO"
    YZERO(2) = P(12)    !"CP_ZERO"
```

```
    YZERO(3) = P(10)    !"IR_ZERO"
    YZERO(4) = P(12)*K12/K21

    CALL INTEGRATE_USERMODEL_ODE(T,C,P,NP,IFUN,TZERO,YZERO,NEQN,JY)
  END IF

  IF (IFUN.EQ.0) THEN
    CALL PROMT(SHOWIT)

    IF(SHOWIT)THEN
      CALL GETDATAFILENAME(DATAFILENAME)
      CALL ADDMARGINTEXT(DATAFILENAME)
      CALL TITLE('FITTED INSULIN AND CPEPTIDE')

      CALL XLABEL('TIME(MINUTES)')
      CALL LEFTLABEL('INSULIN (PMOL/L)')
      CALL ADDOBSERVATIONSLEFT(1)
      CALL ADDFITTEDCURVELEFT(1)
      CALL PLOT_IN_AREA(1,2)

      CALL LEFTLABEL('CPEPTIDE (PMOL/L)')
      CALL ADDOBSERVATIONSLEFT(2)
      CALL ADDFITTEDCURVELEFT(2)
      CALL PLOT_IN_AREA(2,2)

      CALL DISPLAYPLOT
      CALL GETLUNOUTPUT(LUN)
      CALL RECORDPLOTIFSAVED(LUN)
      CALL RECORDPLOTIFSAVED(3)
    END IF
 END IF
 RETURN
!---------------------------------------------------------------------


!**
CONTAINS
SUBROUTINE XY_DATA_FOR_SPLIN_FROM_FUNFIT_FILE (X,Y,N,F)
IMPLICIT NONE
INTEGER, INTENT (INOUT) :: N
REAL*8,  INTENT (INOUT) :: X(*), Y(*)
CHARACTER (LEN=256), INTENT(OUT)  :: F
INTEGER, PARAMETER :: MAXLINES = 10000, LENSTRING = 80
INTEGER :: J, JS, K, NN, IERR
CHARACTER (LEN=256) :: DATAFILENAME
CHARACTER (LEN=LENSTRING) :: STRING

  PRINT*," NEXT SELECT THE FILE CONTAINING THE BLOOD INSULIN C-T DATA "
  CALL FILESELECT("DAT", DATAFILENAME, J)
  PRINT*, 'This is the *.DAT file selcted:', DATAFILENAME

  OPEN(UNIT=101, FILE=DATAFILENAME, STATUS='OLD', IOSTAT = IERR)
  IF(IERR /= 0) STOP ' XY_DATA_FOR_SPLIN_FROM_FUNFIT_FILE: &
                       ERROR IN OPENING DATA FILE'
  NN = 0
  F=DATAFILENAME
  DO J= 1, MAXLINES
    JS = J
    STRING(1:LENSTRING) = ''
    READ (101,"(A)", END = 10, IOSTAT = IERR) STRING
    IF(IERR /= 0) STOP 'GET_XY_DATA_FROM_FUNFIT_FILE:  &
                        ERROR IN READING DATA FILE'
    K = LEN_TRIM(ADJUSTL(STRING))
    IF(STRING(1:1) == 'C' .OR. STRING(1:1) == 'c' .OR. &
```

```
      STRING(1:1) == '' .OR. K <= 2) CYCLE
    NN = NN + 1

    IF(NN > N) STOP ' XY_DATA_FOR_SPLIN_FROM_FUNFIT_FILE:  &
                     ASSIGNED DIMENSION OF X, Y TOO SMALL'
    READ(STRING,*, IOSTAT = IERR) X(NN), Y(NN)

    IF(IERR /= 0) STOP ' XY_DATA_FOR_SPLIN_FROM_FUNFIT_FILE:  &
                         ERROR IN DATA FILE LIKELY, PLEASE CHECK'
  ENDDO

  10 IF (JS == MAXLINES) STOP ' XY_DATA_FOR_SPLIN_FROM_FUNFIT_FILE: &
                       DATA FILE CONTAINS TOO MANY LINES (RECORDS)'
  N = NN
  CLOSE (101,STATUS='SAVE')
END SUBROUTINE XY_DATA_FOR_SPLIN_FROM_FUNFIT_FILE
END SUBROUTINE USERMODEL
!--------------------------END---------------------------------
```

****Begin prologue
This Monolix script yields population statistics of the proposed PK/PD model for OGTT in Chapter 6 (Eq. 6.1 -6.5). A nonlinear mixed-effects model was used for the population analysis and the status of glucose tolerance, type 2 diabetes and obesity as covariates were included in the population model. The population model is described by:

$$y_{ij} = f(\varphi_i, t_{ij}) + b \cdot f(\varphi_i, t_{ij}) \cdot \varepsilon_{ij} \qquad \text{Eq. 6.6}$$

$$\ln(\varphi_i) = \mu + \beta c_i + \eta_i \qquad \text{with} \quad \eta_i \sim_{i.i.d} N(0, \Omega) \qquad \text{Eq. 6.7}$$

where $f$ is the proposed PK/PD model described by Eq. 6.1 -6.5; A proportional error structure was used, in which $b$ is the coefficient and $\varepsilon_{ij}$ is a random variable following a normal distribution with mean 0 and variance 1.

The program runs under a computer-based program Monolix, standalone version 3.1. The analysis involves 3 files in CD:
(1). Monolix script: \monolix\MARI_ORAL_WO_1ST_2CP_FIX_PAR.TXT
(2). Data file: \monolix\ORAL.TXT
(3). Output file: \ORAL
****End prologue

```
$PROBLEM SIMUTANEOUSLY ANALYZE OGTT DATA OF INSULIN AND C-PEPTIDE

$MODEL
COMP = (I)
COMP = (IR)
COMP = (CP1)
COMP = (CP2)

$PSI  KG EMAX C50 ALPHA E KE IR0 CIB VI CP1B RK12 VP1

$REG  t_start t_end g_start g_end t1 t2 f

$PK

A1=f/VP1
A2= (1-f)/VP1
lamda1=0.693/t1
lamda2=0.693/t2
K21=(A1*lamda2+A2*lamda1)/(A1+A2)
KC=lamda1*lamda2/K21
K12=lamda1+lamda2-K21-KC

IB=CIB*VI
CPB=CP1B*VP1

$ODE

;STIFF           ;solver for stiff ODE's systems

I_0=IB
IR_0=IR0
CP1_0=CPB
CP2_0=RK12*CPB

if (T < 500)
```

```
  C = g_start + (T - t_start)*(g_end - g_start)/(t_end-t_start)
else
  C = g_end
end

DDT_I = (IR*EMAX*(C^ALPHA)/(C^ALPHA+C50^ALPHA))*(1-E) -KE*I
DDT_IR = KG*C - IR*EMAX*(C^ALPHA)/(C^ALPHA+C50^ALPHA)
DDT_CP1= IR*EMAX*(C^ALPHA)/(C^ALPHA+C50^ALPHA) -KC*CP1-K12*CP1+K21*CP2
DDT_CP2=K12*CP1-K21*CP2

$OUTPUT
OUTPUT1=I/VI
OUTPUT2=CP1/VP1
```

****Begin prologue
This FORTRAN program simulates the prehepatic insulin secretion rate of subjects with various levels of glucose tolerance OGTT based on the PK/PD model proposed In Chapter 6 and population estimates of parameters from Monolix. The prehepatic insulin secretion rate, *R(t)*, is given by:

$$R(t) = \frac{E_{\max} C_G(t)^{\alpha}}{C_G(t)^{\alpha} + C_{50}(t)^{\alpha}} \qquad \text{Eq. 6.3}$$

The program runs under a computer-based program WINFUNFIT. The analysis involves 9 files in CD:
(1). program files: \fortran\ORAL_ISR.F90
\fortran\LinearSpline2Step.for
\fortran\dlsode
(2). WINFUNFIT files: \fortran\ALLWINFUNFIT
\fortran\FUNFIT_RESOURCES.res
(3). data file: \fortran\ ORAL_ISR\mean_insulin*.DAT (e.g. oral_obs_pop_nd.DAT )
\fortran\ ORAL_ISR\mean_glucose*.DAT (e.g. oral_pop_glu_nd.DAT
\fortran\ ORAL_ISR\para.PAR (e.g. para_nd_nob)
(4).output file: \fortran\ ORAL_ISR\RATE.DAT (e.g. RATE_ND.DAT
****End prologue

```
SUBROUTINE USERMODEL_ODE(T,Y,YPRIME,P,NP,IFUN)     !
IMPLICIT NONE

INTEGER NP,IFUN
REAL*8 T, YPRIME(*),Y(*),P(*)
REAL*8 KG,EMAX,C50,ALPHA,E,VI,VP,KE,KC, K12,K21
REAL*8 G,LNG,IR,IRR,I,CP,CI,CCP,CP2
REAL*8 IR_ZERO,IRR_ZERO,CP_ZERO,I_ZERO,CP2_ZERO
REAL*8 IR_PRIME,CP_PRIME,I_PRIME,CP2_PRIME
REAL*8 WEIGHT,RATE
LOGICAL EVENT_IS_ACTIVE

  IF(IFUN == 1 .OR. IFUN==2) THEN
    CALL LIN_SPLIN_EVALUATE(T,G)

    I = Y(1)             ! INSULIN IN PLASMA
    CP  = Y(2)           ! C-PEPTIDE IN COMPARTMENT 1
    IR = Y(3)            ! RESERVED INSULIN
    CP2 = Y(4)           ! C-PEPTIDE IN COMPARTMENT 2

    KG = P(1)
    EMAX = P(2)
    C50 = P(3)
    ALPHA = P(4)
    E = P(5)
    VI= P(6)
    KE =P(7)
    KC =P(8)
    VP= P(9)
    K12 = P(13)
    K21 = P(14)

    I_PRIME = (1-E)*EMAX*(G**ALPHA)*IR/(C50**ALPHA    &
```

```
                + G**ALPHA)/VI - KE*I
    CP_PRIME = (EMAX*(G**ALPHA)*IR/(C50**ALPHA + G**ALPHA))/VP   &
                - KC*CP + K21*CP2/VP -K12*CP
    IR_PRIME = KG*G - EMAX*(G**ALPHA)*IR/(C50**ALPHA + G**ALPHA)
    CP2_PRIME = K12*CP*VP -K21*CP2

    YPRIME(1) = I_PRIME
    YPRIME(2) = CP_PRIME
    YPRIME(3) = IR_PRIME
    YPRIME(4) = CP2_PRIME

  END IF

END SUBROUTINE USERMODEL_ODE


! DEFINE JACOBIAN OF ODE
SUBROUTINE USERMODEL_ODE_JACOBIAN(T,Y,DFDT,DFDY,N,P,NP,IFUN)
IMPLICIT NONE
INTEGER, INTENT(IN):: N, NP, IFUN
DOUBLE PRECISION, INTENT(IN)::T
DOUBLE PRECISION, DIMENSION(N), INTENT(IN)::Y
DOUBLE PRECISION, DIMENSION(N),INTENT(OUT)::DFDT
DOUBLE PRECISION, DIMENSION(N,N), INTENT(OUT):: DFDY
DOUBLE PRECISION, DIMENSION(NP), INTENT(IN)::P
END SUBROUTINE USERMODEL_ODE_JACOBIAN

SUBROUTINE USERMODEL(T,C,P,NP,IFUN)
IMPLICIT NONE

INTEGER NP,IFUN
REAL*8 T,C,P(*)
INTEGER, PARAMETER :: NEQN =4,NPT=150
INTEGER NOBS,J,JY,NUM,LUN,NN, II
REAL*8 TOBS(NPT), COBS(NPT)
REAL*8 KG,EMAX,C50,ALPHA,E,VI,KE,KC,VP,K12,K21
REAL*8 IR,IRR,I
REAL*8 IR_ZERO,IRR_ZERO,CP_ZERO,I_ZERO,CP2_ZERO
REAL*8 DT, LNG
REAL*8 D,XEND
REAL*8 Y(NEQN),YZERO(NEQN) , LG(100)
REAL*8 TSP(NPT),GSP(NPT), TIME_STEP1,TIME_STEP2,G_STEP1,G_STEP2
REAL*8 GGS(NPT),GGL(NPT),TTS(NPT),G
LOGICAL SHOWIT
CHARACTER*256 ID,DATAFILENAME
REAL*8 ::TZERO
DATA  TZERO/0.0D0/
INTEGER NEVENTS
REAL*8 RATE,T_START, T_STOP
EXTERNAL FEX, JEX
INTEGER IOPT, IOUT, ISTATE, ITASK, ITOL,IWORK(24),LIW, LRW,MF,NEQ
DOUBLE PRECISION ATOL(4), RTOL,RWORK(74),  TOUT, YY(4),TT
DOUBLE PRECISION CI(2000),CIR(2000),CI2(2000),CP(2000)
DOUBLE PRECISION CR1(2000),CR2(2000),TC(2000)
DOUBLE PRECISION CNR1(2000),CNR2(2000),POP_IR(2000),POP_IRR(2000)
INTEGER N
DOUBLE PRECISION PP(14)
COMMON PP

  KG = P(1)
  EMAX = P(2)
  C50 = P(3)
  ALPHA = P(4)
  E = P(5)
```

```
VI= P(6)
KE =P(7)
KC =P(8)
VP= P(9)
IR_ZERO =P(10)
I_ZERO = P(11)
CP_ZERO =P(12)
K12 = P(13)
K21 = P(14)

NEQ=4
YY(1) = I_ZERO
YY(2) = CP_ZERO
YY(3) = IR_ZERO
YY(4) = IR_ZERO*K12/K21
TT=0.D0
ITOL=1
RTOL=1.D-4
ISTATE=1
IOPT=0
LRW=74
ATOL(1)=1.D-6
ATOL(2)=1.D-6
ATOL(3)=1.D-6
ATOL(4)=1.D-6
ITASK=1
LIW=24
MF=22

IF(IFUN.EQ.-1000) THEN
  NOBS=NPT
  CALL XY_DATA_FOR_SPLIN_FROM_FUNFIT_FILE(TOBS,COBS,NOBS)

  CALL LIN_SPLIN_SETUP(TOBS,COBS,NOBS)
  XEND=1.2*TOBS(NOBS)
  D=XEND/FLOAT(NPT-1)

  DO J=1,NPT
    TTS(J) = D*FLOAT(J-1)
    CALL LIN_SPLIN_EVALUATE(TTS(J),GGS(J))
  END DO

  CALL TITLE('PLOT OF GLUCOSE CONCENTRATION')
  CALL XLABEL('TIME(MIN)')
  CALL ADDPOINTSLEFT_D(TOBS,COBS,NOBS)
  CALL ADDCURVELEFT_D(TTS,GGS,NPT)
  CALL DISPLAYPLOT

  CALL SetFunfitParameterName(1,"KG")
  CALL SetFunfitParameterName(2,"EMAX")
  CALL SetFunfitParameterName(3,"C50")
  CALL SetFunfitParameterName(4,"ALPHA")
  CALL SetFunfitParameterName(5,"E")
  CALL SetFunfitParameterName(6,"VI")
  CALL SetFunfitParameterName(7,"KE")
  CALL SetFunfitParameterName(8,"KC")
  CALL SetFunfitParameterName(9,"VP")
  CALL SetFunfitParameterName(10,"IR_ZERO")
  CALL SetFunfitParameterName(11,"I_ZERO")
  CALL SetFunfitParameterName(12,"CP_ZERO")
  CALL SetFunfitParameterName(13,"K12")
  CALL SetFunfitParameterName(14,"K21")

END IF
```

```
IF(IFUN == 1 .OR. IFUN ==2) THEN
  JY=IFUN
  YZERO(1) = P(11)    !"I_ZERO"
  YZERO(2) = P(12)     !"CP_ZERO"
  YZERO(3) = P(10)     !"IR_ZERO"
  YZERO(4) = P(10)*P(13)/P(14)

  CALL INTEGRATE_USERMODEL_ODE(T,C,P,NP,IFUN,TZERO,YZERO,NEQN,JY)
END IF

IF (IFUN.EQ.0) THEN
  PP(1)=P(1)
  PP(2)=P(2)
  PP(3)=P(3)
  PP(4)=P(4)
  PP(5)=P(5)
  PP(6)=P(6)
  PP(7)=P(7)
  PP(8)=P(8)
  PP(9)=P(9)
  PP(10)=P(10)
  PP(11)=P(11)
  PP(12)=P(12)
  PP(13)=P(13)
  PP(14)=P(14)

  TOUT=0.D0
  DO N=1,181
    CALL DLSODE(FEX,NEQ,YY,TT,TOUT,ITOL, RTOL, ATOL,      &
                       ITASK,ISTATE,IOPT,RWORK,LRW,IWORK,LIW,JEX,MF)

    CI(N)=YY(1)
    CI2(N)=YY(2)
    CIR(N)=YY(3)
    CR1(N)=YY(4)
    TC(N)=TOUT

    CALL LIN_SPLIN_EVALUATE(TOUT,G)
    POP_IR(N) = PP(2)*(G**PP(4))*CIR(N)/(PP(3)**PP(4) + G**PP(4))
    TOUT=TOUT+1.D0
  END DO

  OPEN(26,FILE='RATE_ND.TXT')
  WRITE(26,'(2F12.6)') (TC(N), POP_IR(N), N=1,181)

  CALL PROMT(SHOWIT)
  IF(SHOWIT)THEN
    CALL GETDATAFILENAME(DATAFILENAME)
    CALL ADDMARGINTEXT(DATAFILENAME)
    CALL TITLE('FITTED INSULIN AND CPEPTIDE')

    CALL XLABEL('TIME(MINUTES)')
    CALL LEFTLABEL('INSULIN (PPMOL/L)')
    CALL ADDOBSERVATIONSLEFT(1)
    CALL ADDFITTEDCURVELEFT(1)
    CALL PLOT_IN_AREA(1,5)
    CALL X_LABEL("TIME(MIN)")
    CALL ADDCURVELEFT_D(TC,CI,181)
    CALL ADDOBSERVATIONSLEFT(1)
    CALL LEFT_LABEL("LSODE PREDICTION")
    CALL PLOT_IN_AREA(2,5)

    CALL XLABEL('TIME(MINUTES)')
```

```
      CALL LEFTLABEL('CP')
      CALL ADDOBSERVATIONSLEFT(2)
      CALL ADDFITTEDCURVELEFT(2)
      CALL PLOT_IN_AREA(3,5)

      CALL ADDCURVELEFT_D(TC,CI2,181)
      CALL X_LABEL("TIME(MIN)")
      CALL ADDOBSERVATIONSLEFT(2)
      CALL LEFT_LABEL("LSODE PREDICTION")
      CALL PLOT_IN_AREA(4,5)

      CALL RIGHTLABEL(' RATE (PMOL/MIN)' )
      CALL ADDCURVELEFT_D(TC,POP_IR,181)
      CALL PLOT_IN_AREA(5,5)

      CALL DISPLAYPLOT
      CALL GETLUNOUTPUT(LUN)
      CALL RECORDPLOTIFSAVED(LUN)
      CALL RECORDPLOTIFSAVED(3)
    ENDIF
  ENDIF
RETURN


!**
CONTAINS
SUBROUTINE XY_DATA_FOR_SPLIN_FROM_FUNFIT_FILE (X,Y,N,F)
IMPLICIT NONE
INTEGER, INTENT (INOUT) :: N
REAL*8,  INTENT (INOUT) :: X(*), Y(*)
CHARACTER (LEN=256), INTENT(OUT)  :: F
INTEGER, PARAMETER :: MAXLINES = 10000, LENSTRING = 80
INTEGER :: J, JS, K, NN, IERR
CHARACTER (LEN=256) :: DATAFILENAME
CHARACTER (LEN=LENSTRING) :: STRING

  PRINT*," NEXT SELECT THE FILE CONTAINING THE BLOOD INSULIN C-T DATA "
  CALL FILESELECT("DAT", DATAFILENAME, J)
  PRINT*, 'This is the *.DAT file selcted:', DATAFILENAME

  OPEN(UNIT=101, FILE=DATAFILENAME, STATUS='OLD', IOSTAT = IERR)
  IF(IERR /= 0) STOP ' XY_DATA_FOR_SPLIN_FROM_FUNFIT_FILE: &
                       ERROR IN OPENING DATA FILE'
  NN = 0
  F=DATAFILENAME
  DO J= 1, MAXLINES
    JS = J
    STRING(1:LENSTRING) = ''
    READ (101,"(A)", END = 10, IOSTAT = IERR) STRING
    IF(IERR /= 0) STOP 'GET_XY_DATA_FROM_FUNFIT_FILE:  &
                        ERROR IN READING DATA FILE'
    K = LEN_TRIM(ADJUSTL(STRING))
    IF(STRING(1:1) == 'C' .OR. STRING(1:1) == 'c' .OR. &
       STRING(1:1) == '' .OR. K <= 2) CYCLE
    NN = NN + 1

    IF(NN > N) STOP ' XY_DATA_FOR_SPLIN_FROM_FUNFIT_FILE:  &
                     ASSIGNED DIMENSION OF X, Y TOO SMALL'
    READ(STRING,*, IOSTAT = IERR) X(NN), Y(NN)


    IF(IERR /= 0) STOP ' XY_DATA_FOR_SPLIN_FROM_FUNFIT_FILE:  &
                        ERROR IN DATA FILE LIKELY, PLEASE CHECK'
  ENDDO
```

```
  10 IF (JS == MAXLINES) STOP ' XY_DATA_FOR_SPLIN_FROM_FUNFIT_FILE: &
                        DATA FILE CONTAINS TOO MANY LINES (RECORDS)'
  N = NN
  CLOSE (101,STATUS='SAVE')
END SUBROUTINE XY_DATA_FOR_SPLIN_FROM_FUNFIT_FILE
END SUBROUTINE USERMODEL


SUBROUTINE FEX(NEQ, TT, YY, YDOT)
IMPLICIT NONE
COMMON PP
DOUBLE PRECISION  PP(10)
INTEGER NEQ
DOUBLE PRECISION TT, YY(7), YDOT(7)
DOUBLE PRECISION KG,K1,K2,PE,KE,KRR,IRR_ZERO,G_ZERO, EMAX, C50, ALPHA
DOUBLE PRECISION I_ZERO,I1_ZERO,I2_ZERO,G

  KG = PP(1)
  EMAX = PP(2)
  C50 = PP(3)
  PE = PP(4)
  KE = PP(5)
  KRR=PP(6)
  ALPHA=PP(7)
  I2_ZERO=PP(8)
  I_ZERO=PP(9)
  IRR_ZERO = PP(10)

  CALL LIN_SPLIN_EVALUATE(TT,G)

  YDOT(1) = PE*EMAX*(G**ALPHA)/(C50**ALPHA + G**ALPHA)*YY(2) &
            - KE*YY(1) + PE*KRR*YY(3)
  YDOT(2) = KG*G - EMAX*(G**ALPHA)/(C50**ALPHA + G**ALPHA)*YY(2)
  YDOT(3) = -KRR*YY(3)
  YDOT(4)=EMAX*(G**ALPHA)/(C50**ALPHA + G**ALPHA)*YY(2)*PE
  YDOT(5)=KRR*YY(3)*PE
  YDOT(6)=EMAX*(G**ALPHA)/(C50**ALPHA + G**ALPHA)*YY(2)*PE - KE*YY(6)
  YDOT(7)=KRR*YY(3)*PE-KE*YY(7)

RETURN
END
```

!----------END----------

## APPENDIX D. THE LIST OF PEER REVIEWED PUBLICATIONS

## BY LANYI XIE

**Xie L**, Hoffman RP, and Veng-Pedersen P. Noncompatmental pharmacokinetics analysis of glucose-stimulated insulin response in African-American and Caucasian youths. *Biopharm Drug Dispos* 30(3): 117-125 (2009)

**Xie L**, Hoffman RP, and Veng-Pedersen P. Population analysis of ethnicity and first-phase insulin release. *Diabetes Res Clin Pract* 89(3): 243-249 (2010)

**Xie L**, Kautzky-Willer A, Ferrannini E, and Veng-Pedersen P. A population kinetic analysis of prehepatic insulin secretion. *JCMD* 1(2), online (2011)

## REFERENCES


1. Center for Disease Control and Prevention (CDC). General information and national estimates on diabetes in the United States. Available from http://www.cdc.gov/diabetes/pubs/pdf/ndfs_2007.pdf. National Diabetes Fact Sheet (2007).

2. Bergman RN. Lilly lecture 1989. Toward physiological understanding of glucose tolerance. Minimal-model approach. Diabetes 38(12): 1512-1527 (1989).

3. Bliss M. Who Discovered Insulin. News Physiol Sci 1(1): 31-36 (1986).

4. Yalow RS, Berson SA. Assay of plasma insulin in human subjects by immunological methods. Nature 184(Suppl 21): 1648-1649 (1959).

5. Rawdon BB, Andrew A. Origin and differentiation of gut endocrine cells. Histol Histopathol 8(3): 567-580 (1993).

6. Bell GI, Pictet RL, Rutter WJ, et al. Sequence of the human insulin gene. Nature 284(5751): 26-32 (1980).

7. Steiner DF, Oyer PE. The biosynthesis of insulin and a probable precursor of insulin by a human islet cell adenoma. Proc Natl Acad Sci USA 57(2): 473-480 (1967).

8. Tager HS, Steiner DF, Patzelt C. Biosynthesis of insulin and glucagon. Methods Cell Biol 23: 73-88 (1981).

9. Grant PT, Coombs TL. Proinsulin, a biosynthetic precursor of insulin. Essays Biochem 6: 69-92 (1970).

10. Kemmler W, Steiner DF. Conversion of proinsulin to insulin in a subcellular fraction from rat islets. Biochem Biophys Res Commun 41(5): 1223-1230 (1970).

11. Exton JH. Hormonal control of gluconeogenesis. Adv Exp Med Biol 111: 125-167 (1979).

12. Cryer PE, Gerich JE. Glucose counterregulation, hypoglycemia, and intensive insulin therapy in diabetes mellitus. N Engl J Med 313(4): 232-241 (1985).

13. Klip A, Paquet MR. Glucose transport and glucose transporters in muscle and their metabolic regulation. Diabetes Care 13(3): 228-243 (1990).

14. Beck-Nielsen H. Insulin resistance in skeletal muscles of patients with diabetes mellitus. Diabetes Metab Rev 5(6): 487-493 (1989).

15. Baron AD, Brechtel G, Wallace P, et al. Rates and tissue sites of non-insulin- and insulin-mediated glucose uptake in humans. Am J Physiol 255(6 Pt 1): E769-774 (1988).

16. Rorsman P, Renstrom E. Insulin granule dynamics in pancreatic beta-cells. Diabetologia 46(8): 1029-1045 (2003).

17. Straub SG, Shanmugam G, Sharp GW. Stimulation of insulin release by glucose is associated with an increase in the number of docked granules in the beta-cells of rat pancreatic islets. Diabetes 53(12): 3179-3183 (2004).

18. Halban PA. Structural domains and molecular lifestyles of insulin and its precursors in the pancreatic beta-cell. Diabetologia 34(11): 767-778 (1991).

19. Duckworth WC. Insulin degradation: mechanisms, products, and significance. Endocr Rev 9(3): 319-345 (1988).

20. Morishima T, Pye S, Bradshaw C, et al. Posthepatic rate of appearance of insulin: measurement and validation in the nonsteady state. Am J Physiol 263(4 Pt 1): E772-779 (1992).

21. Sato H, Terasaki T, Mizuguchi H, et al. Receptor-recycling model of clearance and distribution of insulin in the perfused mouse liver. Diabetologia 34(9): 613-621 (1991).

22. Duck MM, Hoffman RP. Impaired endothelial function in healthy African-American adolescents compared with Caucasians. J Pediatr 150(4): 400-406 (2007).

23. Field JB. Extraction of insulin by liver. Annu Rev Med 24: 309-314 (1973).

24. Bonora E, Zavaroni I, Coscelli C, et al. Decreased hepatic insulin extraction in subjects with mild glucose intolerance. Metabolism 32(5): 438-446 (1983).

25. Xie L, Hoffman RP, Veng-Pedersen P. Noncompartmental pharmacokinetics analysis of glucose-stimulated insulin response in African-American and Caucasian youths. Biopharm Drug Dispos 30(3): 117-125 (2009).

26. Rabkin R, Ryan MP, Duckworth WC. The renal metabolism of insulin. Diabetologia 27(3): 351-357 (1984).

27. Rabkin R, Kitaji J. Renal metabolism of peptide hormones. Miner Electrolyte Metab 9(4-6): 212-226 (1983).

28. Hysing J, Tolleshaug H, Kindberg GM. Renal uptake and degradation of trapped-label insulin. Ren Physiol Biochem 12(4): 228-237 (1989).

29. Nielsen S. Time course and kinetics of proximal tubular processing of insulin. Am J Physiol 262(5 Pt 2): F813-822 (1992).

30. O'Connor MD, Landahl H, Grodsky GM. Comparison of storage- and signal-limited models of pancreatic insulin secretion. Am J Physiol 238(5): R378-389 (1980).

31. Luzi L, DeFronzo RA. Effect of loss of first-phase insulin secretion on hepatic glucose production and tissue glucose disposal in humans. Am J Physiol 257(2 Pt 1): E241-246 (1989).

32. Calles-Escandon J, Robbins DC. Loss of early phase of insulin release in humans impairs glucose tolerance and blunts thermic effect of glucose. Diabetes 36(10): 1167-1172 (1987).

33. Srikanta S, Ganda OP, Gleason RE, et al. Pre-type I diabetes. Linear loss of beta-cell response to intravenous glucose. Diabetes 33(8): 717-720 (1984).

34. Ganda OP, Srikanta S, Brink SJ, et al. Differential sensitivity to beta-cell secretagogues in "early," type I diabetes mellitus. Diabetes 33(6): 516-521 (1984).

35. Srikanta S, Ganda OP, Rabizadeh A, et al. First-degree relatives of patients with type I diabetes mellitus. Islet-cell antibodies and abnormal insulin secretion. N Engl J Med 313(8): 461-464 (1985).

36. Kahn SE, Montgomery B, Howell W, et al. Importance of early phase insulin secretion to intravenous glucose tolerance in subjects with type 2 diabetes mellitus. J Clin Endocrinol Metab 86(12): 5824-5829 (2001).

37. Daniel S, Noda M, Straub SG, et al. Identification of the docked granule pool responsible for the first phase of glucose-stimulated insulin secretion. Diabetes 48(9): 1686-1690 (1999).

38. Henquin JC, Ishiyama N, Nenquin M, et al. Signals and pools underlying biphasic insulin secretion. Diabetes 51(Suppl 1): (S60-67 (2002).

39. Ohara-Imaizumi M, Fujiwara T, Nakamichi Y, et al. Imaging analysis reveals mechanistic differences between first- and second-phase insulin exocytosis. J Cell Biol 177(4): 695-705 (2007).

40. Barg S, Lindqvist A, Obermuller S. Granule docking and cargo release in pancreatic beta-cells. Biochem Soc Trans 36(Pt 3): 294-299 (2008).

41. DeFronzo RA, Tobin JD, Andres R. Glucose clamp technique: a method for quantifying insulin secretion and resistnace. Am. J. Physiol. 237(3): E214-E223 (1979).

42. Soop M, Nygren J, Brismar K, et al. The hyperinsulinaemic-euglycaemic glucose clamp: reproducibility and metabolic effects of prolonged insulin infusion in healthy subjects. Clin Sci (Lond) 98(4): 367-374 (2000).

43. Morris AD, Ueda S, Petrie JR, et al. The euglycaemic hyperinsulinaemic clamp: an evaluation of current methodology. Clin Exp Pharmacol Physiol 24(7): 513-518 (1997).

44. Nijpels G, van der Wal PS, Bouter LM, et al. Comparison of three methods for the quantification of beta-cell function and insulin sensitivity. Diabetes Res Clin Pract 26(3): 189-195 (1994).

45. Davis SN, Piatti PM, Monti L, et al. A comparison of four methods for assessing in vivo beta-cell function in normal, obese and non-insulin-dependent diabetic man. Diabetes Res 19(3): 107-117 (1992).

46. Uwaifo GI, Parikh SJ, Keil M, et al. Comparison of insulin sensitivity, clearance, and secretion estimates using euglycemic and hyperglycemic clamps in children. J Clin Endocrinol Metab 87(6): 2899-2905 (2002).

47. Matthews DR, Hosker JP, Rudenski AS, et al. Homeostasis model assessment: insulin resistance and beta-cell function from fasting plasma glucose and insulin concentrations in man. Diabetologia 28(7): 412-419 (1985).

48. Turner RC, Holman RR, Matthews D, et al. Insulin deficiency and insulin resistance interaction in diabetes: estimation of their relative contribution by feedback analysis from basal plasma insulin and glucose concentrations. Metabolism 28(11): 1086-1096 (1979).

49. Lee JM, Okumura MJ, Davis MM, et al. Prevalence and determinants of insulin resistance among U.S. adolescents: a population-based study. Diabetes Care 29(11): 2427-2432 (2006).

50. Arslanian S, Suprasongsin C, Janosky JE. Insulin secretion and sensitivity in black versus white prepubertal healthy children. J Clin Endocrinol Metab 82(6): 1923-1927 (1997).

51. Arslanian S, Suprasongsin C. Differences in the in vivo insulin secretion and sensitivity of healthy black versus white adolescents. J Pediatr 129(3): 440-443 (1996).

52. Bergman RN. Minimal model: perspective from 2005. Horm Res 64(Suppl 3): 8-15 (2005).

53. Boston RC, Stefanovski D, Moate PJ, et al. MINMOD Millennium: a computer program to calculate glucose effectiveness and insulin sensitivity from the frequently sampled intravenous glucose tolerance test. Diabetes Technol Ther 5(6): 1003-1015 (2003).

54. Bergman RN, Phillips LS, Cobelli C. Physiologic evaluation of factors controlling glucose tolerance in man: measurement of insulin sensitivity and beta-cell glucose sensitivity from the response to intravenous glucose. J Clin Invest 68(6): 1456-1467 (1981).

55. Toffolo G, Bergman RN, Finegood DT, et al. Quantitative estimation of beta-cell sensitivity to glucose in the intact organism: a minimal model of insulin kinetics in the dog. Diabetes 29(12): 979-990 (1980).

56. Bergman RN, Ider YZ, Bowden CR, et al. Quantitative estimation of insulin sensitivity. Am J Physiol 236(6): E667-677 (1979).

57. Saad MF, Anderson RL, Laws A, et al. A comparison between the minimal model and the glucose clamp in the assessment of insulin sensitivity across the spectrum of glucose tolerance. Insulin Resistance Atherosclerosis Study. Diabetes 43(9): 1114-1121 (1994).

58. Bergman RN, Prager R, Volund A, et al. Equivalence of the insulin sensitivity index in man derived by the minimal model method and the euglycemic glucose clamp. J Clin Invest 79(3): 790-800 (1987).

59. Beard JC, Bergman RN, Ward WK, et al. The insulin sensitivity index in nondiabetic man. Correlation between clamp-derived and IVGTT-derived values. Diabetes 35(3): 362-369 (1986).

60. Welch S, Gebhart SS, Bergman RN, et al. Minimal model analysis of intravenous glucose tolerance test-derived insulin sensitivity in diabetic subjects. J Clin Endocrinol Metab 71(6): 1508-1518 (1990).

61. Finegood DT, Hramiak IM, Dupre J. A modified protocol for estimation of insulin sensitivity with the minimal model of glucose kinetics in patients with insulin-dependent diabetes. J Clin Endocrinol Metab 70(6): 1538-1549 (1990).

62. Matsuda M, DeFronzo RA. Insulin sensitivity indices obtained from oral glucose tolerance testing: comparison with the euglycemic insulin clamp. Diabetes Care 22(9): 1462-1470 (1999).

63. Hays NP, Starling RD, Sullivan DH, et al. Comparison of insulin sensitivity assessment indices with euglycemic-hyperinsulinemic clamp data after a dietary and exercise intervention in older adults. Metabolism 55(4): 525-532 (2006).

64. Abdul-Ghani MA, Williams K, DeFronzo RA, et al. What is the best predictor of future type 2 diabetes? Diabetes Care 30(6): 1544-1548 (2007).

65. Gutt M, Davis CL, Spitzer SB, et al. Validation of the insulin sensitivity index (ISI(0,120)): comparison with other measures. Diabetes Res Clin Pract 47(3): 177-184 (2000).

66. Haffner SM, Miettinen H, Stern MP. The homeostasis model in the San Antonio Heart Study. Diabetes Care 20(7): 1087-1092 (1997).

67. Anderson RL, Hamman RF, Savage PJ, et al. Exploration of simple insulin sensitivity measures derived from frequently sampled intravenous glucose tolerance (FSIGT) tests. The Insulin Resistance Atherosclerosis Study. Am J Epidemiol 142(7): 724-732 (1995).

68. Stumvoll M, Mitrakou A, Pimenta W, et al. Use of the oral glucose tolerance test to assess insulin release and insulin sensitivity. Diabetes Care 23(3): 295-301 (2000).

69. Phillips DI, Clark PM, Hales CN, et al. Understanding oral glucose tolerance: comparison of glucose or insulin measurements during the oral glucose tolerance test with specific measurements of insulin resistance and insulin secretion. Diabet Med 11(3): 286-292 (1994).

70. Tura A, Ludvik B, Nolan JJ, et al. Insulin and C-peptide secretion and kinetics in humans: direct and model-based measurements during OGTT. Am J Physiol Endocrinol Metab 281(5): E966-974 (2001).

71. Rubenstein AH, Melani F, Pilkis S, et al. Proinsulin. Secretion, metabolism, immunological and biological properties. Postgrad Med J 45(Suppl): 476-481 (1969).

72. Steiner DF. On the role of the proinsulin C-peptide. Diabetes 27(Suppl 1): 145-148 (1978).

73. Horwitz DL, Starr JI, Mako ME, et al. Proinsulin, insulin, and C-peptide concentrations in human portal and peripheral blood. J Clin Invest 55(6): 1278-1283 (1975).

74. Polonsky K, Jaspan J, Pugh W, et al. Metabolism of C-peptide in the dog. In vivo demonstration of the absence of hepatic extraction. J Clin Invest 72(3): 1114-1123 (1983).

75. Bratusch-Marrain PR, Waldhausl WK, Gasic S, et al. Hepatic disposal of biosynthetic human insulin and porcine C-peptide in humans. Metabolism 33(2): 151-157 (1984).

76. Polonsky KS, Pugh W, Jaspan JB, et al. C-peptide and insulin secretion. Relationship between peripheral concentrations of C-peptide and insulin and their secretion rates in the dog. J Clin Invest 74(5): 1821-1829 (1984).

77. Faber OK, Hagen C, Binder C, et al. Kinetics of human connecting peptide in normal and diabetic subjects. J Clin Invest 62(1): 197-203 (1978).

78. Polonsky KS, Licinio-Paixao J, Given BD, et al. Use of biosynthetic human C-peptide in the measurement of insulin secretion rates in normal volunteers and type I diabetic patients. J Clin Invest 77(1): 98-105 (1986).

79. Eaton RP, Allen RC, Schade DS, et al. Prehepatic insulin production in man: kinetic analysis using peripheral connecting peptide behavior. J Clin Endocrinol Metab 51(3): 520-528 (1980).

80. Van Cauter E, Mestrez F, Sturis J, et al. Estimation of insulin secretion rates from C-peptide levels. Comparison of individual and standard kinetic parameters for C-peptide clearance. Diabetes 41(3): 368-377 (1992).

81. Ahren B, Pacini G. Importance of quantifying insulin secretion in relation to insulin sensitivity to accurately assess beta-cell function in clinical studies. Eur J Endocrinol 150(2): 97-104 (2004).

82. Kahn SE. The relative contributions of insulin resistance and beta-cell dysfunction to the pathophysiology of Type 2 diabetes. Diabetologia 46(1): 3-19 (2003).

83. Mari A, Ahren B, Pacini G. Assessment of insulin secretion in relation to insulin resistance. Curr Opin Clin Nutr Metab Care 8(5): 529-533 (2005).

84. Report of the Expert Committee on the Diagnosis and Classification of Diabetes Mellitus. Diabetes Care 20(7): 1183-1197 (1997).

85. Bonadonna RC, Groop L, Kraemer N, et al. Obesity and insulin resistance in humans: a dose-response study. Metabolism 39(5): 452-459 (1990).

86. Ginsberg HN. Insulin resistance and cardiovascular disease. J Clin Invest 106(4): 453-458 (2000).

87. Reaven GM, Lithell H, Landsberg L. Hypertension and associated metabolic abnormalities--the role of insulin resistance and the sympathoadrenal system. N Engl J Med 334(6): 374-381 (1996).

88. Carey DG, Jenkins AB, Campbell LV, et al. Abdominal fat and insulin resistance in normal and overweight women: Direct measurements reveal a strong

relationship in subjects at both low and high risk of NIDDM. Diabetes 45(5): 633-638 (1996).

89. Kahn SE, Hull RL, Utzschneider KM. Mechanisms linking obesity to insulin resistance and type 2 diabetes. Nature 444(7121): 840-846 (2006).

90. Montague CT, O'Rahilly S. The perils of portliness: causes and consequences of visceral adiposity. Diabetes 49(6): 883-888 (2000).

91. Mayer EJ, Newman B, Austin MA, et al. Genetic and environmental influences on insulin levels and the insulin resistance syndrome: an analysis of women twins. Am J Epidemiol 143(4): 323-332 (1996).

92. Cobelli C, Caumo A, Omenetto M. Minimal model SG overestimation and SI underestimation: improved accuracy by a Bayesian two-compartment model. Am J Physiol 277(3 Pt 1): E481-488 (1999).

93. Cobelli C, Pacini G, Toffolo G, et al. Estimation of insulin sensitivity and glucose clearance from minimal model: new insights from labeled IVGTT. Am J Physiol 250(5 Pt 1): E591-598 (1986).

94. Vicini P, Caumo A, Cobelli C. The hot IVGTT two-compartment minimal model: indexes of glucose effectiveness and insulin sensitivity. Am J Physiol 273(5 Pt 1): E1024-1032 (1997).

95. Chiu KC, Cohan P, Lee NP, et al. Insulin sensitivity differs among ethnic groups with a compensatory response in beta-cell function. Diabetes Care 23(9): 1353-1358 (2000).

96. Watanabe RM, Steil GM, Bergman RN. Critical evaluation of the combined model approach for estimation of prehepatic insulin secretion. Am J Physiol 274(1 Pt 1): E172-183 (1998).

97. Gupta N, Hoffman RP, Veng-Pedersen P. Pharmacokinetic/pharmacodynamic differentiation of pancreatic responsiveness in obese and lean children. Biopharm Drug Dispos 26(7): 287-294 (2005).

98. Toffolo G, De Grandi F, Cobelli C. Estimation of beta-cell sensitivity from intravenous glucose tolerance test C-peptide data. Knowledge of the kinetics avoids errors in modeling the secretion. Diabetes 44(7): 845-854 (1995).

99. De Gaetano A, Arino O. Mathematical modelling of the intravenous glucose tolerance test. J Math Biol 40(2): 136-168 (2000).

100. de Winter W, DeJongh J, Post T, et al. A mechanism-based disease progression model for comparison of long-term effects of pioglitazone, metformin and gliclazide on disease processes underlying Type 2 Diabetes Mellitus. J Pharmacokinet Pharmacodyn 33(3): 313-343 (2006).

101. Topp B, Promislow K, deVries G, et al. A model of beta-cell mass, insulin, and glucose kinetics: pathways to diabetes. J Theor Biol 206(4): 605-619 (2000).

102. Silber HE, Jauslin PM, Frey N, et al. An integrated model for glucose and insulin regulation in healthy volunteers and type 2 diabetic patients following intravenous glucose provocations. J Clin Pharmacol 47(9): 1159-1171 (2007).

103. Avogaro A, Vicini P, Valerio A, et al. The hot but not the cold minimal model allows precise assessment of insulin sensitivity in NIDDM subjects. Am J Physiol 270(3 Pt 1): E532-540 (1996).

104. Best JD, Kahn SE, Ader M, et al. Role of glucose effectiveness in the determination of glucose tolerance. Diabetes Care 19(9): 1018-1030 (1996).

105. Finegood DT, Tzur D. Reduced glucose effectiveness associated with reduced insulin release: an artifact of the minimal-model method. Am J Physiol 271(3 Pt 1): E485-495 (1996).

106. Vicini P, Caumo A, Cobelli C. Glucose effectiveness and insulin sensitivity from the minimal models: consequences of undermodeling assessed by Monte Carlo simulation. IEEE Trans Biomed Eng 46(2): 130-137 (1999).

107. Cobelli C, Bettini F, Caumo A, et al. Overestimation of minimal model glucose effectiveness in presence of insulin response is due to undermodeling. Am J Physiol 275(6 Pt 1): E1031-1036 (1998).

108. Quon MJ, Cochran C, Taylor SI, et al. Non-insulin-mediated glucose disappearance in subjects with IDDM. Discordance between experimental results and minimal model analysis. Diabetes 43(7): 890-896 (1994).

109. Callegari T, Caumo A, Cobelli C. Bayesian two-compartment and classic single-compartment minimal models: comparison on insulin modified IVGTT and effect of experiment reduction. IEEE Trans Biomed Eng 50(12): 1301-1309 (2003).

110. Hoffman RP, Vicini P, Cobelli C. Comparison of insulin sensitivity and glucose effectiveness determined by the one- and two-compartment-labeled minimal model in late prepubertal children and early adolescents. Metabolism 51(12): 1582-1586 (2002).

111. Caumo A, Giacca A, Morgese M, et al. Minimal models of glucose disappearance: lessons from the labelled IVGTT. Diabet Med 8(9): 822-832 (1991).

112. Caumo A, Cobelli C. Hepatic glucose production during the labeled IVGTT: estimation by deconvolution with a new minimal model. Am J Physiol 264(5 Pt 1): E829-841 (1993).

113. Krudys KM, Dodds MG, Nissen SM, et al. Integrated model of hepatic and peripheral glucose regulation for estimation of endogenous glucose production during the hot IVGTT. Am J Physiol Endocrinol Metab 288(5): E1038-1046 (2005).

114. Polonsky KS, Rubenstein AH. C-peptide as a measure of the secretion and hepatic extraction of insulin. Pitfalls and limitations. Diabetes 33(5): 486-494 (1984).

115. Watanabe RM, Volund A, Roy S, et al. Prehepatic beta-cell secretion during the intravenous glucose tolerance test in humans: application of a combined model of insulin and C-peptide kinetics. J Clin Endocrinol Metab 69(4): 790-797 (1989).

116. Toffolo G, Breda E, Cavaghan MK, et al. Quantitative indexes of beta-cell function during graded up&down glucose infusion from C-peptide minimal models. Am J Physiol Endocrinol Metab 280(1): E2-10 (2001).

117. Breda E, Cavaghan MK, Toffolo G, et al. Oral glucose tolerance test minimal model indexes of beta-cell function and insulin sensitivity. Diabetes 50(1): 150-158 (2001).

118. Gupta N, Hoffman RP, Veng-Pedersen P. Pharmacokinetic/pharmacodynamic insulin-glucose analysis for differentiation of beta-cell function: an 18 month follow-up study in pre-pubertal lean and obese children. Biopharm Drug Dispos 27(6): 257-265 (2006).

119. Hovorka R, Koukkou E, Southerden D, et al. Measuring pre-hepatic insulin secretion using a population model of C-peptide kinetics: accuracy and required sampling schedule. Diabetologia 41(5): 548-554 (1998).

120. Hovorka R, Soons PA, Young MA. ISEC: a program to calculate insulin secretion. Comput Methods Programs Biomed 50(3): 253-264 (1996).

121. Volund A, Polonsky KS, Bergman RN. Calculated pattern of intraportal insulin appearance without independent assessment of C-peptide kinetics. Diabetes 36(10): 1195-1202 (1987).

122. Pacini G. Mathematical models of insulin secretion in physiological and clinical investigations. Comput Methods Programs Biomed 41(3-4): 269-285 (1994).

123. Rorsman P, Eliasson L, Renstrom E, et al. The Cell Physiology of Biphasic Insulin Secretion. News Physiol Sci(15): 72-77 (2000).

124. Watanabe RM, Bergman RN. Accurate measurement of endogenous insulin secretion does not require separate assessment of C-peptide kinetics. Diabetes 49(3): 373-382 (2000).

125. Kjems LL, Christiansen E, Volund A, et al. Validation of methods for measurement of insulin secretion in humans in vivo. Diabetes 49(4): 580-588 (2000).

126. Kjems LL, Volund A, Madsbad S. Quantification of beta-cell function during IVGTT in Type II and non-diabetic subjects: assessment of insulin secretion by mathematical methods. Diabetologia 44(10): 1339-1348 (2001).

127. Pacini G, Cobelli C. Estimation of beta-cell secretion and insulin hepatic extraction by the minimal modelling technique. Comput Methods Programs Biomed 32(3-4): 241-248 (1990).

128. Toffolo G, Campioni M, Basu R, et al. A minimal model of insulin secretion and kinetics to assess hepatic insulin extraction. Am J Physiol Endocrinol Metab 290(1): E169-E176 (2006).

129. Toffolo G, Cefalu WT, Cobelli C. Beta-cell function during insulin-modified intravenous glucose tolerance test successfully assessed by the C-peptide minimal model. Metabolism 48(9): 1162-1166 (1999).

130. Kloppel G, Lohr M, Habich K, et al. Islet pathology and the pathogenesis of type 1 and type 2 diabetes mellitus revisited. Surv Synth Pathol Res 4(2): 110-125 (1985).

131. Sheiner LB, Rosenberg B, Marathe VV. Estimation of population characteristics of pharmacokinetic parameters from routine clinical data. J Pharmacokinet Biopharm 5(5): 445-479 (1977).

132. Sheiner LB, Beal SL. Evaluation of methods for estimating population pharmacokinetic parameters. III. Monoexponential model: routine clinical pharmacokinetic data. J Pharmacokinet Biopharm 11(3): 303-319 (1983).

133. Sheiner LB, Beal SL. Evaluation of methods for estimating population pharmacokinetics parameters. I. Michaelis-Menten model: routine clinical pharmacokinetic data. J Pharmacokinet Biopharm 8(6): 553-571 (1980).

134. Sheiner BL, Beal SL. Evaluation of methods for estimating population pharmacokinetic parameters. II. Biexponential model and experimental pharmacokinetic data. J Pharmacokinet Biopharm 9(5): 635-651 (1981).

135. Sheiner LB, Rosenberg B, Melmon KL. Modelling of individual pharmacokinetics for computer-aided drug dosage. Comput Biomed Res 5(5): 411-459 (1972).

136. Steimer JL, Mallet A, Golmard JL, et al. Alternative approaches to estimation of population pharmacokinetic parameters: comparison with the nonlinear mixed-effect model. Drug Metab Rev 15(1-2): 265-292 (1984).

137. Jellife RW, Schumitzky A, Van Guillder M. User manual for version 10.7 of the USC*PACK collection of PC programs. Los Angeles: Laboratory for Applied Pharmacokinetics, University of Southern California (1996).

138. Sheiner LB, Beal SL. Pharmacokinetic parameter estimates from several least squares procedures: superiority of extended least squares. J Pharmacokinet Biopharm 13(2): 185-201 (1985).

139. Delyon B, Lavielle M, Moulines E. Convergence of a stochastic approximation version of the EM algorithm. Ann Statist 27(1): 94-128 (1999).

140. Monolix. http://software.monolix.org. (2009).

141. Wang Y, Beydoun MA. The obesity epidemic in the United States--gender, age, socioeconomic, racial/ethnic, and geographic characteristics: a systematic review and meta-regression analysis. Epidemiol Rev 29: 6-28 (2007).

142. Rocchini AP. Childhood obesity and a diabetes epidemic. N Engl J Med 346(11): 854-855 (2002).

143. Arslanian S. Insulin secretion and sensitivity in healthy African-American vs American white children. Clin Pediatr (Phila) 37(2): 81-88 (1998).

144. Moran A, Jacobs DR, Jr., Steinberger J, et al. Insulin resistance during puberty: results from clamp studies in 357 children. Diabetes 48(10): 2039-2044 (1999).

145. Hoffman RP, Vicini P, Sivitz WI, et al. Pubertal adolescent male-female differences in insulin sensitivity and glucose effectiveness determined by the one compartment minimal model. Pediatr Res 48(3): 384-388 (2000).

146. Henquin JC, Boitard C, Efendic S, et al. Insulin secretion: movement at all levels. Diabetes 51(Suppl 1): S1-2 (2002).

147. Cherrington AD, Sindelar D, Edgerton D, et al. Physiological consequences of phasic insulin release in the normal animal. Diabetes 51(Suppl 1): S103-108 (2002).

148. Maheux P, Chen YD, Polonsky KS, et al. Evidence that insulin can directly inhibit hepatic glucose production. Diabetologia 40(11): 1300-1306 (1997).

149. Davies MJ, Rayman G, Grenfell A, et al. Loss of the first phase insulin response to intravenous glucose in subjects with persistent impaired glucose tolerance. Diabet Med 11(5): 432-436 (1994).

150. Hoffman RP. Indices of insulin action calculated from fasting glucose and insulin reflect hepatic, not peripheral, insulin sensitivity in African-American and Caucasian adolescents. Pediatr Diabetes 9(3 Pt 2): 57-61 (2008).

151. Del Prato S, Tiengo A. The importance of first-phase insulin secretion: implications for the therapy of type 2 diabetes mellitus. Diabetes Metab Res Rev 17(3): 164-174 (2001).

152. McCulloch DK, Bingley PJ, Colman PG, et al. Comparison of bolus and infusion protocols for determining acute insulin response to intravenous glucose in normal humans. The ICARUS Group. Islet Cell Antibody Register User's Study. Diabetes Care 16(6): 911-915 (1993).

153. Hutchinson MF. ALGORITHM 642: a fast procedure for calculating minimum cross-validation cubic smoothing splines. ACM Trans. Math. Software 12(2): 150-153 (1986).

154. Warram JH, Martin BC, Soeldner JS, et al. Study of glucose removal rate and first phase insulin secretion in the offspring of two parents with non-insulin-dependent diabetes. Adv Exp Med Biol(246): 175-179 (1988).

155. Mitrakou A, Kelley D, Mokan M, et al. Role of reduced suppression of glucose production and diminished early insulin release in impaired glucose tolerance. N Engl J Med 326(1): 22-29 (1992).

156. Schuster DP, Kien CL, Osei K. Differential impact of obesity on glucose metabolism in black and white American adolescents. Am J Med Sci 316(6): 361-367 (1998).

157. Gower BA, Granger WM, Franklin F, et al. Contribution of insulin secretion and clearance to glucose-induced insulin concentration in african-american and caucasian children. J Clin Endocrinol Metab 87(5): 2218-2224 (2002).

158. Gungor N, Saad R, Janosky J, et al. Validation of surrogate estimates of insulin sensitivity and insulin secretion in children and adolescents. J Pediatr 144(1): 47-55 (2004).

159. Goran MI, Ball GD, Cruz ML. Obesity and risk of type 2 diabetes and cardiovascular disease in children and adolescents. J Clin Endocrinol Metab 88(4): 1417-1427 (2003).

160. Walton C, Godsland IF, Proudler AJ, et al. Effect of body mass index and fat distribution on insulin sensitivity, secretion, and clearance in nonobese healthy men. J Clin Endocrinol Metab 75(1): 170-175 (1992).

161. Potau N, Ibanez L, Rique S, et al. Pubertal changes in insulin secretion and peripheral insulin sensitivity. Horm Res 48(5): 219-226 (1997).

162. Roemmich JN, Clark PA, Lusk M, et al. Pubertal alterations in growth and body composition. VI. Pubertal insulin resistance: relation to adiposity, body fat distribution and hormone release. Int J Obes Relat Metab Disord 26(5): 701-709 (2002).

163. Goran MI, Bergman RN, Cruz ML, et al. Insulin resistance and associated compensatory responses in african-american and Hispanic children. Diabetes Care 25(12): 2184-2190 (2002).

164. Uwaifo GI, Nguyen TT, Keil MF, et al. Differences in insulin secretion and sensitivity of Caucasian and African American prepubertal children. J Pediatr 140(6): 673-680 (2002).

165. Lillioja S, Mott DM, Spraul M, et al. Insulin resistance and insulin secretory dysfunction as precursors of non-insulin-dependent diabetes mellitus. Prospective studies of Pima Indians. N Engl J Med 329(27): 1988-1992 (1993).

166. Warram JH, Martin BC, Krolewski AS, et al. Slow glucose removal rate and hyperinsulinemia precede the development of type II diabetes in the offspring of diabetic parents. Ann Intern Med 113(12): 909-915 (1990).

167. Preeyasombat C, Bacchetti P, Lazar AA, et al. Racial and etiopathologic dichotomies in insulin hypersecretion and resistance in obese children. J Pediatr 146(4): 474-481 (2005).

168. Arslanian SA, Saad R, Lewy V, et al. Hyperinsulinemia in african-american children: decreased insulin clearance and increased insulin secretion and its relationship to insulin sensitivity. Diabetes 51(10): 3014-3019 (2002).

169. Cerasi E, Luft R. The plasma insulin response to glucose infusion in healthy subjects and in diabetes mellitus. Acta Endocrinol (Copenh) 55(2): 278-304 (1967).

170. Grodsky G, M. A threshold distribution hypothesis for packet storage of insulin and its mathematical modeling. J Clin Invest 51(8): 2047-2059 (1972).

171. Panhard X, Samson A. Extension of the SAEM algorithm for nonlinear mixed models with 2 levels of random effects. Biostatistics 10(1): 121-135 (2009).

172. Kuhn E, Lavielle M. Maximum likelihood estimation in nonlinear mixed effects models. Computational Statistics & Data Analysis 49(4): 1020-1038 (2005).

173. Kuhn E, Lavielle M. Coupling a stochastic approximation version of EM with an MCMC procedure. ESAIM: P&S 8: 115-131 (2004).

174. Bratanova-Tochkova TK, Cheng H, Daniel S, et al. Triggering and augmentation mechanisms, granule pools, and biphasic insulin secretion. Diabetes 51(Suppl 1): S83-90 (2002).

175. Grodsky GM, Curry D, Landahl H, et al. Further studies on the dynamic aspects of insulin release in vitro with evidence for a two-compartmental storage system. Acta Diabetol Lat 6(Suppl 1): 554-578 (1969).

176. Melloul D, Marshak S, Cerasi E. Regulation of insulin gene transcription. Diabetologia 45(3): 309-326 (2002).

177. Jarrett RJ, Keen H, Track N. Glucose and RNA synthesis in mammalian islets of Langerhans. Nature 213(5076): 634-635 (1967).

178. Permutt MA, Kipnis DM. Insulin biosynthesis. I. On the mechanism of glucose stimulation. J Biol Chem 247(4): 1194-1199 (1972).

179. Dean PM. Ultrastructural morphometry of the pancreatic -cell. Diabetologia 9(2): 115-119 (1973).

180. Pedersen PV. Curve fitting and modeling in pharmacokinetics and some practical experiences with NONLIN and a new program FUNFIT. J Pharmacokinet Biopharm 5(5): 513-531 (1977).

181. Akaike H. A new look at the statistical model identification. IEEE Trans Automat Contr 19(6): 716-723 (1974).

182. Home PD, Massi-Benedetti M, Shepherd GA, et al. A comparison of the activity and disposal of semi-synthetic human insulin and porcine insulin in normal man by the glucose clamp technique. Diabetologia 22(1): 41-45 (1982).

183. Sherwin RS, Kramer KJ, Tobin JD, et al. A model of the kinetics of insulin in man. J Clin Invest 53(5): 1481-1492 (1974).

184. Juhl C, Grofte T, Butler PC, et al. Effects of fasting on physiologically pulsatile insulin release in healthy humans. Diabetes 51(Suppl 1):S255-257 (2002).

185. Ku CY, Gower BA, Hunter GR, et al. Racial differences in insulin secretion and sensitivity in prepubertal children: role of physical fitness and physical activity. Obes Res 8(7): 506-515 (2000).

186. DeFronzo RA. Lilly lecture 1987. The triumvirate: beta-cell, muscle, liver. A collusion responsible for NIDDM. Diabetes 37(6): 667-687 (1988).

187. Macor C, Ruggeri A, Mazzonetto P, et al. Visceral adipose tissue impairs insulin secretion and insulin sensitivity but not energy expenditure in obesity. Metabolism 46(2): 123-129 (1997).

188. Polonsky K, Frank B, Pugh W, et al. The limitations to and valid use of C-peptide as a marker of the secretion of insulin. Diabetes 35(4): 379-386 (1986).

189. Sparacino G, Cobelli C. A stochastic deconvolution method to reconstruct insulin secretion rate after a glucose stimulus. IEEE Trans Biomed Eng 43(5): 512-529 (1996).

190. Campioni M, Toffolo G, Basu R, et al. Minimal model assessment of hepatic insulin extraction during an oral test from standard insulin kinetic parameters. Am J Physiol Endocrinol Metab 297(4): E941-948 (2009).

191. Cobelli C, Pacini G. Insulin secretion and hepatic extraction in humans by minimal modeling of C-peptide and insulin kinetics. Diabetes 37(2): 223-231 (1988).

192. Xie L, Hoffman RP, Veng-Pedersen P. Population analysis of ethnicity and first-phase insulin release. Diabetes Res Clin Pract 89(3): 243-249.

193. Mari A, Tura A, Pacini G, et al. Relationships between insulin secretion after intravenous and oral glucose administration in subjects with glucose tolerance ranging from normal to overt diabetes. Diabet Med 25(6): 671-677 (2008).

194. Kuhn E, Lavielle M. Maximum likelihood estimation in nonlinear mixed effects model. Comput Stat Data An 49(4): 1020-1838 (2005).

195. Kuhn E, Lavielle M. Coupling a stochastic approximation version of EM with an MCMC procedure. ESAIM: P&S 8(115-131): (2004).

196. Delyon B. Convergence of a stochastic approximation version of the EM algorithm. Ann Statist 27(1): 94-128 (1999).

197. Radziuk J, Morishima T. New methods for the analysis of insulin kinetics in vivo: insulin secretion, degradation, systemic dynamics and hepatic extraction. Adv Exp Med Biol 189: 247-276 (1985).

198. Madsbad S, Kehlet H, Hilsted J, et al. Discrepancy between plasma C-peptide and insulin response to oral and intravenous glucose. Diabetes 32(5): 436-438 (1983).

199. Shuster LT, Go VL, Rizza RA, et al. Incretin effect due to increased secretion and decreased clearance of insulin in normal humans. Diabetes 37(2): 200-203 (1988).

200. Shapiro ET, Tillil H, Miller MA, et al. Insulin secretion and clearance. Comparison after oral and intravenous glucose. Diabetes 36(12): 1365-1371 (1987).

201. Nauck MA, Homberger E, Siegel EG, et al. Incretin effects of increasing glucose loads in man calculated from venous insulin and C-peptide responses. J Clin Endocrinol Metab 63(2): 492-498 (1986).

202. Meier JJ, Holst JJ, Schmidt WE, et al. Reduction of hepatic insulin clearance after oral glucose ingestion is not mediated by glucagon-like peptide 1 or gastric inhibitory polypeptide in humans. Am J Physiol Endocrinol Metab 293(3): E849-856 (2007).